ENHANCED THERAPEUTIC POTENTIAL OF PREACTIVATED MESENCHYMAL STROMAL CELLS AND THEIR SECRETORY FACTOR STANNIOCALCIN-1 IN MODELS FOR ACUTE INJURIES AND INFLAMMATION

A Dissertation

by

AREZOO MOHAMMADIPOOR

Submitted to the Office of Graduate and Professional Studies of
Texas A&M University
in partial fulfillment of the requirements for the degree of

DOCTOR OF PHILOSOPHY

Chair of Committee,	Darwin J. Prockop
Committee Members,	Ryang Hwa Lee
	Carl A. Gregory
	Fei Liu
	Thomas J. Bartosh
Head of Department,	Van G. Wilson

August 2015

Major Subject: Medical Sciences

ABSTRACT

There has been significant interest in the therapeutic potential of the adult stem/progenitor cells from bone marrow called multipotent mesenchymal stromal cells (MSCs). Signals from injured tissues activate MSCs to secrete beneficial factors and contribute to immune/inflammatory modulation and tissue healing. In order to enhance the therapeutic potential of MSCs hanging drop culture method was used to preactivate the cells in vitro and eliminate the lag period required for their activation in vivo. Stanniocalcin-1 (STC-1) is a potent anti-inflammatory and anti-apoptotic protein secreted from activated MSCs and has been considered as a substitute for MSCs in several disease conditions; therefore, the effects of STC-1 were studied on monocyte fate in vitro and in a mouse model of ischemic myocardial injury.

Aggregated MSCs in hanging drops were self-activated to produce several therapeutic factors such as anti-inflammatory protein STC-1 and TNFα stimulated gene/protein 6 (TSG-6). MSCs dissociated from spheroids were also smaller than MSCs from standard 2 dimensional cultures, and as a result, larger numbers of them trafficked through the lung of mice after intravenous administration. Notably, spheroid MSCs were more effective than MSCs from standard cultures in suppressing inflammatory responses in a co-culture system with activated macrophages and in a mouse model of peritonitis. The data suggest enhanced therapeutic potential of spheroid MSCs for diseases caused by unresolved inflammation. Treatment with STC-1 reduced expression of CD14, a co-receptor for toll-like receptors, in differentiating monocytes/macrophages and suppressed the inflammatory responses of the cells to endotoxin. Administration of STC-1 also reduced CD14 expression in monocytes stimulated with various danger signals and in hearts of mice after myocardial infarction. These findings may explain the observed decreases in cardiac inflammation following myocardial infarction, and the improvements in ejection fraction and infarct size. The results suggest that STC-1 is a promising therapy to protect the heart and other tissues from ischemic injury.

I would like to dedicate this work to my father, late Manouchehr Mohammadipoor, and my mother, Parvin Samari, for their unwavering support and guidance.

ACKNOWLEDGEMENTS

I would like to express the deepest appreciation to my committee chair Dr. Darwin. J. Prockop for his guidance and support throughout the course of this research. I would like to thank my committee members, Dr. Ryang Hwa Lee, Dr. Carl A. Gregory, Dr. Fei Liu, and Dr. Thomas V. Peterson for their constant guidance and support. I would also like to sincerely thank my committee member Dr. Thomas. J. Bartosh for his immense involvement in my work. His mentorship and genuine interest in my personal growth as a graduate student is greatly appreciated.

Thanks also go to my friends and colleagues at the Institute for Regenerative Medicine for their support, specifically Dr. Nikolay Bazhanov, Dr. Andrea Foskett, April Tiblow, Kent and Monica Claypool, Dr. Joni H. Ylostalo, Nrutya Madduri, and Roxanne Reger for all their help and guidance. To all the staff members at Texas A&M University Health Science Center and the Institute for Regenerative Medicine, specially Joyce Adams, Karen Purcella, Kyra Cox, and Betsy Ball for their help and cheerful disposition – thank you so much!

Finally, thanks to my family for their encouragement.

TABLE OF CONTENTS

Page

Page

Page

Page

LIST OF FIGURES

Page

LIST OF TABLES

Page

CHAPTER I
INTRODUCTION AND LITERATURE REVIEW

I.1 Multipotent Mesenchymal Stromal Cells: Characteristics and Therapeutic Potential

There has been significant interest in the therapeutic potential of the adult stem/progenitor cells from bone marrow initially referred to as colony forming units-fibroblasts (CFU-Fs), then as marrow stromal cells and subsequently as mesenchymal stem cells and currently as multipotent mesenchymal stromal cells (MSCs). Each of the names reflect a different property or function of the cells. Marrow-derived MSCs are easy to isolate and expand in culture. These cells divide well in culture and their progeny are further capable of differentiating into one of several mesenchymal phenotypes such as osteoblasts, chondrocytes, and adipocytes. In addition, MSCs secrete a variety of cytokines and growth factors that have both paracrine and autocrine effects on different physiological and pathological processes [1-3].

I.1.1. Isolation and characteristics of bone marrow-derived multipotent mesenchymal stromal cells

Marrow stromal tissue contains variety of cells plus extracellular matrix to support the hematopoietic cells and influence their proliferation and differentiation. In addition to adipocytes, osteoblasts, endothelial cells and macrophages; marrow stromal cells include spindle-shaped cells, previously known as fibroblast-reticular cells, which form the reticular tissue and possess distinct osteogenic potencies [4,5]. The stromal fibroblast-reticular cells were considered histogenetically to be independent of the hematopoietic cells. These cells were shown to contain recipient genotypes in the radiochimeric bone marrow, while macrophages and hematopoietic and lymphoid cells were replaced by donor cells. In semisyngeneic heterotopic transplants of bone marrow, fibroblast-reticular cells were also found to retain their donor origin independent of host hematopoietic cells [4-6]; thus, these cells were considered responsible for the

specificity of the microenvironment. Moreover, developments in the in vitro culturing system led to better understanding of how the signaling pathways played unique roles within the microenvironment of the marrow and characterized the marrow cells within the hematopoietic niche.

In early attempts to culture bone marrow, Friedenstein and colleagues revealed that a small fraction of marrow stromal cells adhered to culture dishes. Friedenstein observed morphological similarity of the adhered cells to the spindle-shaped fibroblast-like cells that formed the stroma of marrow [6,7]. Since these cells expanded as single-cell derived colonies in monolayer cultures, he named them CFU-Fs. The clonal origin of the fibroblastic colonies was confirmed, later, using thymidine labeling, time-lapse photography and chromosome markers [8,9]. The cells from the colonies were easily maintained in vitro. In addition, they were shown to differentiate into bone after retransplantation of diffusion chambers under kidney capsules [4,7]. Further studies showed that multipotent bone-marrow-derived colony forming stromal cells were developmentally originated from mesenchymal tissues and, therefore, were named mesenchymal stromal cells (MSCs) [10].

During the primary cultures of whole bone marrow aspirate, the hematopoietic fraction has been shown to disappear mostly within 2 to 3 weeks. The non-hematopoietic plastic-adherent compartment of bone marrow consists of a variety of heterogeneous populations of cells; thus, since 1990 several groups of investigators have attempted to prepare more homogeneous populations [2,11]. In addition, several multipotent MSC-like cells were recovered from various tissues, particularly from human adipose tissue, umbilical cord blood, placental tissue, and even exfoliated deciduous teeth [12-15]. Because various methods are used in different labs to isolate, expand, and characterize MSCs and MSC-like cells, interpretation and comparison of their outcomes is difficult. Therefore, the Mesenchymal and Tissue Stem Cell Committee of the International Society for Cellular Therapy proposed minimal criteria to define human MSCs. First, the cells must be plastic-adherent when maintained in standard culture conditions. Second, MSCs must express CD105, CD73, and CD90 surface antigens when analyzed by flow

cytometry. In addition, they must lack expression of the following hematopoietic antigens: CD45, CD34, CD14 or CD11b, CD79a or CD19, and human leukocyte antigen (HLA)-DR. Thirdly, MSCs must differentiate into osteoblasts, adipocytes and chondrocytes in vitro. While these criteria will most likely require modification as new knowledge unfolds, the standardization of the minimum criteria for MSC classification will serve to facilitate the exchange of data among investigators [16].

Typically, in order to isolate adult human bone marrow-derived MSCs the bone marrow aspirates are taken from the iliac crest of normal adult donors. Discontinuous density gradient centrifugation is mainly used to separate the mononuclear layer of bone marrow aspirates, which contains the MSCs. The mononuclear cells are then cultured in the plastic based culture dish. After 24 hours, non-adherent cells are discarded and remaining adherent cells are expanded in α-minimal Eagle's medium (αMEM) containing fetal bovine serum (FBS) or fresh human serum [4,17-19]. In some cases, MSCs are purified from mononuclear layer based in the expression of the primitive MSC marker, STRO-1; otherwise, the cells from passage one or higher are used for characterization [20]. After an initial lag phase for MSCs to proliferate in culture, the cells divide rapidly, with a donor-dependent average initial doubling time of 12 to 24 hours. Initial plating density is another factor for MSC proliferation rate. As the cultures approach high density, MSCs enter a stationary phase and transform from a spindle-like morphology to a larger, flatter phenotype; therefore, for expansion purposes the cells are maintained below their confluency level. Typically, the MSCs recovered from a 2-mL bone marrow aspirate can be expanded 500-fold over about 3 weeks resulting in theoretical yield of 12.5 to 35.5 billion cells. The cells generally retain their multipotentiality for at least 6-10 subsequent passages [19]. Since MSCs could be easily isolated from adult bone marrow aspirates or other sources and are rapidly expanded in regular monolayer culture through 30 or more population doublings, the cells could offer broad therapeutic implications for a variety of diseases.

I.1.2. The roles of mesenchymal stromal cells in hematopoiesis

One of the primary roles for marrow-derived MSCs was proposed to be the involvement of those cells in the hematopoietic niche. Confluent cultures of MSCs were shown to be effective feeder layers for the culture of hematopoietic stem cells (HSCs). MSCs were found, subsequently, to influence all stages of hematopoiesis through establishing distinct microenvironments in part by production of regulatory macromolecules. The extracellular matrix molecules synthesized by MSCs include interstitial type I collagen, fibronectin, and the type IV collagen and laminin of basement membranes in cultures. MSCs also secrete cytokines in culture, the most important of which appear to be interleukin-1 (IL-1), IL-7, IL-11, stem cell factor (c-kit ligand), colony-stimulating factor–1 (CSF-1), granulocyte-macrophage-CSF (GM-CSF), and macrophage-CSF (M-CSF). These macromolecules could provide molecular signals to modulate mitotic, metabolic, and or development states of neighboring cells. Also, marrow-derived MSCs were shown to dynamically respond to environmental components resulting in modulation of their own mitotic, metabolic, and or developmental activity [10,21-24]. The niche role of MSCs was observed in vivo as well. Islands of hematopoiesis formed within the ceramic cubes seeded with human MSCs, which were transplanted subcutaneously into immunodeficient mice [25]. Moreover, this role was supported in clinical trials when autologous MSCs were expanded ex vivo and then infused in breast cancer patients. MSCs were shown to hasten the recovery of the hematopoietic system after bone marrow transplants [26]. Together, these observations demonstrated that the primary role of the cells is to form niches for HSCs [3].

I.1.3. Therapeutic potential of multipotent mesenchymal stromal cells

I.1.3.1. Engraftment and differentiation paradigm

Friedenstein et al. originally reported that MSCs became mineralizing cells or chondrocytes in vitro and in vivo [9]. Further studies confirmed that isolated marrow-derived MSCs were capable of differentiating into multiple cell lineages, including bone,

fat, tendon and cartilage [9,10,27]. Also, several reports suggested that under specific experimental conditions MSCs could differentiate into skeletal and cardiac muscle, hepatocytes, glia and neurons [28-35]. Although the exact mechanisms of MSC differentiation are not fully understood, multipotent MSCs have been proposed to repair injured tissues by engraftment and differentiation. This paradigm was supported by early observations that local administration of MSCs improved bone repair [36]. Other studies also determined that MSCs administered to animals, either locally or systemically, could home to multiple tissues and improve tissue healing [37-39]. These observations led to a few clinical trials using MSCs in children with severe osteogenesis imperfecta [40] and children with severe lysosomal storage diseases [41]. Notably, minimal adverse effects were detected after administration of MSCs; one of the children developed a mild allergic reaction to FBS in which the MSCs were expanded [40]. The promising results from these experimental studies and clinical trials encouraged investigators to further examine the long term engraftment and differentiation potential of MSCs in several settings [3].

Numerous reports described functional improvements after administration of MSCs in models for human diseases such as osteogenensis imperfecta [38], stroke [42], myocardial infarction [43], acute kidney injury [44], and diabetes [45,46]; however, series of technical challenges limited validating engraftment of MSCs and thus influenced the interpretation of the outcomes of those studies. For instance, the available tracking methods used to follow MSC differentiation in vivo produced unidentifiable artifacts. In addition, species differences in characteristics and behaviors of MSCs created a significant experimental barrier [3]. Moreover, some of the observations from the studies on the fate of administered MSCs in vivo were inconsistent with the engraftment and differentiation hypothesis. In fact, after local administration of MSCs into animals the majority of cells were reported to disappear within a few weeks [47-49]. Observations with whole body imaging techniques also revealed that most MSCs became trapped in the lungs after intravenous (i.v.) infusions into rodents [50]. Lee and colleagues (2009) employed quantitative polymerase chain reaction (PCR) assay for

human Alu sequences to track tissue distribution of MSCs after i.v. infusion. They demonstrated that all of the MSCs were cleared from the circulation within 5 minutes of infusion. Most of the cells were recovered in the lungs. MSCs in the lungs disappeared with a half-life of about 24 hours and the remaining trace amounts of the cells were detected in brain, heart, liver, spleen, and kidney [51]. Interestingly in some disease models the medium conditioned (CM) by MSCs in cultures was reported to be as effective as the cells themselves [52,53]; therefore, all these observations indicate that in many situations MSCs could repair injured tissues and improve functions without significant engraftment or differentiation.

I.1.3.2. Crosstalk paradigm

Because the engraftment and differentiation paradigm failed to explain all of the reparative effects of administered MSCs in vivo, other paradigms were proposed. MSCs were shown to express a distinct cytokine profile to maintain HSCs in a quiescent state as part of the stromal-cells physiological niche. Interestingly, several investigators observed that variety of stimuli could alter the profile of MSC cytokine expression to promote proliferation, differentiation, and migration of HSCs. Subsequently, others reported the crosstalk between MSCs and injured cells in which signals from injured cells or MSCs activated other cells to alter the expression of large arrays of genes [2,3,54,55]. For instance, Ohtaki and colleagues (2008) reported that local injection of human MSCs into the hippocampi of mice following transient cerebral ischemia, reduced neuronal death and improved the neurological deficits. Human-specific microarrays of RNA from hippocampi demonstrated that in the injured brain, the expression of genes involved in modulation of immune and inflammatory responses were increased in human MSCs. Assays of the same RNA on mouse-specific microarrays revealed that the presence of the human MSCs modulated expression of mouse genes involved in immune responses to the ischemic environment [48]. More evidence of crosstalk was observed between MSCs and multiple myeloma cells [55]. Co-culture studies demonstrated that signals from the myeloma cells stimulated the MSCs to increase secretion of IL-6. IL-6 was then shown to stimulate the proliferation of

myeloma cells. At the same time, the myeloma cells secreted high levels of Dkk-1, an inhibitor of Wnt signaling. DKK-1 in turn, inhibited MSCs from differentiating into osteoblasts [54]. The dynamic and transient crosstalk between MSCs and injured tissues was suggested as a new paradigm to explain some of the beneficial effects of MSCs in vivo. Based on the crosstalk theory, MSCs respond to the injured tissue and enhance tissue repair via different mechanisms such as promoting endogenous tissue regeneration, modulation of immune and inflammatory responses, and reduction in cell death [2,3,56].

MSCs could promote endogenous regeneration by providing a niche to enhance proliferation and differentiation of tissue-specific stem/progenitor cells. Munoz et al. (2005) reported that in the experiments in which human MSCs were injected directly into the hippocampus of immune-deficient rats, MSCs engrafted briefly in hippocampus and enhanced proliferation of the endogenous neural stem cells found in the hippocampus. In addition, the cells increased migration of neural stem cells and their differentiation into neural cells [47].

Numerous investigators have studied the immune modulatory effects of MSCs on both innate and adaptive immune responses. The cells could suppress proliferation, maturation, and pro-inflammatory functions of different types of immune cells such as monocytes, dendritic cells, T-cells, B-cells, and neutrophils. Parallel with suppressing pro-inflammatory responses, MSCs have been demonstrated to increase the generation of anti-inflammatory immune cells, that include regulatory T-cells as well as anti-inflammatory phenotypes of macrophages [2]. One of the first preclinical experiments focusing on immune modulatory potential of MSCs was done by Bartholomew and colleagues (2002). They observed that injection of allogeneic MSCs prolonged skin-graft survival in primates [57]. Other investigators also reported i.v. infusion of MSCs significantly reduced demyelination of neurons, loss of function, and infiltration of pro-inflammatory cells in the experimental autoimmune encephalitis (EAE) model for multiple sclerosis [58,59]. For the first time, immune modulatory effects of tMSCs were reported in clinical trials to improve bone marrow transplants with MSCs: administration

of allogeneic MSCs improved the manifestations of graft-versus-host disease (GVHD) in a few patients [60]. Despite all the reports about immunosuppressive roles of the cells, underlying mechanisms of their actions are partially known. Some observations suggest that cell-to-cell contact with immune cells is required for these effects. In addition, immune modulatory effects of MSCs may be explained by the soluble factors secreted by these cells, including inducible nitric oxide synthase (iNOS), indoleamine dioxygenase (IDO), monocyte chemoattractant protein (MCP-1, also known as chemokine (C–C motif) ligand 2 (CCL2)), and prostaglandin E2 (PGE_2) [2].

Recent reports demonstrated that MSCs also modulate inflammation [56]. Even though inflammatory responses have essential roles in eliminating foreign agents, removing damaged cells, and promoting tissue repair, a growing body of evidence suggests accentuation, prolongation, or expansion of inflammation worsen tissue deterioration and loss of function. Excessive or non-resolving inflammation has also been known to contribute to the pathogenesis of diseases such as obesity, diabetes, myocardial infarction, stroke, Parkinsonism, and Alzheimer's disease [61]. Inflammatory stimuli have been shown to activate MSCs to secrete arrays of soluble factors and affect different aspects of inflammatory responses; therefore, MSCs could modulate excessive inflammation without significant tissue engraftment as was suggested in the crosstalk paradigm [56]. Searching for the mechanisms in which MSCs reduced inflammation and protected cardiac function in the murine model of myocardial infarction, Dr. Lee et al. (2009) analyzed transcriptomal alteration of trapped MSCs in the lungs of experimental mice 10 hours after i.v. infusion. Using both human- and mouse-specific microarrays for RNA isolated from the lungs, they observed wide ranges of human and mouse transcripts upregulated or downregulated post MSCs administration. Among several candidate genes, upregulation of human TNFAIP6 gene, which encodes tumor necrosis factor (TNF) stimulating gene 6 protein (TSG-6), was confirmed by real-time RT-PCR assays [51]. TSG-6 is a 35 kDa secreted protein. Previous studies demonstrated that TSG-6 expression has been observed in different pathological contexts that are associated with inflammation. The strong anti-

inflammatory activity of this protein has been studied in both wild-type and transgenic mice [62,63]. Experiments with recombinant human TSG-6 and siRNA demonstrated that secreted TSG-6 largely accounted for the anti-inflammatory and cardio-protective effects of MSCs mouse model of myocardial infarction. Paralleled with in vivo observation, treated MSCs with recombinant TNFα in culture were activated to express TSG-6 mRNA [51]. Secretion of TSG-6 by MSCs was also demonstrated in a model of chemical-induced cornea injury in rats. Intraperitoneal (i.p.) and i.v administration of human MSCs were shown to significantly reduce the amount of myeloperoxidase (MPO, enzyme released in injured tissue mainly by activated neutrophils) and pro-inflammatory cytokines [64]. In addition, MSC therapy decreased development of opacity in the cornea. Similar to the mouse model of myocardial infarction, knockdown of the TSG-6 gene negated the beneficial effects of MSCs. Also, administration of recombinant human TSG-6 could reproduce the beneficial outcomes of MSC therapy. A quantitative assay for human mRNA for glyceraldehyde 3-phosphate dehydrogenase (GAPDH) demonstrated insignificant numbers of MSCs detectable in the corneas of rats 1 day and 3 days after i.v. or i.p. administration [64]. In a mouse model of zymosan-induced peritonitis, Choi et al. (2011) demonstrated that secreted TSG-6 from MSCs and its recombinant protein suppressed the initial production of pro-inflammatory cytokines: TSG-6 decreased activation of nuclear factor (NF)-κB in the resident macrophages and therefore fewer neutrophils were recruited to the site of injury, which led to lesser tissue damage [65]. In addition to TSG-6, stimulation of MSCs with different pro-inflammatory cytokines activated the cells to secrete variety of anti-inflammatory mediators such as transforming growth factor beta (TGF-β), PGE_2, IL-10, IL-1 receptor antagonist (IL-1ra), soluble receptor 1 for TNF (sTNFR1), and stanniocalcin-1 (STC-1) indicating that MSCs can suppress inflammation through a variety of mechanisms [56].

Another therapeutic potential of MSCs was shown to be cytoprotection [56]. Hypoxic culture conditions activated MSCs to increase production of several angiogenesis and anti-apoptosis factors such as IL-6, vascular endothelial growth factor (VEGF), and MCP-1/CCL2 [66]. In addition, Block and colleagues (2009) observed that

apoptosis was reduced in the previously UV irradiated fibroblasts co-cultured with MSCs in a transwell system [67]. Comparative microarray analysis of cultured MSCs in the presence or absence of UV irradiated fibroblasts demonstrated that apoptotic cells activated MSCs to secrete STC-1. The use of anti-STC-1 blocking antibody attenuated the anti-apoptotic effect of MSCs [67].

Overall, the current data indicate that although bone marrow-derived MSCs were first proposed to differentiate into injured tissue, their therapeutic effects mostly result from their broad range of responses to different microenvironments. MSCs release anti-inflammatory cytokines as well as anti-apoptotic and trophic molecules to protect the damaged tissues and promote tissue repair. These cells produce significant beneficial effects when administered to experimental animals. Also, they have demonstrated few if any adverse effects; therefore, MSCs are likely to continue to be the most widely used cells for new clinical trials in patients.

I.2 Stanniocalcin-1: the Multitasking Secretory Protein

STC-1 is the mammalian homologue of STC, which was originally identified as a calcium/phosphate-regulating hormone in bony fish. Formerly called hypocalcin or teleocalcin, STC is a homodimeric glycoprotein secreted by small endocrine glands in fish called corpuscles of Stannius. STC-1 in mammals is produced by a variety of tissues and has been proposed to regulate a variety of physiological and pathological functions in a paracrine/intracrine fashion [68-70].

I.2.1. Stanniocalcin in fish

In 1839, Stannius described corpuscles of Stannius as cream-colored bodies located ventrally on the surface of the fish kidney. He thought corpuscles of Stannius were fish adrenal glands; therefore, initially emphasis was on identifying their steroidogenic capacity, but to no avail [68,71]. More than a century after the discovery of corpuscles of Stannius, Fontaine (1964) found that the surgical removal of these glands led to a transparent hypercalcemia in European eel. Interestingly, the animals

were unperturbed by elevated serum calcium levels in the 5-6 mM range and eventually restored their normocalcemia. The mode of recovery is still not completely understood. Stanniectomized eels held in acalcemic water did not develop hypercalcemia, which suggested the significant role of exogenous calcium in the calcium hemostasis in fish [71,72]. Fenwick and his colleagues identified that the gills of eels lacking corpuscles had at least 10 fold higher rates of calcium transport [72]. Furthermore, the injection of corpuscles of Stannius glandular extracts were found to reduce gill calcium transport, both in vivo and in vitro in isolate perfused gills. This finding hinted that an active principle(s) or inhibitory factor(s) in the corpuscles of Stannius extracts might regulate the rate of gill calcium transport [73,74]. Other investigators showed hypocalcemic activity in the corpuscles of Stannius of different types of fish as well [71,75,76].

I.2.1.1. Structure of fish stanniocalcin protein

Two major active principles were later isolated from corpuscles of Stannius: a substance with pressor activity [77] and a glycosylated protein [78,79]. While the characteristic of pressor substance was still being investigated [80], the studies for the hypocalcemic principle of corpuscles of Stannius of fish, STC, indicated that the protein had a unique amino acid sequence as compared to other known mammalian hormones [79,81-83]. In most fish species, STC is a homodimeric molecule. On the basis of cDNA sequencing in salmonids, the precursor of proSTC monomer is 256 residues in length. A hydrophobic segment is cleaved off during translation to yield a 64 kDa proSTC, which is then processed over a period of minutes into the mature monomer of 223 residues. Glycosylation at an Asn-linked consensus site adds ~5 kDa to the protein core. Two-dimensional gel electrophoresis indicated the presence of several isoforms of proSTC and mature STC molecules that may reflect different stages of maturation of the (pro)hormone [71,84]. During translation, 10 of the 11 cysteines form intrachain disulfide linkages, leaving the last (Cys_{169}) to form the interchain dimer [83]. In arawana and several other osteoglossiform species the 11th cysteine is replaced by arginine (Cys_{169}-Arg_{169}), making these the only known vertebrates in which STC exists in monomeric form [85]; however, the effect of this mutation on STC bioactivity has not

yet been addressed. Synthetic N-terminal fragments (1–20) of fish STC monomers were shown to have inhibitory effects on gill calcium transport, albeit at much reduced potency. Also, the loss of the first four N-terminal amino acids significantly reduced the effect of STC [86,87], suggesting that the bioactive portion of this hormone resides in the N-terminus. Verbost et al. observed that the midfragment of STC conceivably contained a major antigenic site of the hormone [87]. In salmon, the C-terminus of STC has been shown to undergo truncation [88], but the effect of this process on hormone potency has not yet been identified [71].

I.2.1.2. Tissue expression of fish stanniocalcin

STC was originally believed to be made only by corpuscles of Stannius cells in fish. However, the gene is now known to be expressed in most tissues at much lower levels and could account for the ability of fish to re-establish normal calcium balance after stanniectomy. Gonads and kidneys have the highest levels of extra-corpuscular gene expression. The ovaries have been shown to produce a more heavily glycosylated form of STC hormone [89,90]. The function of this STC variant remains to be seen. Despite the tissue pattern of gene expression, the immunoassay of sera from fish maintained in waters of wide-ranging calcium concentrations (0.02-10 mM Ca^{2+}) indicated that STC was always present in the blood, although not always in its bioactive form. Fish serum contained at least four smaller immunoreactive forms of STC in addition to the pro and mature hormone. It would appear that fish serum contains factors capable of modifying hormone activity, such as proteolytic enzymes cleaving STC at one or more sites in the protein core [91]. A rise in serum calcium levels is known to be the primary stimulus for promoting STC release from the corpuscles of Stannius glands [91]. The sensitivity of the cells to calcium is mediated by membrane-associated calcium sensing receptors (CaSR) [92,93]. This mechanism ensures that as serum calcium levels rise, STC is released to slow the rate of calcium entry via the gills. Calcium also stimulates STC translation [94], stabilizes pre-existing transcript [95], and increases transcript levels as much as 6-fold in cultured corpuscles of Stannius cells [71]. Recent

studies suggested that Na^+ and Cl^- ions might regulate STC release from corpuscles of Stannius as well [96].

I.2.1.3. Function of fish stanniocalcin

Calcium transport is an important and evolutionarily conserved process. In fish, STC regulates serum calcium homeostasis via the inhibition of branchial/ intestinal calcium uptake [91]. In addition, STC promotes phosphate reabsorption by the kidneys [97], which might be intended to chelate excess calcium in the serum and deposit into bone and scales. Although the exact mechanism by which STC inhibits gill calcium transport is not known; this biological action of STC has been widely used as a standard bioassay to test the hypocalcemic potency of corpuscles of Stannius extracts or the recombinant STC protein [79,91,98]. In studies on isolated flounder proximal tubules, Renfro and colleagues have shown that STC has dose-dependent stimulatory effects on G protein coupled signaling cascade activating the PKA pathway [97]; however, the structure of STC receptors in fish or mammals have not been identified. Chloride cells of the gills are responsible for regulated calcium transport and have been suggested to be sites of STC action [99]. Butler and colleagues have suggested that STC may redirect blood flow away from areas of the gill that are rich in chloride cells as a means of reducing calcium transport [100]. One other proposed mechanism could be the transfer of calcium back to water by yet-uncharacterized transporters. Alternatively, STC might promote calcium chelation within the cytosol of chloride cells or its uptake by a subcellular organelle such as mitochondria. Then the trapped cation could be released to the bloodstream in accordance with normal physiological demands. While studying fractionated gills, Flik (1990) ruled out low- and high-affinity Ca^{2+}-ATPases as being regulated by STC. He suggested that STC might close calcium channels in the apical membranes of chloride cells, thereby reducing their calcium permeability [94]. Recently, STC has been found to reduce calcium uptake via the inhibition of epithelial Calcium channel mRNA expression [101], which could explain the calcium regulatory mechanism of STC in fish.

I.2.2. Stanniocalcin-1 in mammals

Originally, STC was assumed to be unique to fish. No corpuscles of Stannius glands or any comparable structures have been identified in mammals. In addition, calcium/phosphate homeostasis in mammals has been replaced by parathyroid hormone, calcitonin, and 1,25-dihydroxyvitamin D [70]. The first suggestion that there might be a mammalian STC was based on immunoreaction of STC with human serum and kidneys [102]. Mammalian homologue of STC was thereafter isolated independently in two laboratories. Chang et al. (1995) identified a cDNA that was downregulated following immortalization of simian virus 40 (SV40) early region-transformed human fibroblasts. The sequence of the new cDNA was found to share ~60% identity and ~73% similarity with amino acid sequences of various fish STCs. Due to its high degree of homology to fish STC, this novel mammalian protein was also named STC [103]. Olsen and colleagues (1996) identified the same gene during random sequencing of an early-stage human fetal lung cDNA library [98]. Two years after the identification of the mammalian STC, a second human and mouse STC gene was identified by several groups searching expressed sequence tag (EST) databases for sequences related to human STC [104-107]; Consequently, fish and mammalian STC was renamed STC-1 and STC-related protein was named STC-2. In 2005, fish STC-2 was also cloned from various fish species [108].

I.2.2.1. Structure of mammalian stanniocalcin-1 protein

The human STC-1 cDNA encodes a protein of 247 amino acids. The level of sequence similarity to salmon STC-1 is 92% over the first 204 amino acids; however, the last 43 residues at the C-terminus are completely different. The human STC-2 cDNA encodes a protein of 302 amino acids that has 34% identity to human STC-1. The relatedness of STC-2 to STC-1 is greatest at the N-terminus [109]. In addition, an unusual feature of STC-2 is the presence of 15 histidine residues, four of which are present as a cluster at the C-terminus of the protein. Moore et al. (1999) utilized a nickel-chelating column to purify STC-2 [107], which suggest that these histidines may bind to transition metals [109]. Together, these findings suggest that STC-1 is more closely

related to fish STC-1 than to human STC-2 [107,109]. Nevertheless, mammalian STC-1 and STC-2 are secreted phosphoglycoproteins and the site of a glycosylation consensus sequence [Asn-X- Thr(Ser)] is conserved between the two proteins. They both contain PKC/PKA consensus sequences. Another conserved feature of STC proteins is the presence and location of cysteine residues, which cause mammalian STC proteins to form homodimers in their native state. Also, mammalian stanniocalcin genes have four exons and display conserved exon-intron boundaries implying that STC-1 and STC-2 may be derived from a common ancestral gene [71,110].

I.2.2.2. Tissue distribution of mammalian stanniocalcin-1

Mammalian STC-1 mRNA is expressed in various tissues. The highest level of expression is found in the kidney, ovary, prostate, and thyroid [98,103]. It was previously assumed that STC-1 protein does not circulate in the blood of mammals [111]; however, recent reports suggest that mammalian STC-1 is blood borne and likely attached to a soluble protein [110,112]. Interestingly, the distributions of STC-1 mRNA and protein do not always parallel. In the kidney for example, STC-1 protein was detected along the entire nephron, albeit the mRNA expression that was restricted to the cortical and medullary collecting ducts [113,114]. Recently, STC-1 binding protein (receptor) has been detected in cells of the kidney, liver, breast, and ovaries using stanniocalcin-alkaline phosphatase fusion protein, which can explain the wide distributions of STC-1 protein [115-118]. STC-1 binding sites were found mainly on mitochondria and to a lesser extent to the external cell membranes and nucleus. Analysis of membrane fractions also revealed that STC-1 was associated with the inner matrix of mitochondria [115]. Structural information on STC-1 receptor, its role in ligand sequestration, or its possible involvement in subsequent hormone action have not yet been described. Nevertheless, these findings suggest that STC-1 functions in a paracrine/intracrine manner [69].

Like STC-1, mammalian STC-2 is ubiquitously expressed. The primary sites of STC-2 expression are the pancreas, spleen, kidney and skeletal muscle [105,106]. Its localization in pancreatic alpha cells suggests involvement of STC-2 in glucose and

energy metabolism [107]. Consistent with this, deletion of STC-2 produces overweight mice [119]. Abnormalities in the expression of STC-2 have also been associated with various malignancies [109]. There is no available information on the serum level of STC-2 in mammals and it is believed that STC-2 may function as a paracrine/autocrine factor as well.

I.2.2.3. Regulation of stanniocalcin-1 expression

To better understand the possible roles for STC-1 in mammals, regulation of its mRNA expression was examine by several investigators. Chang et al. (1995) found that the steady-state STC-1 mRNA level in immortalized human fibroblasts was elevated almost 10-fold by a 2.5-fold increase in the calcium concentration of the culture medium [103]; therefore, mammalian STC-1 mRNA levels are affected by extracellular calcium concentration. The active metabolite of vitamin D_3 was also shown to increase STC-1 mRNA levels in rat kidneys more than 3-fold, which could be due to vitamin D_3-induced hypercalcemia. Interestingly, regulation of STC-1 expression was tissue-specific; vitamin D_3 metabolite didn't increase the STC-1 mRNA levels in the ovaries [120]. Sheikh-Hamad et al. (2000) also observed 8-fold increase in STC-1 mRNA caused by growth in hypertonic medium of canine renal cell line. This induction of STC-1 mRNA, however, was dependent upon an extracellular calcium concentration greater than 0.1 mM, confirming a role for extracellular calcium in STC-1 regulation [121].

Likewise, STC-1 mRNA was significantly increased during endothelial differentiation of human umbilical vein cells observed by Kahn et al. (2000) [122] and during capillary morphogenesis in 3-dimensional collagen matrices [123]. STC-1 was later identified as a downstream target of VEGF/Wnt2 signaling pathway [122,124,125] indicating STC-1 involvement in angiogenesis. Utilizing differential display analysis of mRNA from human umbilical vein endothelial cells treated with lysophosphatidylcholine, a component of oxidized lipoproteins with proatherogenic properties, Sato et al. (1998) observed transitory expression of STC-1 mRNA [126]. Expression of STC-1 was also found to be induced in human glioblastoma cells and in the brain and heart of mice in response to hypoxia [127-129]. A study of temporal gene

expression in serum-stimulated human fibroblasts, often used to investigate wound repair, demonstrated that STC-1 mRNA was upregulated two hours after stimulation [130]. The expression of STC-1 has further been associated with tumor suppression. BRCA1 is a tumor-suppressor gene, which its mutations can lead to breast and ovarian cancer. In an in vitro study designed to identify transcriptional targets of BRCA1, STC-1 was shown to be induced by 2-4 fold increases in the expression of BRCA1 [131]. Together these results indicate that expression of mammalian STC-1 is controlled in a tissue-specific manner by a variety of stimuli and suggest STC-1 may play distinct roles in angiogenesis, in wound repair, in the response to hypoxia, and in the pathogenesis of carcinogenesis and atherosclerosis.

Studies on human tumor samples revealed that STC-1 was differentially expressed in a number of cancers compared with the relevant normal tissues; some examples include breast carcinomas, ovarian cancers, colorectal cancers, hepatocellular carcinoma, and non-small cell lung cancers [70,109]. Since, STC-1 mRNA has been considered to be a molecular marker for various types and stages of cancers. Furthermore, some clinical studies on different cancer types have correlated the high expression levels of STC-1 to poor prognostic outcome. For example, the survival rate of leukemia patients with high STC-1 mRNA levels in their peripheral blood was lower [132]. However, a larger sample size with identified developmental stage is necessary to support this diagnostic relationship.

I.2.2.4. Stanniocalcin-1 function in mammals

As a result of STC-1 being highly expressed in ovaries and due to the fact it is detectable in serum during pregnancy and lactation, its roles in development were studied by generating two transgenic STC-1-overexpressing mice. Circulating STC-1 protein was detectable in both transgenic mouse lines [133,134]. The muscle-specific STC-1 transgenic mice displayed the dwarf phenotype. These mice had increased cartilage matrix and decreased bone length with smaller muscles. There were abnormalities in skulls and long bones of the transgenic mice proposing that STC-1 has a role in both intramembranous and endochondral bone formation. Blood pressure and

serum phosphate levels were normal, but serum calcium levels were elevated; the latter finding was attributed to stimulated osteoclast activity. Notably, transgenic mice were hyperphagic compared with wild-type littermates and consumed more oxygen. Muscle-specific STC-1 transgenic mice also had leaner fat pads and faster clearance of glucose. These mice were noted to have mitochondrial swelling [133]that can arise from increased respiration and/or enhanced mitochondrial ion transport. In the second STC-1 transgenic mouse line(s), strong preferential expression of the transgene was detected mostly in the liver, heart, brain, endothelial cells, and macrophages [134,135]. Overexpression of STC-1 resulted in permanent and severe dwarfism. In addition, the reproductive ability of female transgenic mice was compromised. Serum calcium levels were normal, while serum phosphate levels were slightly higher. Overall, these observations suggested that STC-1 is involved in different stages of development.

Subsequently, the STC-1 knockout mouse line was generated to identify the normal function of this protein. However, no anatomical or histological abnormalities were detected in any tissues [136]. Because physiological parameters and animal phenotypes are regulated by complex signaling crosstalk and the function of many gene products, the observed changes in the knockout and transgenic mice may not accurately reflect the functions of STC-1 gene [70].

Due to the similarity of STC-1 to its fish counterpart, it seemed likely that mammalian STC-1 was involved in regulation of calcium and phosphate concentration at a tissue or cellular level. In addition, calcium concentration was shown already to influence expression of STC-1. Interestingly, recombinant human STC-1 was shown to inhibit branchial calcium transport in fish [98] and intestinal calcium absorption in swine and rat [137]. Also, recombinant STC-1 stimulated the renal and intestinal reabsorption of phosphate [137,138]. Analysis of phosphate uptake in vesicles isolated from rat renal tubular brush-border membrane has suggested that the sodium-phosphate transporter may be a target of STC-1 activity [138]. Furthermore, STC-1 was found to play a role in bone mineralization via a functional relationship with the type III sodium-phosphate transporter in osteoblasts [139]. Sheikh-Hamad et al. (2003) reported a regulatory role of

STC-1 on intracellular calcium. STC-1 was shown to inhibit transmembrane calcium currents via L-type channels in rat cardiomyocytes [140]. Collectively, these studies imply that mammalian STC-1 can locally regulate calcium and phosphate levels [70].

The local action of mammalian STC-1 was further studied on neural cells. Zhang et al. (2000) observed that treatment of Paju cells with recombinant STC-1 in vitro stimulated their uptake of phosphate. Phosphate is known to buffer intracellular free calcium and protect neural cells from apoptosis, since elevation of intracellular free calcium, during brain injuries such as ischemia, is neurotoxic and can cause apoptosis in neural cells. In addition, the cytoprotective role of this protein was studied in STC-1-overexpressing Paju cells in vitro. The cell viability was significantly increased in these cells compared to control cells in response to hypoxia stress as well as toxic levels of intracellular free calcium. Interestingly, transient upregulation of STC-1 was seen in human and rat brain neurons at the edges of infarcted areas suggesting therapeutic potential of STC-1 in neural cells challenged by ischemia and calcium-mediated injuries [141].

Observations from transgenic mice suggested that STC-1 might regulate metabolism of energy via its localization at the inner membrane of mitochondria and its concentration-dependent stimulatory effect on electron transfer [115,133]. In order to better address the effects of STC-1 on mitochondria, Ellard and colleagues (2007) isolated intact mitochondria from rat muscle and liver and exposed them to increasing concentrations of recombinant human STC-1. They observed that respiration rate was significantly increased in isolated mitochondria; while ATP synthesis was reduced thereby suggesting STC-1 was involved in uncoupling of oxidative phosphorylation [142]. Subsequently, Wang et al. (2009) reported that recombinant human STC-1 upregulated the expression of mitochondrial uncoupling protein-2 (UCP2) in cultured macrophages. This finding was concurrent with diminishing mitochondrial membrane potential and superoxide generation in both untreated and lipopolysaccharide (LPS)-stimulated macrophages. Despite of the reduction in cellular ATP level, STC-1 appeared to enhance cell viability [143]. UCPs are mitochondrial anion carriers that localize at the

inner membrane of mitochondria and facilitate proton leak from the mitochondrial inter-membrane space to the matrix, which diminishes the proton gradient and uncouples oxidative phosphorylation. UCPs are activated by reactive oxygen species (ROS) and their metabolites during oxidative stress. Excessive ROS and their products could damage cells and induce apoptosis. UCPs create a negative feedback loop to reduce production of ROS in mitochondria and protect cells from oxidative damage. UCP2 is widely expressed in tissues, including the spleen, thymus, macrophages, hypothalamus, pancreatic β-cells, and stomach. UCP3 is another members of the mitochondrial anion carrier family, which induces proton leak in skeletal muscle, brown adipose tissue, and to a lesser extent in the heart [110,144]. Notably, STC-1 was shown later to upregulate expression of UCP3 and reduce superoxide generation in angiotensin II-treated cardiomyocytes in vitro. Recombinant STC-1 failed to suppress superoxide generation in isolated cardiomyocytes from $UCP3^{-/-}$ mice, suggesting that the effects of STC-1 on ROS generation in cardiomyocytes are UCP3-dependent [145]. As mentioned before, MSCs were shown to enhance cell survival through upregulation and secretion of STC-1 [67]. Administration of recombinant STC-1 produced similar effect on hypoxic lung cancer cells and was reported to be partly UCP2 dependent [146]. These observations revealed that STC-1 acts as a key regulator of ROS generation and protects cells from oxidative stress in a tissue-specific manner [70,110].

Kanellis et al. (2004) reported that recombinant STC-1 diminished the intracellular calcium signals in macrophages and attenuated the responses of cultured murine macrophages and human monocytes to chemokines. In addition, they observed that STC-1 is strongly induced in the kidney following obstructive injury and in macrophages, suggesting STC-1 may serve as endogenous anti-inflammatory agent and attenuate the infiltration of inflammatory cells to the site of tissue injury [147]. Later, recombinant STC-1 was shown to attenuate the migration of cultured macrophages and T cells across a quiescent or cytokine-treated endothelial cells in vitro [148]. As mentioned, STC-1 decreased ROS generation in LPS-stimulated macrophages [143]. Production of mitochondrial ROS is known to potentiate NF-κB activity in immune

cells; therefore, emphasizing an anti-inflammatory role for STC-1 [110,149]. Anti-inflammatory actions of STC-1 were further studied in the mouse model of anti-glomerular basement membrane glomerulonephritis. After anti-glomerular basement membrane treatment, STC-1 transgenic mice exhibited diminished infiltration of inflammatory macrophages in the glomeruli, decreased interstitial fibrosis, reduced expression of CXC motif ligand 2 (CXCL2) and TGF-β in the kidney, and preserved kidney function when compared with wild-type mice [135]. Anti-inflammatory and therapeutic potentials of STC-1 were confirmed in various disease models such as ischemia/reperfusion kidney injuries, retinal degeneration, and sepsis, in which STC-1 reduced generation of ROS and infiltration of immune cells to the injured tissues [150-152]. Whether these effects are related to antioxidant property of STC-1, regulation of intracellular calcium concentration, or other mechanisms remains to be determined.

Collectively, these observations revealed that through the evolutionary process from fish to mammals, STC-1 has maintained functional relevance to calcium/phosphate homeostasis, while acquiring additional paracrine/intracrine roles and functions in the various organs in which it is expressed. The mechanisms for pleiotropic actions of the protein have not been entirely defined; however, most studies emphasized the therapeutic applications of STC-1 in numerous diseases.

I.3. Monocytes and Macrophages in Tissue Homeostasis and Disease Pathogenesis

Monocytes and macrophages are heterogeneous mononuclear phagocytes with crucial but distinct roles in tissue homeostasis and immunity. Monocytes play a significant role during inflammation and pathogen challenge, while tissue-resident macrophages have important functions in development, tissue homeostasis and the resolution of inflammation. Moreover, monocytes and macrophages contribute to pathogenesis of a broad spectrum of diseases making these cells attractive therapeutic targets. Therefore, novel clinical strategies are essential that aim to manipulate these cells. For example, depleting monocytes/macrophages when their effects are detrimental or enhancing their mobilization when their activities are advantageous [153].

I.3.1. Monocyte and macrophage development

Monocytes and macrophages as well as dendritic cells (DCs) are part of the mononuclear phagocyte system (MPS) originally described as a main phagocytic population of bone marrow-derived myeloid cells that could circulate in the blood and populate tissues in the steady state and during inflammation [154-156]. Monocytes are a conserved population of leukocytes. Mature cells have heterogeneous morphology, which are defined by their location, phenotype, characteristic gene, and microRNA (miRNA) expression signatures. These cells constitute ~5–10% of peripheral blood leukocytes in mice and humans. In addition, considerable numbers of monocytes are stored in the spleen and lungs that can be mobilized on demand [157]. Monocytes arise from their precursor cells in primary lymphoid organs, including the fetal liver and bone marrow, during both embryonic and adult hematopoiesis. In mice, monocytes are also produced from precursors in the spleen during inflammation [158]. Monocyte development and survival in mice have been suggested to be completely dependent on M-CSF, since mice suffering deficiency in this growth factor or its receptor CSF1R exhibit severe monocytopenia [153,156,159].

Macrophages are the most plastic cells of the hematopoietic system. These cells are found in all tissues. Tissue-resident macrophages are morphologically distinct from one another, have different transcriptional profiles, and diverse functional capabilities. Ebert and Florey (1939) first reported that monocytes emigrated from blood vessels and developed into macrophages in the tissues [155]. Several other investigators also observed that circulating monocytes differentiate into macrophages during inflammation. In addition, studying the fate of monocytes revealed that the cells have a short half-life of 20 hours in blood, which together led to the assumption that blood monocytes constitute the main precursor reservoirs for tissue-resident macrophages. However, the most recent data have demonstrated that monocytes do not significantly contribute to most tissue-resident macrophages in the steady state or during certain types of inflammation. Adult tissue-resident macrophages are found to originate prenatally from

the yolk sac- or fetal liver-derived precursors that seed the tissues before birth. These cells can maintain themselves in adults by self-renewal, including the macrophages in the central nervous system (CNS) called microglia. Nevertheless, monocytes can, and do, give rise to macrophages in certain settings as well as during inflammatory circumstances [153,156,160]; for instance, at the tissues with considerable exposure to microorganisms and their products such as intestine recruitment and differentiation of circulating monocytes have been observed to maintain macrophage pools. That perhaps is the result of low-grade chronic inflammation caused by the constant presence of commensal microorganisms [161]; therefore, resident macrophages are constituted from mixed lineage-committed precursors in healthy adult animals [160].

I.3.2. Monocyte and macrophage subsets in human and mouse

Monocytes are divided into subsets on the basis of expression of chemokine receptors and the presence of specific surface molecules. Human monocytes were initially identified by their expression of large amounts of CD14 (which is a co-receptor for LPS). Currently, there are two main human monocyte subpopulations: $CD14^{high}$ ($CD14^{hi}$) monocytes and $CD14^{low}$ monocytes. Differential expression of CD16 (also known as Fc receptor FcγRIII) allowed the first population of monocytes to be divided into two subsets of $CD14^{hi}CD16^{-}$ and $CD14^{hi}CD16^{+}$ monocytes. $CD14^{hi}CD16^{-}$ monocytes, referred to as classical monocytes, are the most abundant subset of circulating monocytes in humans. $CD14^{low}$ monocytes express CD16 as well, which are referred to as non-classical monocytes. Distinct expression of chemokine-receptors has been recognized between all these subsets [153,162,163]: for example, $CD14^{hi}CD16^{+}$ monocytes expressed CC-chemokine receptor 5 (CCR5), whereas $CD14^{hi}CD16^{-}$ monocytes expressed CCR2.

Murine monocyte subsets were first identified by differential expression of CCR2. CCR2 is also expressed in HSCs and is a subset of natural killer (NK) cells mediating migration of the leukocytes (monocytes) from bone marrow to the blood stream. $CCR2^{+}$ subset shows higher migratory and infiltration capacity than $CCR2^{-}$

subset of monocytes and was initially considered to be the inflammatory monocyte. Currently, mouse monocyte subsets are characterized by differential expression of an inflammatory monocyte marker Ly6C (Gr1). The cells are grouped as $CD11b^{+}Ly6C^{hi}$ and $CD11b^{+}Ly6C^{low}$. Moreover, mouse $CD11b^{+}Ly6C^{hi}$ monocytes, which are similar to human $CD14^{hi}$ monocytes, express CCR2 on their surface and have been shown to represent approximately 2–5% of circulating white blood cells in an uninfected mouse. Whereas, $CD11b^{+}Ly6C^{low}$ mouse monocytes express low levels of CCR2 and are considered being equivalent to human $CD14^{low}CD16^{+}$. The latest subset of mouse and human monocytes express high levels of CX_3-chemokine receptor 1 (CX_3CR1) that is important in leukocyte adhesion to the endothelial cells [153,163,164].

Macrophages are categorized into subpopulations based on their anatomical location and functional phenotypes. Specialized tissue-resident macrophages include alveolar macrophages (lung), Langerhans cells (skin), osteoclasts (bone), and Kupffer cells (liver) [162,165]. Macrophages isolated from the lamina propria have a unique phenotype, which is characterized by high phagocytic and bactericidal activity but weak production of pro-inflammatory cytokines. Interestingly, this phenotype can be induced in peripheral blood-derived macrophages by products of intestinal stromal cells indicating the influence of microenvironment on macrophage polarization and function [161,162]. In addition to macrophage heterogeneity in different organs, different subpopulations of macrophages have been observed in a single organ, such as spleen, skin, and CNS [162,165,166].

There is a great overlap in surface marker expression between the different macrophage subsets; thus, a useful characterization approach has been based on the profile of gene expression in response to cytokine or microbial stimulation. Several macrophage subsets with distinct functions have been described, including classically activated macrophages (M1) and alternatively activated macrophages (M2) consist of regulatory macrophages and wound-healing macrophages as well as tumor-associated macrophages (TAMs). Although there are obvious differences among the M2, regulatory macrophages, and TAMs, they all exhibit immune suppressive activity. Numerous

studies have documented macrophages switching from one functional phenotype to another in response to diverse stimuli indicating that macrophages represent a spectrum of activated phenotypes rather than discrete stable subpopulations [165,167].

I.3.3. Monocyte and macrophage function in tissue homeostasis and disease

I.3.3.1. Monocyte/macrophage tissue homeostasis in the steady state

In regards to the fate of circulating monocytes under normal circumstances, there is some evidence to suggest that $Ly6C^{hi}$ monocytes differentiate into $Ly6C^{low}$ cells in the circulation. Mouse $Ly6C^{low}$ monocytes, and their human $CD14^{low}CD16^{+}$ equivalent, have been demonstrated to patrol the integrity of the luminal side of endothelium of small vessels and migrate to non-inflamed organs [163,164,168]. Moreover, $Ly6C^{low}$ cells have recently been shown to coordinate intraluminal stress responses. They induce the recruitment of neutrophils, which trigger focal necrosis of endothelial cells and, then, $Ly6C^{low}$ monocytes clear the cellular debris [153,168].

The function of $Ly6C^{hi}$ monocytes in the steady state remains poorly defined. Highlighting their potential physiological importance, however, it was recently reported that $Ly6C^{hi}$ monocytes are mobilized from the bone marrow in diurnal rhythmic waves, suggesting a role for these monocytes in supporting the innate immune system against predicted environmental challenges. Since chronic inflammatory diseases, such as myocardial infarction, asthma, and rheumatoid arthritis, exhibit diurnal clustering in humans, circadian release of inflammatory $Ly6C^{hi}$ monocytes might also contribute to the pathogenesis of those diseases [153,169].

Experimental depletion of tissue-resident macrophages has been shown that, under certain conditions, circulating monocytes can reconstitute the populations of Langerhans cells, microglial cells, and CX_3CR1^{+} mononuclear phagocytes in the intestinal lamina propria. Monocyte-to-macrophage differentiation following the experimental depletion of resident macrophages does not necessarily reflect the natural processes that occur during the development tissues homeostasis as mentioned before [153,162]. Nevertheless, the ability of monocytes to reconstitute distinct tissue

macrophage and DC populations suggests an important physiological role for monocytes following tissue trauma or infection.

Metchnikoff initially described macrophages in the late 19th century as phagocytic cells. Currently, macrophages are known for their vital roles in tissue development and homeostasis in addition to their involvement in immune responses [164,165]. Phagocytosis, particularly of apoptotic cells, is a critical function for macrophages in the remodeling of tissues during development, for example the resolution of the inter-digit areas during limb formation [159]. The importance of macrophages in development has been studied in *Csf1*$^{op/op}$ mice, which lack many macrophage populations, and revealed a cluster of developmental abnormalities. Most notable among these was the development of osteopetrosis (stone bone). In these mice bone formation was unchanged but the tissue remodeling and expression of growth factors were deficient, which is caused by the loss of bone-reabsorbing osteoclasts [159,170]. Macrophages also have been shown to regulate angiogenesis during development through a number of mechanisms [160,171].

Macrophages are found in mammalian metabolic organs, including liver, pancreas and adipose tissue, which function together with parenchymal cells to maintain metabolic homeostasis. By regulating this interaction, mammals are able to make marked adaptations to changes in their environment and in nutrient availability such as during infection. Tissue-resident macrophages are also involved in maintaining tissue homeostasis by removing dead or dying cells and toxic materials. For example, alveolar macrophages facilitate the removal of allergens from the lung, while Kupffer cells participate in the clearance of pathogens and toxins from the circulation [160]. Macrophages are also involved in recycling erythrocytes and neutrophils in the spleen and liver to maintain the steady state of hematopoiesis [160,172]. Additionally, macrophages ingest the extruded nuclei of maturing erythroblasts, which is crucial for host survival [173]. All together, these processes occur independently of immune-cell signaling, and the removal of apoptotic or dying cells seems to result in little or no production of immune responses by unstimulated macrophages.

I.3.3.2. Monocyte/macrophage responses to danger signals

Tissue-resident macrophages and other mononuclear phagocytes are part of first line of the host defense. They are located throughout the body and constantly survey their surroundings for signs of tissue damage or invading organisms. Sensing danger signals is crucial for activation of macrophages. Activated macrophages then largely polarized to the inflammatory M1 phenotype to phagocytize pathogens and terminally injured cells. They also secrete pro-inflammatory mediators to recruit monocytes and neutrophils from their reservoir such as peripheral blood, bone marrow, and spleen to migrate to the site of injury or infection. Moreover, these mediators stimulate bone marrow to generate large pools of monocytes and neutrophils from HSCs beyond the normal requirements of a healthy organism. The production of monocytes and neutrophils is dependent on cytokines such as G-CSF and chemokines including MCP-1/CCL2 and CCL5. Then, a mixture of mature and immature monocytic and granulocytic cells exits the bone marrow. Monocytes enter the damaged organs and differentiate into a spectrum of mononuclear phagocytes in response to microenvironmental signals, and contribute to the establishment of local inflammation, host defense, and tissue and wound repair. Antigen-presenting mononuclear phagocytes also migrate to the nearest lymph nodes and activate lymphocytes to initiate adaptive immunity [61,165,167].

Mouse Ly6C^{hi} monocytes, and their human CD14^{hi} equivalent, express CCR2 and can be rapidly mobilized to the injured tissues. During early stages of immunity/inflammation, these monocytes are more likely to mature to inflammatory mononuclear phagocytes. They have a high phagocytic capability to remove infectious agents, apoptotic neutrophils, and cell debris. In addition, these cells secrete pro-inflammatory mediators such as TNFα, nitric oxide (in murine) and IL-1, which participate in the activation of various antimicrobial mechanisms, including oxidative processes. ROS and reactive nitrogen intermediates produced by inflammatory monocytes and monocyte-derived cells are highly toxic for microorganisms; however, they are also highly damaging to neighboring tissues and lead to aberrant inflammation.

Therefore, pro-inflammatory and antimicrobial responses must be controlled to prevent extensive collateral tissue damage to the host [164,165,167].

Recruited Ly6C^{low} monocytes mainly differentiate into M2 phenotype, which exhibit potent anti-inflammatory activity. Some of the inflammatory monocytes/macrophages might also convert into anti-inflammatory M2 phenotype upon exposure to microenvironment. M2 macrophages phagocytose dead cells, debris, and other factors that would promote tissue-damaging responses. In addition, expression of immunoregulatory factors such as IL-10 by these cells have been shown to decrease the magnitude and duration of inflammatory responses and promote wound healing. M2 macrophages produce growth factors, including TGF-β1 and platelet-derived growth factor (PDGF), to stimulate epithelial cells and fibroblasts and regulate wound healing. They also secrete matrix metalloproteinases (MMPs) and tissue inhibitors of MMPs (TIMPs) that control extracellular matrix turnover. In order to inhibit excessive fibrosis, M2 macrophages produce factors that induce apoptosis in activated fibroblasts [165,167]; therefore, macrophages and their factors are integrated into all stages of the fibrotic process.

Recently, tissue-resident macrophages were demonstrated to undergo massive proliferation in T_H2-mediated inflammation. IL-4 produced by T_H2 cells was shown to be the key factor stimulating macrophage proliferation. Although, the signaling mechanism regulated by IL-4 to push macrophages into the cell cycle remains unclear, these observations propose that proliferation at site is an alternative mechanism of inflammation, which allows macrophages to accumulate in sufficient numbers and perform critical functions such as parasite elimination and wound repair in the absence of immune cell recruitment [174].

Migration, differentiation, and function of monocytes and macrophages are crucial for host defense and tissue homeostasis; however, the uncontrolled immune/inflammatory responses also have the potential to do harm. For example, excessive activation of inflammatory monocytes/macrophages can cause damage to host tissues, predispose surrounding tissue to neoplastic transformation and influence glucose

metabolism by promoting insulin resistance. On the other hand, disregulation of M2 macrophages can trigger unwanted fibrosis, which lead to loss of function and exacerbate allergic responses. In addition, parasitic, bacterial, and viral pathogens can induce the development of anti-inflammatory M2 phenotype to enhance their survival in the host. Therefore, maintaining a proper balance between the functions of these different phenotypes in vital for the survival of the host [153,165,167]. Better understanding of the mechanisms involved in regulation of monocyte-to-macrophage differentiation, their polarization and functions would improve therapeutic strategies for pathological conditions such as wound healing, autoimmunity, and cancer.

I.3.3.3. Sensing danger signals via Toll-like receptors and their co-receptor CD14

The first step for innate immunity and inflammatory responses is to sense the danger signals from injured tissues or invading organisms. Tissue-resident macrophages are among the first group of cells to detect danger signals through a group of germline-encoded receptor proteins. These receptors recognize specific patterns that are shared by groups of pathogens, but not the host, and are termed pattern recognition receptors (PRRs). PRRs are expressed in immune and non-immune cells and detect pathogen-associated molecular patterns (PAMPs) such as LPS found on the cell surface of Gram-negative bacteria, or double-stranded RNA present in viruses. It is now evident that PRRs also recognize non-infectious material that can cause tissue damage and endogenous molecules that are released during cellular injury. These endogenous molecules have been named damage-associated molecular patterns (DAMPs) and have similar functions as PAMPs in terms of their ability to activate pro-inflammatory pathways [61,165,175]. Endogenous DAMPs are normally sequestered intracellularly and, therefore, hidden from recognition by immune system. Necrosis, resulting from trauma or stress, generates cellular debris that are loaded with these DAMPs, including heat-shock proteins, nuclear proteins (e.g. high-mobility group box 1 protein (HMGB1)), histones, DNA and other nucleotides, and components of the extracellular matrix [167].

Toll-like receptors (TLRs) are the best characterized class of PRRs and are important regulators of innate immune responses. These receptors are type I transmembrane glycoproteins, which their cytosolic domain involved in the recruitment of different combinations of signaling adaptor molecules such as myeloid differentiation primary-response protein 88 (MyD88). Through the adaptor proteins, TLRs can activate downstream kinases that stimulate transcription factors such as NF-κB and activator protein 1 (AP-1), thus, inducing the production of pro-inflammatory cytokines and type I interferons (IFNs). Markedly, the activation of NF-κB pathways has been shown to upregulate the expression of anti-inflammatory molecules (e.g. IL-10) [61,176]. Thirteen mammalian TLRs have been identified (TLR1-10 in humans, TLR1-9 and TLR11-13 in mice), which are associated with the recognition of one or more PAMPs and DAMPs [175,176].

Different types of membrane-bound or soluble co-receptor proteins assist TLRs to catch and concentrate scattered ligands and present them to TLRs. In addition, they help to define the specificity or increase the affinity of homo- or hetero-TLR dimers for a ligand. Co-receptors also deliver TLRs and their ligands to an optimal subcellular compartment to activate signals. Interestingly, TLR-co-receptors have been shown to transduce TLR-independent signals, which lead to distinct inflammatory responses [176,177]. Glycoprotein CD14 is a co-receptor well known for its role in recognition of endotoxin ligand, LPS. This protein is either anchored to the outer leaflet of the plasma membrane or released in the blood as a soluble mediator. CD14 is predominantly expressed by myeloid lineage cells such as monocytes and macrophages; however, several studies have shown that it can also be present in non-immune cells, including epithelia, smooth muscle cells, and fibroblasts. The co-receptor presents LPS to the TLR4 complex and enhances the following TLR4-mediated responses to the endotoxin [176,177]. CD14 knockout mice were shown to be less sensitive to LPS and more resistant to endotoxic shock, indicating the important role for CD14 [178]. Interestingly, this co-receptor is capable of recognizing several types of non-endotoxin ligands and, thus, contributing to the inflammatory responses mediated by different TLRs, including

TLR2 and TLR3. Lipopeptides, peptidoglycan, HMGB1 as well as dsRNA are examples of the identified ligands for different binding sites of CD14 [176,177,179].

Overall, TLRs and their co-receptors have been recognized as key mediators initiating inflammatory responses by immune and non-immune cells and have been linked to the pathogenesis of many conditions, including autoimmune diseases, cancers, and cardiovascular diseases [175,176]. Therefore, understanding the detailed mechanisms regulating the expression and function of TLRs and their co-receptor could facilitate developing therapeutic strategies to modulate inflammatory responses by activated immune cells such as monocytes/macrophages.

CHAPTER II
PROJECT HYPOTHESES AND SPECIFIC AIMS

II.1. Enhanced Therapeutic Potential of Preactivated Mesenchymal Stromal Cells and Their Secretory Factor Stanniocalcin-1 in Models for Acute Injuries and Inflammation

MSCs are a heterogeneous subset of stromal stem cells. These cells are relatively easy to isolated from bone marrow of human donors and patients. A large number of the cells can also be isolate from adipose and synovial tissues as well as umbilical cord blood. In addition, MSCs can expand rapidly for 30 or more population doublings in culture are highly clonogenic, but not tumorigenic. They can differentiate into cells of the mesodermal lineage, such as adipocytes, osteoblasts and chondrocytes. Together, these attractive features of MSCs offer broad implications in clinic; therefore, therapeutic potential of the cells were tested in numerous animal models and in clinical trials. Initially, it was assumed that MSCs repaired tissues by engrafting and differentiating to replace injured cells. Instead, the cells were shown to enhance tissue repair and limit tissue destruction by paracrine secretions, cell-to-cell contacts, and transfer of exosomes or mitochondria [180-183].

The potential paracrine effects of MSCs have been suggested by the observations that the cells in culture secrete a large number of cytokines and growth factors; however, these cells are activated by danger signals from injured cells to express high levels of additional genes [1,54,55]. Several studies have shown that stimulation of MSCs with different pro-inflammatory cytokines activated the cells to secrete variety of anti-inflammatory mediators [56]. One of the anti-inflammatory molecules secreted by MSCs is the TSG-6 molecule. Expression of this protein was shown to upregulate in i.v. infused MSCs in a mouse model of myocardial infarction. MSCs were aggregated in pulmonary microvasculature and activated to secrete TSG-6. During the activation of MSCs, however, a large number of the cells underwent apoptosis and necrosis. Administration of recombinant human TSG-6 protein produced was shown to reduce

inflammation and protect cardiac function after induction of myocardial injury, similar to the MSCs treatment [51]. TSG-6 has also been reported to play a major role in anti-inflammatory and immune modulatory effects of MSCs in several animal models, such as zymosan-induced peritonitis, cornea injury, and lung injury [64,65,184]. Interestingly, MSCs do not produce TSG-6 in standard 2 dimensional (2D) cultures. Incubation of MSCs with recombinant TNF-α in the cultures activates the cells over time to secrete TSG-6 [51,65]. Another stress responsive molecule secreted by MSCs is STC-1. Expression of STC-1 was upregulated in MSCs by signals from dying cells and is involved in anti-apoptosis properties of MSCs [67]. Also, STC-1 was secreted in response to caspase activation and inflammatory cytokines in vitro [185,186]. Anti-inflammatory and anti-apoptotic properties of STC-1 have been reported recently in a number of disease models, including anti-glomerular basement membrane glomerulonephritis, ischemia/reperfusion kidney injuries, retinal degeneration, and sepsis [135,150-152]. In addition to pretreatment of MSCs with exogenous factors, modifications of the culture conditions, such as hypoxia and serum deprivation, were demonstrated to promote their self-activation and expression of wide ranges of factors for cell protection [187]. These observations suggest that stimulation of MSCs in culture before administration might enhance their potential for therapeutic applications by eliminating the lag period for upregulation of beneficial factors in the host. This approach would be especially important in modulation of acute inflammatory phase.

Recently, there has been increasing interest in culturing cells in non-adherent 3D conditions to overcome many limitations of using MSCs and other stem cells for clinical applications. The traditional 2D culture and differentiation methods widely used in current MSCs research yield single cells with limited cell-to-cell contact and result in low differentiation efficacy for the cells [188]. One of the advantages of culturing cells in 3D is that it more closely reproduces their natural environment. In 3D cell cultures, cells can form aggregates, in which nearly all of cell surface area being exposed to other cells or extracellular matrix. These cells extensively interact with each other and with their environment via soluble and membrane bound factors. In addition, extracellular

matrix is made of complexes of proteins, which are important mediators of numerous biological processes. Therefore, growing cells in 3D cultures generates important differences in cellular characteristics and behavior such as differentiation, proliferation, viability, drug metabolism, gene expression, morphology, and responses to stimuli [189].

Different 3D culture methods have been used to generate MSC spheroids in vitro, that include culture in spinner flask or gyratory rotation system, microcarrier beads, microchannel culture system, and hanging drops [189]. A number of investigators have demonstrated that assembly into spheroids enhanced many properties of MSCs. For instance, culturing MSCs in low adherent plates or on micropatterned glass substrates could significantly improve their differentiation potency [188,190,191]. In addition, medium conditioned by MSCs cultured in hanging drops was shown to stimulate cell survival, proliferation, and in vitro migration and invasion of endothelial cells to a much higher extent than CM of 2D-cultured MSCs [192]. 3D cultures also altered expression of cell surface molecules responsible for the regulation of MSC homing [193]. Notably, MSCs aggregates were shown to attach to the underlying tissue and improve cardiac function more efficiently than dissociated cells, when injected into the peri-infarcted zone following myocardial infarction in rats [194]. Overall, 3D culture systems were indicated as a practical method to preactivate MSCs in culture in order to enhance their therapeutic potential in clinic.

In order to benefit from MSCs in medicine and extend their therapeutic applications, alternative approaches have been also considered by investigators. Several soluble factors released by activated MSCs have been able to reproduce many of the anti-inflammatory responses in the cells suggesting these factors could replace MSC therapy. Protein therapy has many attractions; especially for the patients whom cell administration is not an option. Also, therapeutic application of recombinant proteins is preferred in acute injuries such as myocardial infarction or stroke since immediate care is crucial for short- and long-term prognosis after the injury. Several factors secreted by MSCs are not promising candidates for medical therapy. Some of them were shown to have short half-lives or limited applications and some could generate adverse effects

when administered systemically [56]. However, there appears to be adequate reasons for testing certain proteins such as STC-1 for therapeutic uses. Administration of STC-1 was reported to diminish intracellular calcium signal in macrophages and reduce their responses to chemokines. Also, it could suppress ROS production in LPS-stimulated macrophages. Moreover, anti-inflammatory and anti-apoptotic effects of STC-1 have been demonstrated in several models [150-152]. Thus, STC-1 is considered as a potential alternative in several pathological conditions such as acute ischemia-induced injuries.

Myocardial infarction is a leading cause of morbidity and mortality worldwide. Despite advances in therapy to reduce mortality in acute phase, the incidence of chronic heart failure in patients surviving form myocardial damage has increased [195,196]. Following myocardial infarction, infarct area and the non-infarcted myocardium of the left ventricle undergo extreme structural alterations, referred to as ventricular remodeling. Excessive ventricular remodeling manifests clinically as increased chamber dilation and myocardial hypertrophy, which leads to impaired cardiac function and subsequently heart failure. The size of the necrotic area and the quality of cardiac repair are important factors in development of post-infarct heart failure [196,197]. Cardiac repair is supported by a well-orchestrated inflammatory response that serves to clear the wound from dead cells and debris, while activates reparative pathways necessary for scar formation. Timely repression and containment of inflammatory signals are essential to ensure optimal formation of a supportive scar in the infarcted area and to prevent development of adverse ventricular remodeling. For instance, excessive early inflammation may augment matrix degradation, which causes cardiac rupture. It can also activate apoptosis in cardiomyocytes of border zones and expand the scar size. In addition, ineffective containment of inflammatory responses may lead to extension of inflammation to the non-infarcted myocardium enhancing fibrosis and worsening diastolic function [195-197]. Therefore, strategies to regulate post-infarct inflammatory pathways will improve the prognosis of patients with myocardial infarction.

Myocardial tissue injury induces the release of endogenous danger signals, including inflammatory cytokines and chemokines, ROS, and intracellular DAMPs (e.g. HMGB1, heat shock proteins, membrane fractions). These signals trigger intense inflammatory responses by activating the innate immune system. Timely suppression and resolution of post-infarct inflammation requires the coordinated actions of several different cell types such as monocytes and macrophages. Several observations from experimental animals and patients have indicated that distinct subsets of monocytes are recruited at different stages of post myocardial infarction and can differentiate into a spectrum of macrophage populations. The first wave of monocytes facilitates the removal of dead cardiomyocytes and the later phase promotes the resolution of inflammation and tissue repair [163,165]. The detailed mechanisms that regulate activation, deactivation, and differentiation of monocytes/macrophages in myocardial injury are not defined yet; however, developing multifunctional strategies that regulate these processes could help improving the prognosis of patients with acute myocardial injuries.

In this work we proposed two hypotheses: “aggregation of MSCs in 3D cultures provides an effective procedure to pre-activate the cells, and thereby, enhance their therapeutic effects through reduction in the lag period for secretion of anti-inflammatory factors in vivo” and “STC-1, a pleotropic factor secreted by MSCs, modulates differentiation and function of monocytes/macrophages and protects heart from ischemic cardiac damage in part by suppressing inflammation after myocardial infarction.”

II.2. Specific Aims

To test these hypotheses, we performed experiments based on two aims.

II.2.1. To study the enhanced therapeutic potentials of spheroid MSCs

II.2.1.1. Establish the optimal conditions to improve anti-inflammatory properties of cultured MSCs in the hanging drop system

In order to identify a new approach for self-activation of MSCs in vitro, the hanging drop method was used to culture the cells in a 3D system. This method is simple, inexpensive, and does not require specific equipment. Spheroids produced in the hanging drop system are uniform in size and shape. It is also possible to control the culture conditions in the hanging drop system. Therefore, this approach could facilitate studying the unique properties of 3D-cultured MSCs. There is a wide range of factors that can be modified in the hanging drop system and can influence the characteristics and the functions of MSCs. Since the main goal of this study was to enhance production of anti-inflammatory factors by MSCs, the optimal conditions for hanging drop cultures that maximizes expression of TSG-6 were defined. Previous studies on the properties of MSCs in standard 2D culture system revealed that morphology of the cells alters in the confluent cultures and following several passages. In addition, certain environmental modifications could cause remarkable changes in the characteristics of MSCs [19,56]; therefore, some of the properties of MSCs dissociated from spheroids were tested, including survival rate as well as their colony formation and differentiation potentials. The findings of this study would help establish the optimal 3D culture conditions, which yield MSCs with enhanced anti-inflammatory potential. As a result, the therapeutic benefits of MSCs from donors with low rate of paracrine secretion in standard 2D culture, could be improved as well.

II.2.1.2. Demonstrate anti-inflammatory effects of activated spheroid MSCs in vitro and in vivo

Resident macrophages are stimulated at early stages of tissue injury to secrete a large number of pro-inflammatory cytokines and chemokines, activate immune system, destroy pathogens, and remove the death cells. The balance between pro- and anti-inflammatory actions of these cells is important in the outcome of tissue repair [160]. In the current work, the effects of spheroids and their derived MSCs were investigated on

LPS-stimulated macrophages in vitro. In addition, the enhanced anti-inflammatory potential of these cells was compared to the standard 2D cultured cells in a mouse model of zymosan-induced peritonitis. Zymosan binds to TLR2 on resident macrophages. This complex stimulates NF-κB signaling and secretion of TNF-α and other pro-inflammatory cytokines and chemokines. These observations would help determine future therapeutic applications of 3D cultured MSCs.

II.2.2. Study the therapeutic benefits of recombinant STC-1 protein

II.2.2.1. Examine anti-inflammatory effects of recombinant STC-1 on monocyte and macrophages in vitro

In response to danger signals, circulating monocytes activate and migrate to the site of injury, where they differentiate into a spectrum of macrophage subsets. Regulation of these processes is crucial for the outcomes of different conditions such as myocardial injuries and heart failure. Previously, STC-1 was reported to diminish intracellular calcium signals in monocytes/macrophages in response to different chemokines and reduce their migratory potential in vitro and in vivo [147]. In the current work, the effects of STC-1 on monocyte-to-macrophage differentiation by a number of stimuli were studied. In addition, the effects of STC-1 treatment on inflammatory responses of LPS-stimulated monocytes/macrophages were determined. These results can help better understand the mechanisms for anti-inflammatory actions of STC-1.

II.2.2.2. Demonstrate therapeutic potentials of recombinant STC-1 in preclinical model of myocardial infarction

Suppression of inflammatory pathways has been reported to improve outcome after myocardial infarction. Pro- and anti-inflammatory roles of monocytes/macrophages are crucial for the progression and resolution of myocardial infarction. To determine the effects of STC-1 on cardiac inflammation and function a mouse model of myocardial infarction was used. The recombinant protein was intravenously administered to the experimental animals and the amounts of inflammatory mediators in the cardiac tissue were measured. In addition, cardiac function and infarct size of STC-1 treated mice was

compare with controls. These observations, for the first time, revealed anti-inflammatory and cardiac protective roles of STC-1 in ischemia-induced myocardial injury.

CHAPTER III

MANUSCRIPT 1:

AGGREGATION OF HUMAN MESENCHYMAL STROMAL CELLS INTO 3D SPHEROIDS ENHANCES THEIR ANTI-INFLAMMATORY PROPERTIES

Previous reports suggested that culture as 3D aggregates or as spheroids can increase the therapeutic potential of the adult stem/progenitor cells referred to as mesenchymal stem cells or multipotent mesenchymal stromal cells (MSCs). Here we used a hanging drop protocol to prepare human MSCs as spheroids that maximally expressed TSG-6, the anti-inflammatory protein that was expressed at high levels by MSCs trapped in the lung after i.v. infusion and that largely explained the beneficial effects of MSCs in mice with myocardial infarcts. The properties of spheroid MSCs were found to depend critically on the culture conditions. Under optimal conditions for expression of TSG-6, the MSCs also expressed high levels of STC-1, a protein with both anti-inflammatory and anti-apoptotic properties. In addition, they expressed high levels of three anticancer proteins: IL-24, TNFα-related apoptosis inducing ligand, and CD82. The spheroid MSCs were more effective than MSCs from adherent monolayer cultures in suppressing inflammatory responses in a co-culture system with LPS-activated macrophages and in a mouse model for peritonitis. In addition, the spheroid MSCs were about one-fourth the volume of MSCs from adherent cultures. Apparently as a result, larger numbers of the cells trafficked through the lung after i.v. infusion and were recovered in spleen, liver, kidney, and heart. The data suggest that spheroid MSCs may be more effective than MSCs from adherent cultures in therapies for diseases characterized by sterile tissue injury and unresolved inflammation and for some cancers that are sensitive to anti-inflammatory agents. Bartosh et al., PNAS (2010) [198].

III.1. Introduction

There has been considerable interest in the therapeutic potentials of the cells from bone marrow referred to initially as colony forming units-fibroblastic, then as marrow stromal cells, subsequently as mesenchymal stem cells, and most recently as multipotent MSCs [10,16,21,181,199,200]. The cells are relatively easy to isolate from human donors or patients, expand rapidly for 30 or more population doublings in culture, and differentiate into several cellular phenotypes in vitro and in vivo. These and related properties prompted testing the therapeutic potential of the cells in animal models and in clinical trials for a large number of diseases (see www.clinicaltrials.gov). The initial assumption in exploring the therapeutic benefits of MSCs was that they might engraft and differentiate to replace injured cells. Engraftment and differentiation was observed in rapidly grown embryos, with extreme tissue injury, or after local administrations of large concentrations of the cells. Frequently, however, therapeutic benefits were observed without evidence of engraftment. Instead, the cells enhanced tissue repair or limited tissue destruction by paracrine secretions or cell-to-cell contacts that modulated inflammatory or immune reactions [2,10,180,181]. The potential paracrine effects of the cells were suggested by the observations that the cells in culture secrete a large number of cytokines [1,55]. Recent reports, however, have demonstrated that MSCs are activated by crosstalk with injured cells to express high levels of a large number of additional genes [48,51,54,55,67,201].

We previously observed [51] that i.v.-infused human MSCs (hMSCs) improved cardiac function and decreased scarring in a mouse model of myocardial infarction in part because the cells that were trapped in the lung as microemboli were activated to secrete the anti-inflammatory protein, TSG-6 [62]. The TSG-6 decreased the inflammatory reactions in the heart and thereby limited deterioration of the cardiac tissue. However, the hMSCs did not express TSG-6 until 12–24 h after they created microemboli in lungs and until about half the hMSCs had undergone destruction through apoptosis and necrosis. We also observed that standard cultures of hMSCs did not

express TSG-6 but were activated to express the protein if incubated for 24 h or longer with the inflammatory cytokine TNFα [51].

The observations suggested that appropriate manipulation of hMSCs in culture before in vivo administration might enhance their therapeutic benefits by eliminating the lag period for activation on the cells by signals from injured tissues.

Recently there has been a series of publications on aggregation of MSCs either as a procedure for enhancing chrondrogenic differentiation of the cells [188,190,191] or to increase their therapeutic potential [193,194,202,203]. Because aggregated hMSCs were detected in the pulmonary microemboli observed after i.v. infusion of the cells [51,204], we tested the hypothesis that aggregation of hMSCs in culture may provide an effective procedure to preactivate the cells to express TSG-6, and thereby, enhance their anti-inflammatory effects through a reduction in the lag period for expression of the gene in vivo.

III.2. Materials and Methods

III.2.1. hMSC cell culture

Frozen vials containing about 1 million passage 1 hMSCs from bone marrow were obtained from the Center for the Preparation and Distribution of Adult Stem Cells (formerly http://www.som.tulane.edu/gene_therapy/distribute.shtml; currently http://medicine.tamhsc.edu/irm/msc-distribution.html). hMSCs were isolated from 1–4 mL bone marrow aspirates of the iliac crest in normal adult donors. Nucleated cells, obtained by density gradient centrifugation (Ficoll-Paque; GE Healthcare), were resuspended in CCM: α-MEM (Gibco), 17% (v/v) FBS (Atlanta Biologicals), 100 units/mL penicillin (Gibco), 100 μg/mL streptomycin (Gibco), and 2 mM L-glutamine (Gibco), seeded in 175 cm^2 flasks (Nunc), and subsequently cultured at 37 °C in a humidified atmosphere with 5% (v/v) CO_2. After 24 h, non-adherent cells were discarded. Adherent cells were incubated 4–11 d until approximately 70% confluent, harvested with 0.25% (w/v) trypsin and 1 mM EDTA (Gibco) for 5 min at 37 °C, and

replated at 50 cells/ cm^2 in an intercommunicating system of culture flasks (Nunc). The cells were incubated for 7–12 d until approximately 70% confluent, harvested with trypsin/EDTA, and frozen as passage 1 cells in α-MEM containing 30% (v/v) FBS and 5% (v/v) DMSO (Sigma). A frozen vial of passage 1 hMSCs (donor 1, 7064 L; donor 2, 7068 L) was thawed, resuspended in CCM, and plated in a 152-cm^2 culture dish (Corning). After 24 h, adherent cells were harvested using trypsin/EDTA, plated at 100 cells/cm^2, and expanded for 7 d before freezing. In this study, passage 1 or 2 frozen hMSCs were recovered, seeded at 100 cells/cm^2 24 h later, and grown 7–8 d in CCM for various assays.

III.2.2. Spheroid generation and dissociation

To generate spheroids, hMSCs were plated as hanging drops on an inverted culture dish lid in 35 μL of CCM at 10,000–250,000 cells/drop. The lid was flipped and placed on a culture dish containing PBS (Gibco) to prevent evaporation. Hanging drop cultures were grown at 37 °C up to 4 d in a humidified atmosphere with 5% CO_2. Spheroid generation in hanging drops was captured using a Photometrics Coolsnap HQ2 camera mounted on a Nikon Eclipse Ti-E inverted microscope containing a temperature controlled environmental chamber. To collect spheroids, drops were harvested using a cell lifter, transferred to a 15 or 50 mL conical tube (Falcon), washed with PBS, and centrifuged at 453 × g for 5–10 min. To obtain spheroid derived cells, spheroids were incubated with trypsin/EDTA at 37 °C for 5–30 min (5 min for 10k, 10 min for 25k, 20 min for 100k, and 30 min for 250k spheroids), while pipetting every 2–3 min. When no cell aggregates were visible, spheroid derived cells were collected by centrifugation at 453 × g for 5–10 min to be used in described assays.

III.2.3. Histology

hMSC spheroids were collected with cell lifter (Corning), transferred into a 15-mL conical tube, washed twice with PBS, and fixed with 2% (v/v) paraformaldehyde (PFA, USB Corporation) in PBS for 15 min at room temperature. Fixed spheroids were

washed twice with PBS, centrifuged at 500 × g for 10 min, and incubated at 4 °C overnight in 500 μL of 30% (w/v) sucrose solution (Sigma) in 0.1 M phosphate buffer (Sigma). After incubation, 800 μL of 30% (v/v) OCT (Sakura Finetek) in sucrose solution was added gently and the suspension was transferred into a histology mold. The mold was frozen in isopentane (Sigma) chilled by liquid nitrogen and stored at −80 °C. Cryosections (6 μm) were prepared with a Microm HM560 cryostat. For H&E staining, slides were first incubated at room temperature for 10–15 min, fixed in 4% PFA for 15 min, and washed twice with deionized water. Rehydration was performed by incubating the samples in 100% ethanol (EMD Chemical) for 5 min, 95% ethanol for 2 min, 70% ethanol for 2 min, and deionized water twice for 5 min. The slides were stained with Mayer's Hematoxylin (Electron Microscopy Science) for 15 min, rinsed with deionized water, incubated with Scott's Tap Water Substitute (Ricca Chemical Company) for 2 min, rinsed with deionized water, washed with warm tap water for 20 min, rinsed with deionized water, immersed in 95% ethanol for 1 min, and stained with Eosin Y (Mallinckrodt Baker) for 1 min. Slides were then dehydrated by immersion in 95% ethanol for 1 min, 95% ethanol for 5 min, 100% ethanol for 5 min, and xylene (EMD Chemical) for 5 min. Samples were air-dried and overlaid with coverslips for examination. Mounting media (VECTA Mount; Vector Laboratories) was used to preserve staining. Images were acquired on a Nikon Eclipse 80i upright microscope and processed using NiS Elements AR 3.0 software (Nikon).

III.2.4. Real-time RT-PCR assays

Total RNA was isolated from monolayer and spheroid hMSCs using RNeasy Mini Kit (Qiagen) with DNase (RNase-Free DNase Set; Qiagen) digestion step. RNA was converted into cDNA with High-Capacity cDNA RT Kit (Applied Biosystems). Real-time RT-PCR was performed in triplicate for *18 s, TSG-6 (TNFAIP6), STC1, LIF, IL-24, TNFα-related apoptosis inducing ligand (TRAIL), CXC chemokine receptor 4 (CXCR4), and dickkopf 1 (DKK1)* using TaqMan Gene Expression Assays (Applied Biosystems). A total of 15–60 ng of cDNA was used for each 20-μL reaction. Thermal

cycling was performed with 7900HT System (Applied Biosystems) by incubating the reactions at 95 °C for 20 s followed by 40 cycles of 95 °C for 1 s and 60 °C for 20 s. Data were analyzed with Sequence Detection Software V2.3 (Applied Biosystems) and relative quantities (RQs) were calculated with comparative CT method using RQ Manager V1.2 (Applied Biosystems). If no amplification occurred, CT value of 35 was used in calculating the RQs.

III.2.5. Viability assays

Spheroid viability was measured by flow cytometry (FC500; Beckman Coulter) using Annexin V-FITC apoptosis detection kit (Sigma) per manufacturer's instructions. Spheroids were collected and washed in PBS, followed by debris removal with a 40-μm cell strainer (Fisher). Spheroids were then transferred into a sterile centrifuge tube by inversion of the strainer and subsequently pelleted by centrifugation at 453 × g for 5 min. The supernatant was aspirated and the spheroids dissociated in a six-well plate (Corning) at 37 °C using 2–3 mL trypsin/EDTA. After 5–30 min, the digest was neutralized with FBS, filtered through a 40 μm cell strainer to remove nondissociated particles, and centrifuged at 453 × g for 5–10 min to acquire a cell pellet. Approximately 200,000 hMSCs derived from monolayer cultures or spheroids were incubated for 10 min with 0.5 μg/mL annexin V-FITC and 2 μg/mL propidium iodide (PI) in 400 μL of 1× binding buffer (10 mM Hepes, 0.14 M NaCl, 2.5 mM $CaCl_2$). The cells were immediately placed on ice and analyzed. Cell fragments were removed by morphological gating. Cells negative for annexin V-FITC and PI were considered viable, annexin V-FITC positive and PI negative considered apoptotic, and annexin V-FITC positive and PI positive considered necrotic.

III.2.6. Cell cycle analysis

The cell cycle distribution in spheroids and monolayer cultures was determined by analyzing DNA content of permeabilized hMSCs labeled with PI (Sigma). hMSCs derived from monolayer or spheroid cultures were resuspended in 1 mL of ice cold PBS

containing 2% FBS followed by fixing with 3 mL cold absolute ethanol added dropwise while vortexing. The cells were incubated for 2–4 h in 4 mL of 75% ethanol to complete fixation, washed 3 times in PBS, then pelleted by centrifugation at 800 × g for 10 min. Cells were incubated with 7 U/mL RNase A (Qiagen) in 1 mL of PBS at room temperature. After 1 h, 50 μg/mL PI was added and the cells were incubated overnight at 4 °C. DNA content was measured with a flow cytometer and data analyzed using MultiCycle software (Phoenix Flow Systems).

III.2.7. Cell surface protein detection

To analyze cell surface markers, hMSCs resuspended at 3.0×10^6 cells/mL in αMEM containing 2% FBS were labeled with the antibodies described (Table 1) for 40 min on ice. The cells were washed 3 times with PBS and surface expression of proteins was determined with a flow cytometer.

III.2.8. Spheroid derived cell sizing

The size of hMSCs derived from adherent monolayers, or from dissociated spheroids suspended for 3 d in hanging drops at 10,000, 25,000, 100,000, and 250,000 cells/drop, was determined by microscopy and flow cytometry. For microscopic analysis, the cells were transferred into chambers of a Neubauer improved disposable hemocytometer and images captured on a Nikon Eclipse Ti-S inverted microscope using a Ds-Fi1 camera (Nikon). Cell diameter of more than 50 cells per group was subsequently determined using NIS-Elements AR 3.0 software. For flow cytometric analysis of cell size, 2.0×10^5 hMSCs were resuspended in 400 μL αMEM containing 2% FBS then incubated for 20 min with 100 nM of the live cell viability dye calcein AM (Molecular Probes) and 10 min with 2 μg/mL of the dead cell nuclear label 7AAD (Sigma). Cell sizes were estimated from the viable population (Calcein+/7AAD−) by comparing forward scatter (FS) properties of the cells and beads with a known diameter of 3, 7, 15, or 25 μm. Brackets were subsequently applied to the scatter plot at locations corresponding to the respective bead size. Gates established based on bead size FS were

used to group the cells into five populations (<3 μm, 3–7 μm, 7–15 μm, 15–25 μm, and >25 μm).

III.2.9. Intravenous Infusion of hMSCs

Male immunodeficient NOD/scid mice (NOD.CB17-Prkdcscid/J; The Jackson Laboratory), 7–8 week of age, housed on a 12 h light/dark cycle, were used to study the relative tissue distribution of the i.v. infused hMSCs. All animal procedures were performed with approval by the Animal Care and Use Committee of Texas A&M Health Science Center and in accordance with guidelines set forth by the National Institutes of Health. Mice were anesthetized by i.p. injection of a mixture of ketamine (91 mg/kg) and xylazine (9 mg/kg). Total of 10^6 monolayer or spheroid derived hMSCs suspended in 150 μL of HBSS were infused slowly into a tail vein. Mice were anesthetized 15 min later with ketamine/xylazine (90 mg/kg and 9 mg/kg) and euthanized by exsanguination. Heart, lung, liver, spleen, and kidneys were isolated by dissection and stored at −80 °C for further analysis.

III.2.10. Isolation of genomic DNA

After thawing the tissues, 5 mL of 10 mM Tris HCl (pH 8.0) containing 20 μL proteinase K (10 mg/mL), 0.1 mM EDTA (pH 8.0), 0.5% (w/v) SDS, and 20 μg/mL RNase A was added to each sample. Samples were homogenized (PowerGen Model 125 Homogenizer; Fisher Scientific) and incubated at 50 °C overnight on a shaker at 200 rpm. DNA was extracted by mixing 0.5 mL of sample with 0.5 mL phenol/chloroform solution (pH 6.7) followed by centrifugation at 15,300 × g for 5 min in 2 mL phase lock gel tubes (Phase Lock Gel; Eppendorf/Brinkmann Instruments). To precipitate the DNA, 1/2 volume of 2.5 M ammonium acetate, and the same volume of 100% ethanol was added, followed by overnight incubation at 4 °C. The precipitates were washed with ice cold 75% ethanol and resuspended into sterile water.

III.2.11. Real-time PCR assays for Alu sequences

Real-time PCR assays for Alu sequences were performed in 50 μL containing 25 μL Taqman Universal PCR Master Mix (Applied Biosystems), 900 nM each of the forward and reverse primers, 250 nM Taqman probe, and 200 ng of genomic DNA. Reactions were incubated at 50 °C for 2 min and at 95 °C for 10 min followed by 40 cycles at 95 °C for 15 s and 60 °C for 1 min. Real-time PCR assays for human and mouse *GAPDH* genes were performed in 50 μL containing 25 μL SYBR Green Master Mix (Applied Biosystems), 200 nM each of the forward and reverse primers and 200 ng of genomic DNA. All real-time PCR assays were performed in duplicate or triplicate and average values are presented. The final value for total DNA in the sample was corrected by parallel real-time PCR assays with primers that amplified both the human and mouse *GAPDH* genes [51,204,205].

III.2.12. Differentiation assays

hMSCs derived from high density monolayer (5,000 cells/cm^2) or hanging drop cultures (25,000 cells/drop), grown for 3 d, were seeded at low density (100 cells/cm^2) on six-well dishes and were grown until 80–90% confluent. To induce adipogenesis, hMSCs were cultured in CCM supplemented with 500 nM dexamethasone (Sigma), 500 nM isobutylmethylxanthine (Sigma), and 50 μM indomethacin (Sigma) for 14 d with medium changes every 3–4 d. To induce osteogenesis, hMSCs were cultured in CCM supplemented with 10 nM dexamethasone, 10 mM β-glycerolphosphate (Sigma), and 50 μM Ascorbate-2-phosphate (Sigma) for 14 d with medium changes every 3–4 d. Parallel control cultures were maintained in CCM for 14 d with medium changes every 3–4 d. All wells were washed with PBS and fixed with 10% (v/v) neutral buffered formalin (Sigma) for 1 h. The adipogenic differentiation and control wells were washed with PBS and stained with 0.6% (w/v) Oil-Red-O (Sigma) solution in 60% isopropanol (Sigma) and 40% PBS for 20 min followed by washing with PBS. The osteogenic differentiation and control wells were washed with deionized water and stained with 40 mM Alizarin

Red S (Sigma) solution, pH 4.2, in water for 20 min followed by washing with water. Images were captured on a Nikon Eclipse Ti-S inverted microscope.

III.2.13. Growth curves

hMSCs derived from high density monolayer or hanging drop cultures were seeded at 100 cells/cm^2 in 55-cm^2 dishes (Corning) in quadruplicate and cultured for 7 d in CCM with medium changes every 3 d. After 7 d, cells were lifted with trypsin/EDTA, counted with hemocytometer, and replated. The process was repeated until cells reached senescence.

III. 2.14. CFU-F assays

hMSCs derived from high density monolayer or hanging drop cultures were seeded onto 55 cm^2 dishes at 1.5 cells/cm^2 in quadruplicate and cultured for 14 d in CCM. Medium was changed every 3–4 d. After 14 d, the plates were stained with 3% (w/v) crystal violet (Sigma) in 100% methanol (Sigma) for 5 min, washed with water, and air-dried. Plates were scanned on an EPSON Perfection 4490 Photo scanner and images were processed with Adobe Photoshop CS3.

III.2.15. Microarrays

hMSCs from two donors grown at low density for 7 d and at high density or in hanging drops for 3 d were harvested for total RNA. A total of 2 μg of RNA from each sample was applied for microarrays using Whole Transcript Sense Target Labeling Assay protocol (Affymetrix) according to manufacturer's directions. Briefly, to minimize the background and thereby increasing the array detection sensitivity and specificity, rRNA reduction was performed for samples containing the Poly-A RNA controls (GeneChip Eukaryotic Poly-A RNA-Control Kit; Affymetrix) using the RiboMinus Transcriptome Isolation Kit (Invitrogen) with Magna-Sep Magnetic Particle Separator (Invitrogen) and Betaine (Sigma). RNA was concentrated with GeneChip IVT cRNA Cleanup Kit (Affymetrix) and used to prepare double stranded cDNA with

GeneChip WT cDNA Synthesis Kit (Affymetrix). Generated cDNA was used to produce cRNA with GeneChip WT cDNA Amplification Kit (Affymetrix), followed by cleanup with GeneChip Sample Cleanup Module (Affymetrix). The amount of cRNA was determined with spectrophotometer (SmartSpec Plus; Bio Rad) and 10 μg was used to generate cDNA with GeneChip WT cDNA Synthesis Kit (Affymetrix) followed by cRNA hydrolysis and cleanup of single-stranded cDNA with GeneChip Sample Cleanup Module. The amount of cDNA was determined with spectrophotometer and 5.5 μg was used for fragmentation with GeneChip WT Terminal Labeling Kit (Affymetrix). The fragmented cDNA was labeled using GeneChip WT Terminal Labeling Kit and hybridized (GeneChip Hybridization Oven 640; Affymetrix) on Human Exon 1.0 ST arrays (Affymetrix) using GeneChip Hybridization, Wash, and Stain Kit (Affymetrix). Arrays were washed and stained (GeneChip Fluidics Station 450; Affymetrix) using GeneChip Hybridization, Wash, and Stain Kit followed by scanning with GeneChip Scanner (Affymetrix). Data were normalized using robust multiarray (RMA) algorithm and gene level analysis was performed with Partek Genomics Suite 6.4 (Partek). Genes that were either up- or downregulated in spheroids at least twofold, compared with their monolayer counterparts, were used in hierarchical clustering. Significant Gene Ontology terms for up- and downregulated genes in spheroids were determined using the Partek software. The raw microarray data files will be available at the Gene Expression Omnibus website (http://www.ncbi.nlm.nih.gov/geo/).

III.2.16. Analysis of hMSC-secreted soluble anti-inflammatory factors

For TSG-6, STC-1, and LIF ELISAs, monolayer, spheroids, and spheroid derived hMSCs were seeded at equal cell density (200,000 cells/well or 8–25k spheroids/well) on tissue culture treated six-well dishes in 1.5 mL of CCM. In addition, hMSC spheroids were also suspended at 8 spheroids/well on non-adherent six-well dishes (Corning). After 24 h, images were acquired, conditioned medium was collected, and the cells were lyzed with 100 μL of modified RIPA buffer containing HALT protease/phosphatase inhibitors (Thermo Scientific). Conditioned medium was cleared of cellular material by

centrifugation at 500 × g for 10 min and stored at −80 °C. Total cellular protein was measured in whole cells lysates using the bicinchoninic acid (BCA)-dependent colorimetric detection method (Micro BCA Protein Assay Kit; Thermo Scientific). Human TSG-6 protein levels in conditioned medium were determined by ELISA as described [51] with some modifications. Briefly, wells of microplate strips (Costar) were coated overnight at 4 °C with 10 µg/mL TSG-6-specific monoclonal antibody (clone A38.1.20; Santa Cruz Biotechnology, Inc.) in 50 µL of 0.2 M bi- carbonate buffer (pH 9.2). The plates were washed 3 times with 400 µL of 1× wash buffer (R&D Systems), blocked with 100 µL of 1× PBST (Cell Signaling) containing 0.5% BSA (Thermo), and incubated for 2 h with 50 µL of sample or recombinant human TSG-6 protein standards (R&D Systems) diluted in blocking buffer. Wells were subsequently washed and incubated with 0.5 µg/mL biotinylated antihuman TSG-6 (R&D Systems) in 50 µL of 1× PBST. After 2 h, the samples were incubated for 20 min with 50 µL of streptavidin-HRP (R&D Systems), then with 100 µL substrate solution (R&D Systems). The colorimetric reaction was terminated after 15 min with 2 N sulfuric acid (R&D Systems) and the optical density determined on a plate reader (FLUOstar Omega; BMG Labtech) at an absorbance of 450 nm with wavelength correction at 540 nm. Human STC-1 and LIF proteins were detected with commercially available ELISA kits (R&D Systems) following procedures described by the manufacturer. Two hundred µL of sample/well was used for the LIF ELISA and 100 µL for the STC-1 ELISA. The obtained values were normalized to total cellular protein content to account for loss of cell/spheroid transfer.

III.2.17. Macrophage inflammatory assay

J774A.1 mouse macrophages (ATCC) were cultured on 15-cm bacteriological dishes (Falcon) in high glucose DMEM (Invitrogen) supplemented with glutamax, 10% FBS, and penicillin/streptomycin. Subcultures were prepared by washing the cells from the dish every 2–3 d and replating at a ratio of 1:5 to 1:10 (v/v). For the inflammatory assay, macrophages (MΦ) were seeded in the upper chamber of a 24-mm transwell

insert with 0.4-μm pores (Corning) at 400,000 cells/well followed by stimulation with 0.1 μg/mL of LPS (Sigma). After 90 min, LPS was removed and the cultures replaced with fresh medium. Total of 200,000 monolayer hMSCs, 200,000 spheroid derived cells, or 8–25k spheroids were transferred to the plate beneath the transwell. After 5 h, medium conditioned by the macrophages was collected and clarified by centrifugation at 500 × g for 10 min. A total of 50 μL of conditioned medium was used for mTNFα ELISA (Quantikine Kit; R&D Systems). Mouse macrophages were washed with PBS and harvested for RNA to quantify mTNFα expression levels by Real-time RT-PCR using Taqman Gene Expression Assay.

III.2.18. Mouse model of peritonitis

Male C57BL/6J mice (Jackson Laboratories), 6–8 week of age and housed on a 12 h light/dark cycle, were used to study the anti-inflammatory action of hMSC spheroids on zymosan-induced peritonitis. All animal procedures were performed with approval by the Animal Care and Use Committee of Texas A&M Health Science Center and in accordance with guidelines set forth by the National Institutes of Health. The inflammatory compound Zymosan A (Sigma) was prepared at a concentration of 1 mg/mL in PBS and autoclaved for 15 min to sterilize. To induce inflammation, 1 mL of the 0.1% (w/v) zymosan solution was administered i.p. Fifteen minutes later, either 1.5×10^6 monolayer hMSCs, 1.5×10^6 spheroid derived cells, or 60–25k spheroids were administered i.p. through a 20-gauge needle or catheter in 150–200 μL of HBSS (Gibco). After 6 h, animals were killed by cervical dislocation and the exudates retrieved by peritoneal lavage using 1.5 mL sterile PBS, pH 7.4, containing a 1× concentration of Halt protease inhibitors (Thermo Scientific) and 5 mM EDTA (Thermo Scientific). The lavage volume was recorded and the cells removed by centrifugation at 500 × g for 10 min. The protein-rich supernatants were then transferred to fresh microcentrifuge tubes, cleared of debris by centrifugation for 10 min at 10,000 × g, and stored at −80 °C. Amounts of peritoneal exudation were determined by subtracting the measured lavage volume of each sample from the averaged baseline volume. Twenty-four hours after cell

delivery, blood was collected from the right ventricle of anesthetized mice and transferred to Capiject clot activating tubes (Terumo Medical Corporation). The tubes were inverted 8–10 times and incubated at room temperature for 20–30 min to facilitate clot formation. The samples were centrifuged at 1500 × g for 10 min and the serum layer collected for measurements of plasmin activity.

III.2.19. Measurements of inflammation in peritoneal exudates and blood serum

Levels of inflammatory molecules TNFα, IL-1β, CXCL2, and PGE_2 were determined from the peritoneal lavage using commercially available ELISA kits (R&D Systems). Fifty microliters of sample per well was used for the detection of TNFα, 25 μL for IL-1β (1:2 dilution), 6.7 μL for CXCL2 (1:7.5 dilution), and 3 μL for PGE2 (1:50 dilution). Secreted MPO, a marker of neutrophil activity, was measured from the cell-free lavage fluid with a mouse-specific MPO ELISA kit (Hycult Biotech) per manufacturer's instructions. Total protein was evaluated with the Micro BCA protein detection kit (Thermo Scientific). Serum plasmin activity, a marker of inflammatory status, was ascertained by measuring time dependent cleavage of the chromogenic substrate Chromozym PL (Roche Applied Science) into 4-nitranline in 50 mM Tris-HCl (pH 7.4) and 0.9% NaCl. Absorbance at 405 nm was measured every 2 min for 30 min using the plate reader. The values were expressed as average change in absorbance/min.

III.2.20. Data analysis

Data are summarized as mean ± SD. Student's t test was used to calculate the levels of significance (NS, $P \geq 0.05$; *$P < 0.05$; **$P < 0.01$; ***$P < 0.001$).

III.3. Results

III.3.1. Aggregation of hMSCs in hanging drops into spheroids

To aggregate hMSCs, we used a hanging drop protocol. Time-lapse microscopy demonstrated that hMSCs cultured in hanging drops first formed a loose network and

then numerous small aggregates that gradually coalesced into a single central spheroid along the lower surface of the drop (Fig. III.1A). Once assembled, the spheroid did not increase in size but progressively compacted between 48 and 96 h. H&E staining of sections revealed the spheroids were solid throughout with small round cells evenly distributed and embedded in matrix (Fig. III.1B). The surface of the spheroid had a layer of epithelium-like cells that were more elongated and flatter. As expected, the sizes of the spheroids were dependent on the number of hMSCs suspended in the hanging drops (Fig. III.1E). hMSC spheroids of all sizes expressed and secreted very high levels of the anti-inflammatory molecule TSG-6 compared with either low or high density monolayer cultures, but spheroids of 25,000 cells (Sph 25k) showed the highest expression and secretion of TSG-6 (Fig. III.1C and D). Moreover, TSG-6 expression increased in a time dependent manner with spheroids of 25,000 hMSCs and was consistently much higher than in standard cultures of adherent hMSCs (Fig. III.1F).

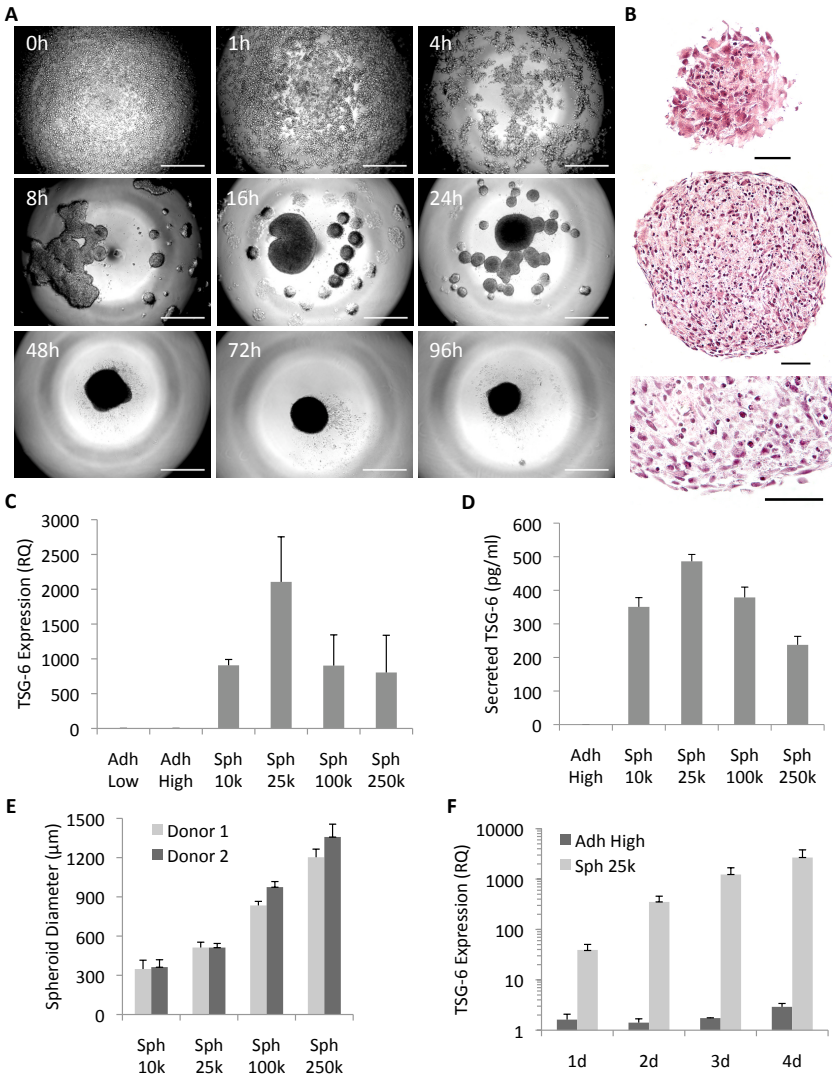

Figure III. 1. The expression of TSG-6 was increased as hMSCs aggregated into spheroids in hanging drops. (A) Phase contrast microscopy showing the time course of the aggregation of 25,000 hMSCs into a spheroid in a hanging drop. (Scale bar, 500 µm.) (B) H&E staining of hMSC spheroid sections from 3-d hanging drop cultures. Surface (Top), and center (Middle and Bottom) of a spheroid. (Scale bar, 50 µm.) (C) Real-time RT-PCR measurements of TSG-6 expression in hMSCs shown as relative to Adh Low sample (n = 3). (D) ELISA measurements of TSG-6 secretion over 24 h from hMSCs grown for 3 d at high density or as hanging drops at different cell densities (n = 4). (E) Sizes of spheroids generated by hMSCs from two donors grown in hanging drops for 3 d. Sizes were measured from captured images of transferred spheroids (n = 7–13). (F) Real-time RT-PCR measurements of TSG-6 expression in hMSCs grown at high density or in hanging drops at 25,000 cells/drop for 1–4 d shown as relative to hMSCs grown at low density (n = 3). Values are mean ± SD. Abbreviations: RQ, relative quantity; Adh Low, hMSCs plated at 100 cells/cm^2 for 7–8 d until about 70% confluent; Adh High, hMSCs harvested from same Adh Low cultures, plated at 5,000 cells/cm^2 and incubated for 3 d; Sph 10k-250k, hMSCs harvested from same Adh Low cultures and incubated for 3 d in hanging drops at 10,000-250,000 cells/drop. Bartosh et al., PNAS (2010) [198].

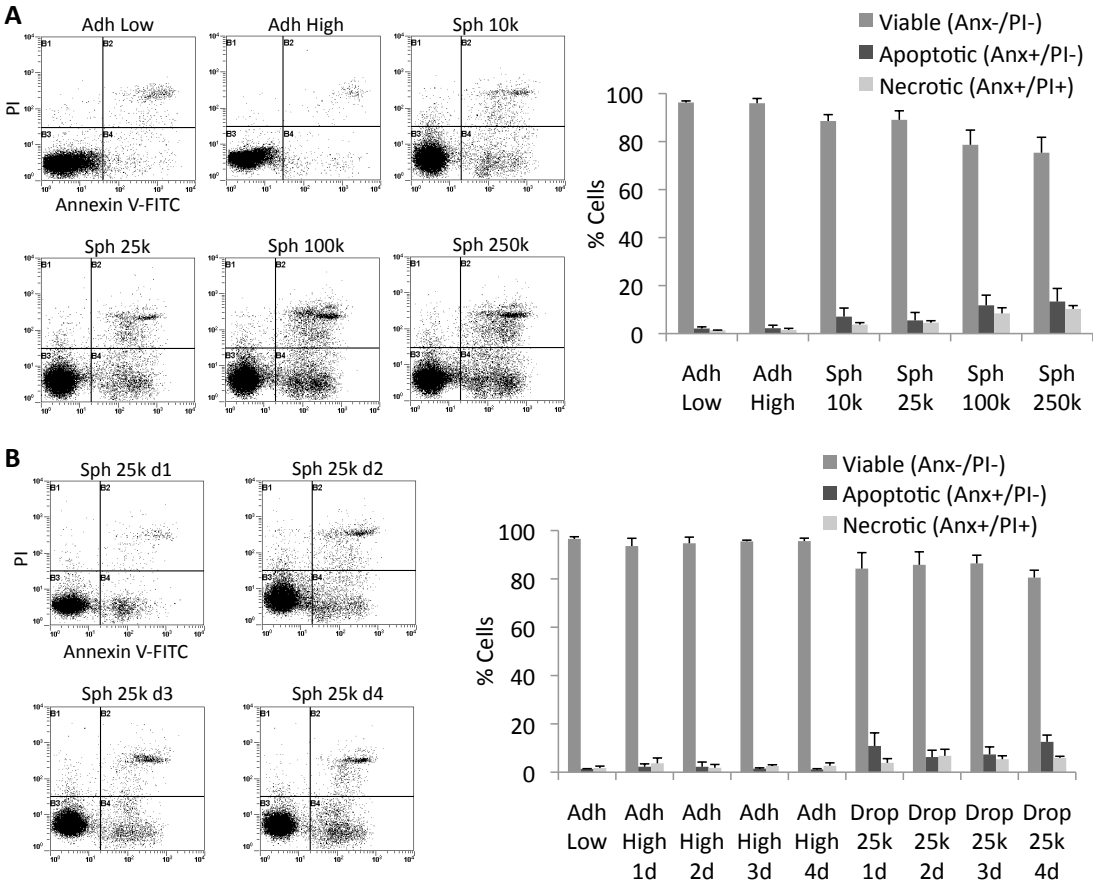

Figure III. 2. Viability of hMSCs in spheroids. (A and B) Viability of hMSCs as determined by flow cytometry measuring PI uptake and annexin V-FITC labeling. Spheroids were dissociated with trypsin/EDTA. Representative log fluorescent dot plots and summary of the data are shown. Values are mean ± SD (n = 3). Abbreviations: As in Fig. 1 with 1 d to 4 d indicating days of incubation. Bartosh et al. PNAS(2010) [198].

III.3.2. Viability of hMSCs in spheroids

Because hMSCs in spheroids may have less access to nutrients, it was of interest to establish whether the cells remained viable. In 3-d cultures of spheroids of 10,000 or 25,000 hMSCs, almost 90% of the harvested cells were viable as assayed by PI uptake and labeling with annexin V-FITC (Fig. III.2A). The number of apoptotic or necrotic cells was greater in spheroids prepared with 100,000 or 250,000 hMSCs (Fig. III.2A).

Also, the number of apoptotic or necrotic cells increased slightly when the incubation period was extended from 3 d to 4 d (Fig. III.2B).

III.3.3. Analysis of spheroid hMSC size in vitro and relative tissue distribution after i.v. infusion

As suggested by histological sections (Fig. III.1B), hMSCs in spheroids appeared smaller than hMSCs from standard monolayer cultures. The cells released from spheroids by trypsinization were nearly half the diameter and approximately one-fourth the volume of hMSCs derived from adherent monolayers as shown by flow cytometry (Fig. III.3 and Fig. III.4A) and microscopy (Fig. III.4B).

To test if the smaller size of the hMSCs dissociated from spheroids would allow the cells to traffic through the lung microvasculature and therefore distribute more efficiently into other tissues, both monolayer and spheroid hMSCs were injected i.v. into the tail vein of NOD/scid mice. Real-time PCR for human Alu sequences in the lungs collected 15 min after hMSC infusion suggested that the number of trapped cells decreased by about 25% with spheroid derived hMSCs compared with monolayer hMSCs, At the same time, a larger fraction of infused spheroid hMSCs were recovered in the liver, spleen, kidney, and heart (Fig. III.4C).

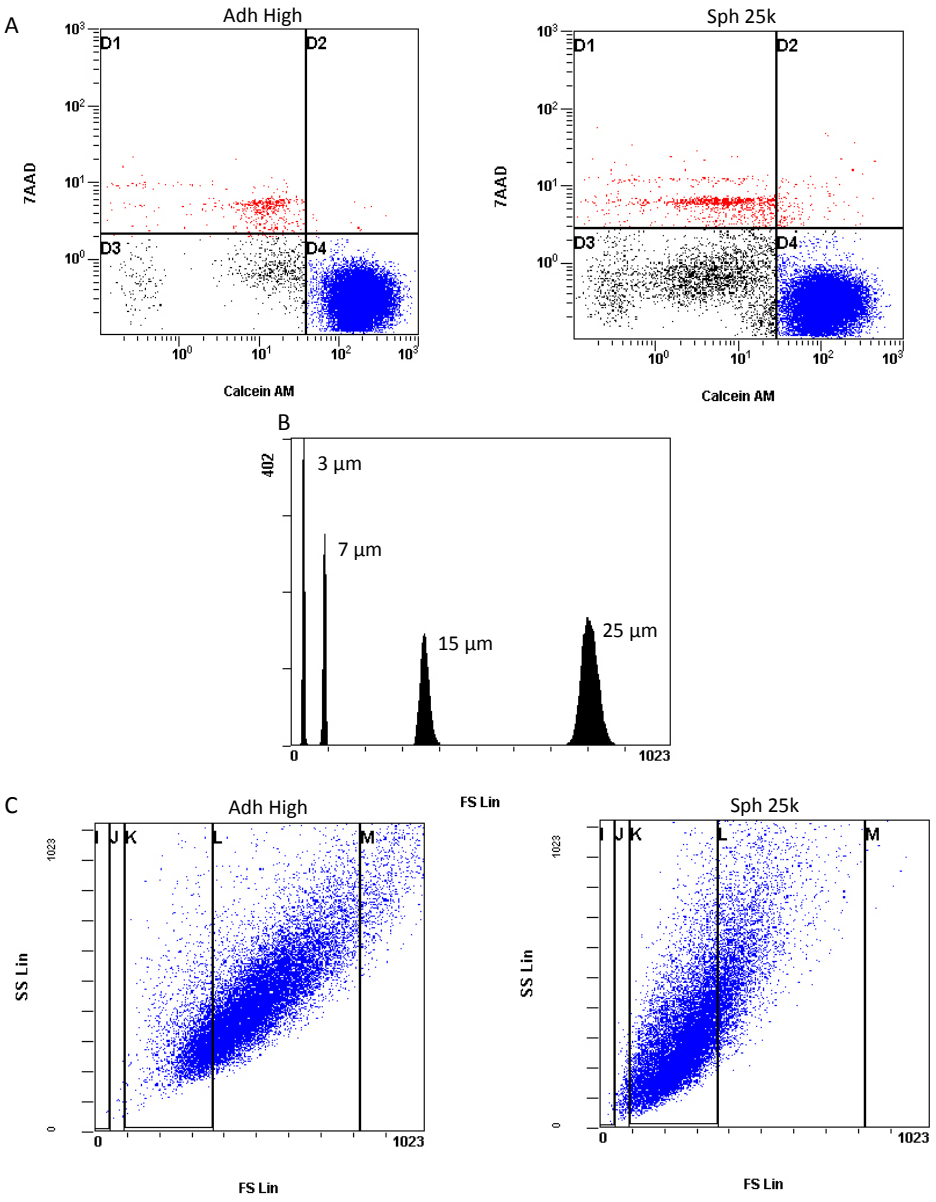

Figure III. 3. Analysis of spheroid derived hMSC size by flow cytometry. Flow cytometric determination of hMSC size from 3-d cultures of adherent monolayers (Adh High) or spheroids (Sph 25k) labeled with the viability dyes calcein AM (live cells, blue) and 7AAD (dead cells, red). (A) Representative log fluorescent dot plots. (B) Histogram of bead standards with diameters of 3, 7, 15, and 25 µm. (C) Representative linear scatter plots of the calcein $AM^{+}/7AAD^{-}$ cell populations. Brackets were applied to the scatter plot at locations corresponding to the appropriate bead size (I = 0, J = 3 µm, K = 7 µm, L = 15 µm, and M = 25 µm). Assays were performed at the same voltages. Bartosh et al., PNAS (2010) [198].

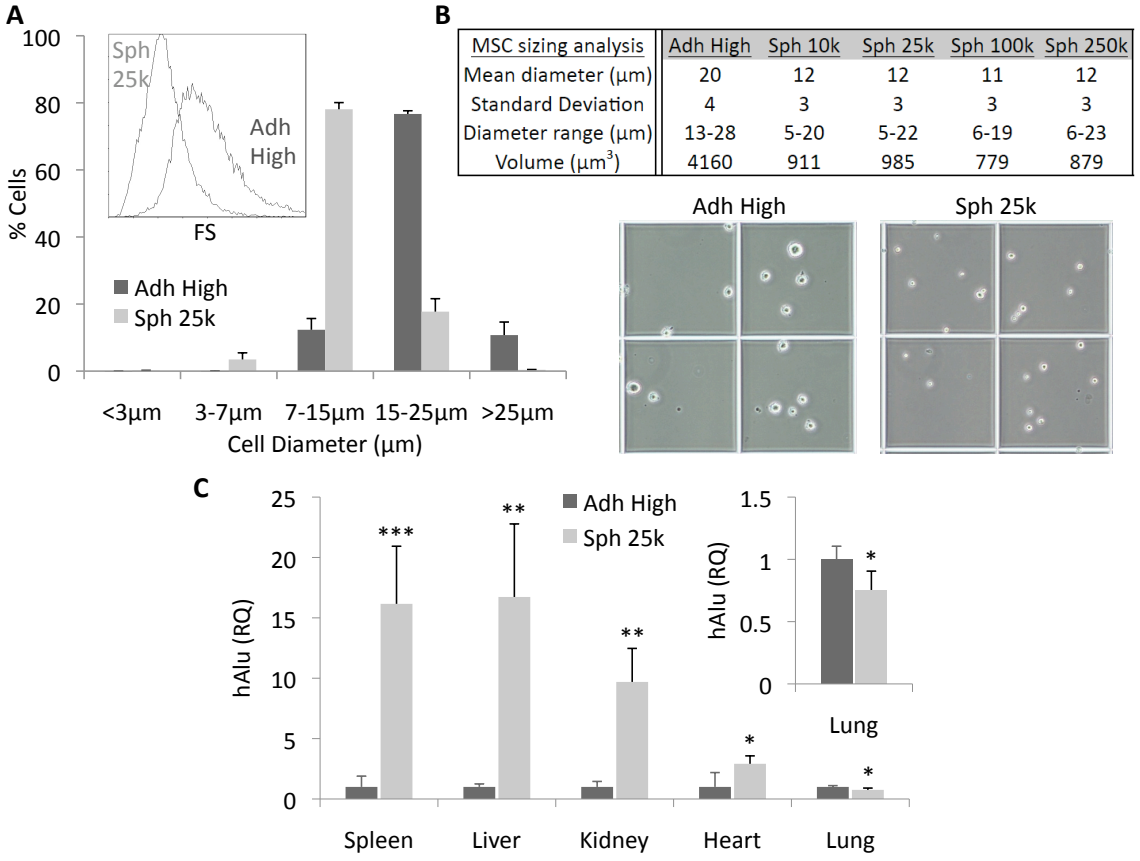

MSC sizing analysis	Adh High	Sph 10k	Sph 25k	Sph 100k	Sph 250k
Mean diameter (µm)	20	12	12	11	12
Standard Deviation	4	3	3	3	3
Diameter range (µm)	13-28	5-20	5-22	6-19	6-23
Volume (μm^3)	4160	911	985	779	879

Figure III. 4. Size analysis and i.v. infusion of spheroid hMSCs. (A) Assays of cell size by flow cytometry (n = 3). hMSC sizes were estimated from forward scatter (FS) (Inset) properties of the viable population (calcein $AM^+/7AAD^-$) relative to beads with known diameters (3, 7, 15, and 25 µm). (B) Cell size assayed by microscopy. (C) Relative tissue distribution of i.v. infused hMSCs. NOD/scid mice were infused i.v. with 10^6 monolayer or spheroid derived hMSCs. After 15 min, tissues were harvested for genomic DNA and tissue distribution of hMSCs was determined with real-time PCR for human Alu and GAPDH (n = 4–5) and shown as relative to Adh High sample. *P < 0.05, **P < 0.01, and ***P < 0.001. Values are mean ± SD. Abbreviations: as in Fig. 1. Bartosh et al., PNAS (2010) [198].

III.3.4. Human MSCs dissociated from spheroids retain the properties of adherent hMSCs

Human MSCs dissociated from spheroids retained the ability to differentiate into mineralizing cells and adipocytes (Fig. III.5A and B). The dissociated cells expanded more slowly during an initial passage and then more rapidly than adherent hMSCs through four passages before reaching senescence at about the same number of

population doublings (Fig. III.5C and Fig. III.6A). In addition, the dissociated cells readily generated colonies (CFUs) when plated at clonal densities (Fig. III.5D and Fig. III.6B). Consistent with the data on rates of propagation (Fig. III.5C), the number of CFUs from spheroid cells was initially less than the number of CFUs from adherent cultures but was greater in later passages (Fig. III.5D and Fig. III.6B). The surface epitopes of the hMSCs dissociated from spheroids were similar to the surface epitopes of hMSCs from adherent monolayers when dissociated under the same conditions with trypsin (10 min at 37 °C): the dissociated cells were negative for hematopoietic markers, and they were slightly less positive for CD73, CD90, and CD105, apparently because of the smaller size of the cells (Fig. III.5E, Figs. III.7–9, and Table III.1).

Figure III. 5. Spheroid hMSCs retain the properties of hMSCs from adherent cultures. (A) Differentiation of hMSCs in osteogenic medium (Osteo Dif) and control medium (Osteo Con). Cultures were stained with Alizarin Red after 14 d. (Scale bar, 200 μm.) (B) Differentiation of hMSCs in adipogenic medium (Adipo Dif) and control medium (Adipo Con). Cultures were stained with Oil Red O after 14 d. (Scale bar, 200 μm.) (C) Growth of hMSCs (donor 2) as monolayers from high density and hanging drop cultures plated at low density (5,500 cells/plate) and passaged every 7 d (n = 4). Cumulative population doublings (PDs) after each passage are shown (Inset). (D) CFU-F assays of hMSCs (donor 2) plated at 83 cells/plate and incubated for 14 d (n = 4). Representative plates at passage 1 and passage 2 after transfer. Values are mean ± SD. (E) Flow cytometry of surface protein expression on hMSCs. Abbreviations: as in Fig. 1 with P1 to P10 indicating passage number. Bartosh et al., PNAS (2010) [198].

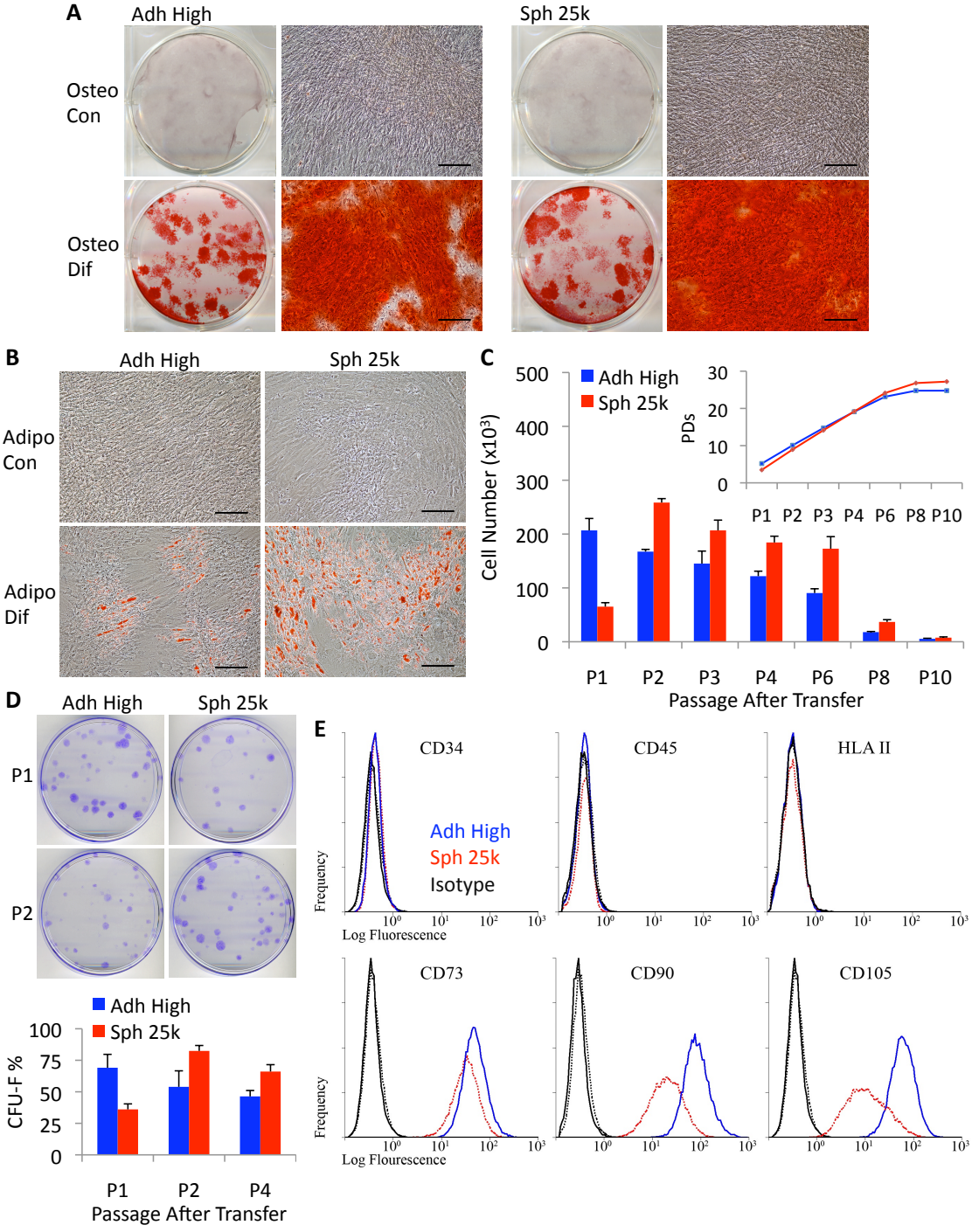
A
Adh High
Sph 25k
Osteo Con
Osteo Dif
B
Adh High
Sph 25k
Adipo Con
Adipo Dif
C
Adh High
Sph 25k
Cell Number (x10³)
PDs
P1 P2 P3 P4 P6 P8 P10
Passage After Transfer
D
Adh High
Sph 25k
P1
P2
CFU-F %
P1 P2 P4
Passage After Transfer
E
CD34
CD45
HLA II
Adh High
Sph 25k
Isotype
Frequency
Log Fluorescence
CD73
CD90
CD105

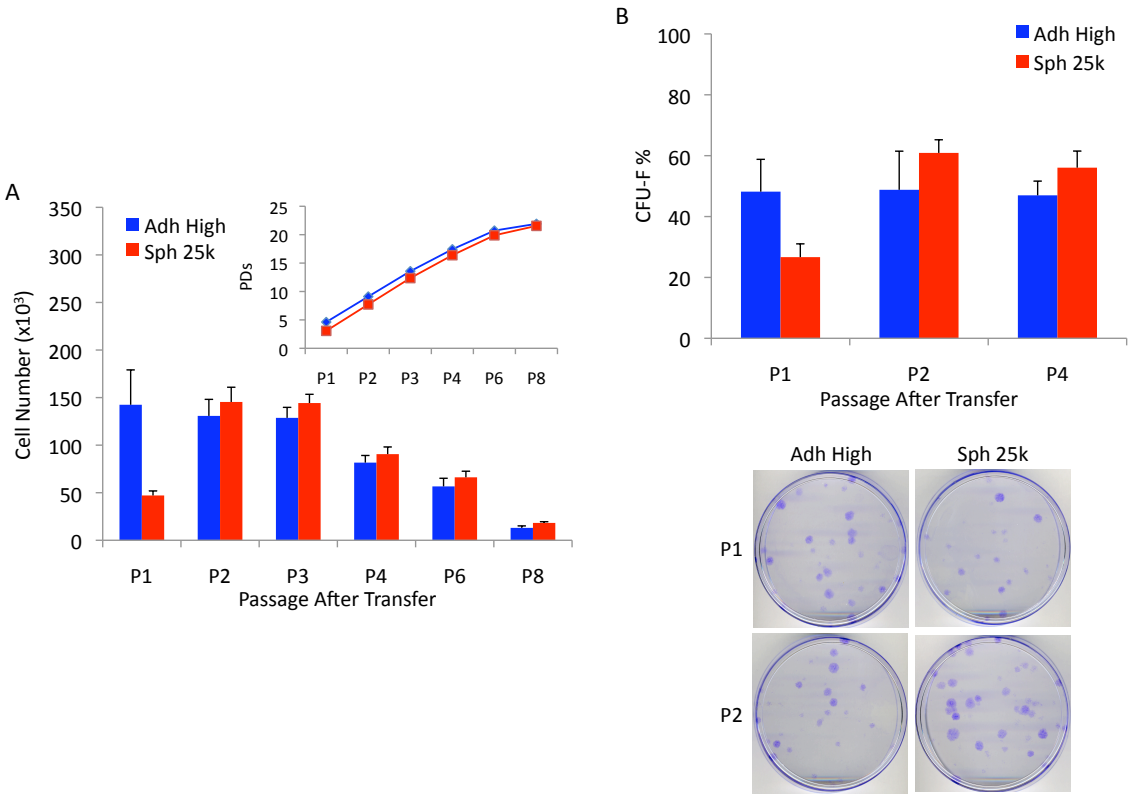

Figure III. 6. hMSCs from spheroids exhibit similar growth characteristics and clonogenicity to monolayer cultures. (A) Growth of hMSCs (donor 1) as monolayers from high density and hanging drop cultures plated at low density (5,500 cells/plate) and passaged every 7 d. Cumulative population doublings (PDs) after each passage are shown (Inset). (B) CFU-F assays of hMSCs (donor 1) plated at 83 cells/plate and incubated for 14 d. Representative plates at passage 1 and passage 2 after transfer. Values are mean CFU-F percentage ± SD (n = 4). Bartosh et al. PNAS (2010) [198].

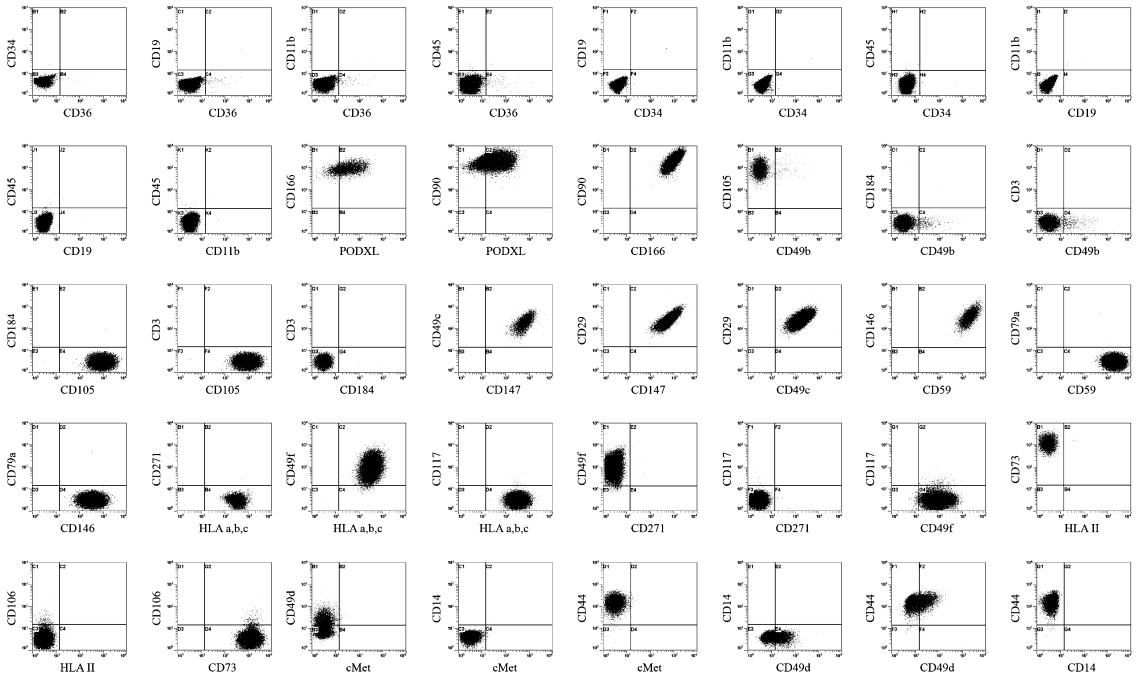

Figure III. 7. Surface phenotype of hMSCs cultured as monolayers at low cell density. Flow cytometry measurements of characteristic hMSC surface proteins. Passage 2 hMSCs were plated at 100 cells/cm^2 and grown for 7 d until approximately 70% confluent before analysis. The cells were harvested by incubation with trypsin/EDTA for 5 min. Bartosh et al. PNAS (2010) [198].

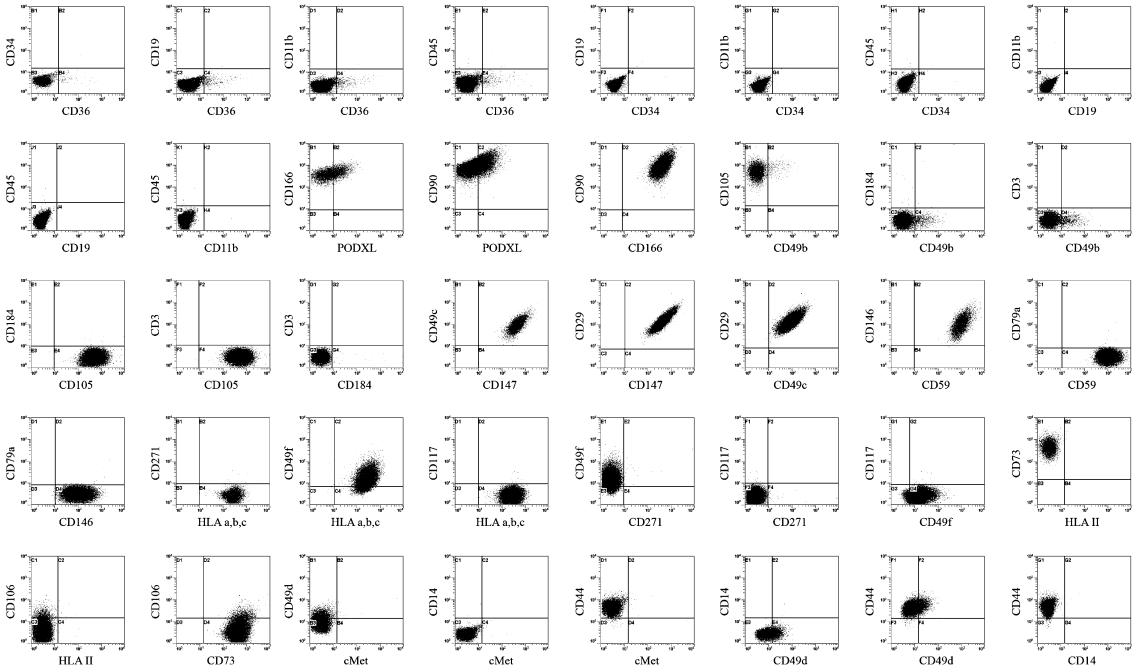

Figure III. 8. Surface phenotype of hMSCs cultured as monolayers at high cell density and harvested by incubation with trypsin for 10 min. Flow cytometry measurements of characteristic hMSC surface proteins. Passage 3 hMSCs were plated at 5,000 cells/cm^2 and grown for 3 d before analysis. The cells were harvested by incubation with trypsin/EDTA for 10 min. Bartosh et al. PNAS (2010) [198].

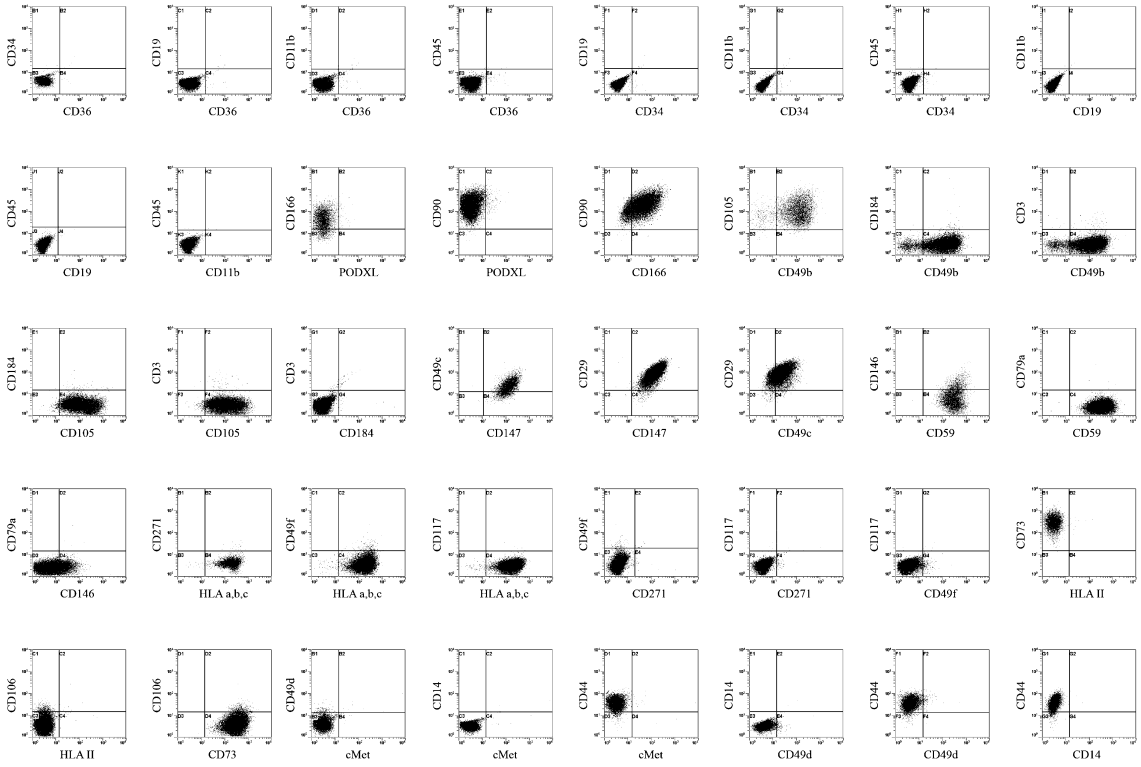

Figure III. 9. Surface phenotype of hMSCs derived from spheroids. Flow cytometry measurements of characteristic hMSC surface proteins. Passage 3 hMSCs were suspended in hanging drops at 25,000 cells/drop and cultured for 3 d before analysis. The spheroids were dissociated for 10 min with trypsin/EDTA to obtain the spheroid cells. Bartosh et al. PNAS (2010) [198].

Table III. 1. List of antibodies used to detect the expression of cell surface proteins in hMSC

Protocol	Protein	Fluorochrome	Isotype	Clone	Manufacturer
Protocol 1	CD36	FITC	Ms IgG-1	FA6.152	Beckman-Coulter
	CD34	PE	Ms IgG-1	581	Beckman-Coulter
	CD19	ECD	Ms IgG-1	J3.119	Beckman-Coulter
	CD11b	PE-Cy5	Ms IgG-1	Bear1	Beckman-Coulter
	CD45	PE-Cy7	Ms IgG-1	J.33	Beckman-Coulter
Protocol 2	PCLP1	FITC	Ms IgG-2a	53D11	MBL International
	CD166	PE	Ms IgG-1	3A6	Beckman-Coulter
	CD90	PE-Cy5	Ms IgG-1	Thy1/310	Beckman-Coulter
Protocol 3	CD49b	FITC	Ms IgG-1	Gi9	Beckman-Coulter
	CD105	PE	Ms IgG-3	IG2	Beckman-Coulter
	CD184	APC	Ms IgG-2a	12G5	BD Biosciences
	CD3	PE-Cy7	Ms IgG-1	UCHT1	Beckman-Coulter
Protocol 4	CD147	FITC	Ms IgG-1	HIM6	BD Biosciences
	CD49c	PE	Ms IgG-1	C3 II.1	BD Biosciences
	CD29	PE-Cy5	Ms IgG-1	MAR4	BD Biosciences
Protocol 5	CD59	FITC	Ms IgG-2a	P282E	Beckman-Coulter
	CD146	PE	Ms IgG-2a	TEA1/34	Beckman-Coulter
	CD79a	PE-Cy5	Ms IgG-1	HM47	Beckman-Coulter
Protocol 6	Class I HLA	FITC	Ms IgG-1	G46-2.6	BD Biosciences
	CD271	PE	Ms IgG-1	C40-1457	BD Biosciences
	CD49f	PE-Cy5	Rat IgG-2a	GoH3	BD Biosciences
	CD117	PE-Cy7	Ms IgG-1	104D2D1	Beckman-Coulter
Protocol 7	Class II HLA	FITC	Ms IgG-2a	TU39	BD Biosciences
	CD73	PE	Ms IgG-1	AD2	BD Biosciences
	CD106	PE-Cy5	Ms IgG-1	51–10C9	BD Biosciences
Protocol 8	HGFR	FITC	Rat IgG-1	eBioclone97	eBioscience
	CD49d	PE	Ms IgG-1	9F10	BD Biosciences
	CD14	ECD	Ms IgG-2a	RMO52	Beckman-Coulter
	CD44	APC	Ms IgG-2b	G44-26	BD Biosciences
Protocol 9	Isotypes	FITC	Ms IgG-1	679.1Mc7	Beckman-Coulter
		PE	Ms IgG-2a	7T4-1FS	Beckman-Coulter
		FITC	Ms IgG-2a	G155-178	BD Biosciences
		FITC	Rat IgG-1, *k*		eBioscience
		PE	Ms IgG-1, *k*	MOPC-31C	BD Biosciences
		PE	Ms IgG-3		Santa Cruz
		ECD	Ms IgG-1	679.1MC7	Beckman-Coulter
		ECD	Ms IgG -2a	7T4-1F5	Beckman-Coulter
		PE-Cy5	Ms IgG-1	679.1Mc7	Beckman-Coulter
		PE-Cy5	Rat IgG-2a	R35-95	BD Biosciences
		APC	Ms IgG-2a	7T4-1F5	Beckman-Coulter
		APC	Ms IgG-2b	27–35	BD Biosciences
		PE-Cy7	Ms IgG-1	679.1Mc7	Beckman-Coulter

Total of nine different protocols were run for each hMSC sample to determine the surface proteins expressed. Bartosh et al. PNAS (2010) [198].

III.3.5. Transcriptome changes in the spheroid hMSCs

Surveys with microarray assays demonstrated that 236 genes were upregulated and 230 genes were downregulated in a comparison of spheroid cells with hMSCs from adherent monolayers (Fig. III.10A and Table III.2). There were increases in genes with ontologies for extracellular region, regulation of cell adhesion, receptor binding, cell communication, extracellular matrix, and negative regulation of cell proliferation (Fig. III.10A). Also, there were parallel decreases in genes with ontologies for cytoskeleton organization and biogenesis, mitosis, cell cycle, and extracellular matrix (Fig. III.10A). Of special interest was the increase in genes with ontologies for response to wounding and inflammatory response (Fig. III.10A). Real-time RT-PCR assays (Fig. III.11A) demonstrated marked increases in the expression of TSG-6; STC-1, an anti-inflammatory/anti-apoptotic protein; leukemia inhibitory factor (LIF), a cytokine for growth and development; IL-24, a tumor suppressor protein; TRAIL, a protein with selectivity for killing certain cancer cells; and CXCR4, a receptor involved in MSC homing. As expected from its stimulatory effect of MSC proliferation [206], there was decreased expression of DKK1, an inhibitor of Wnt signaling (Fig. III.11A).

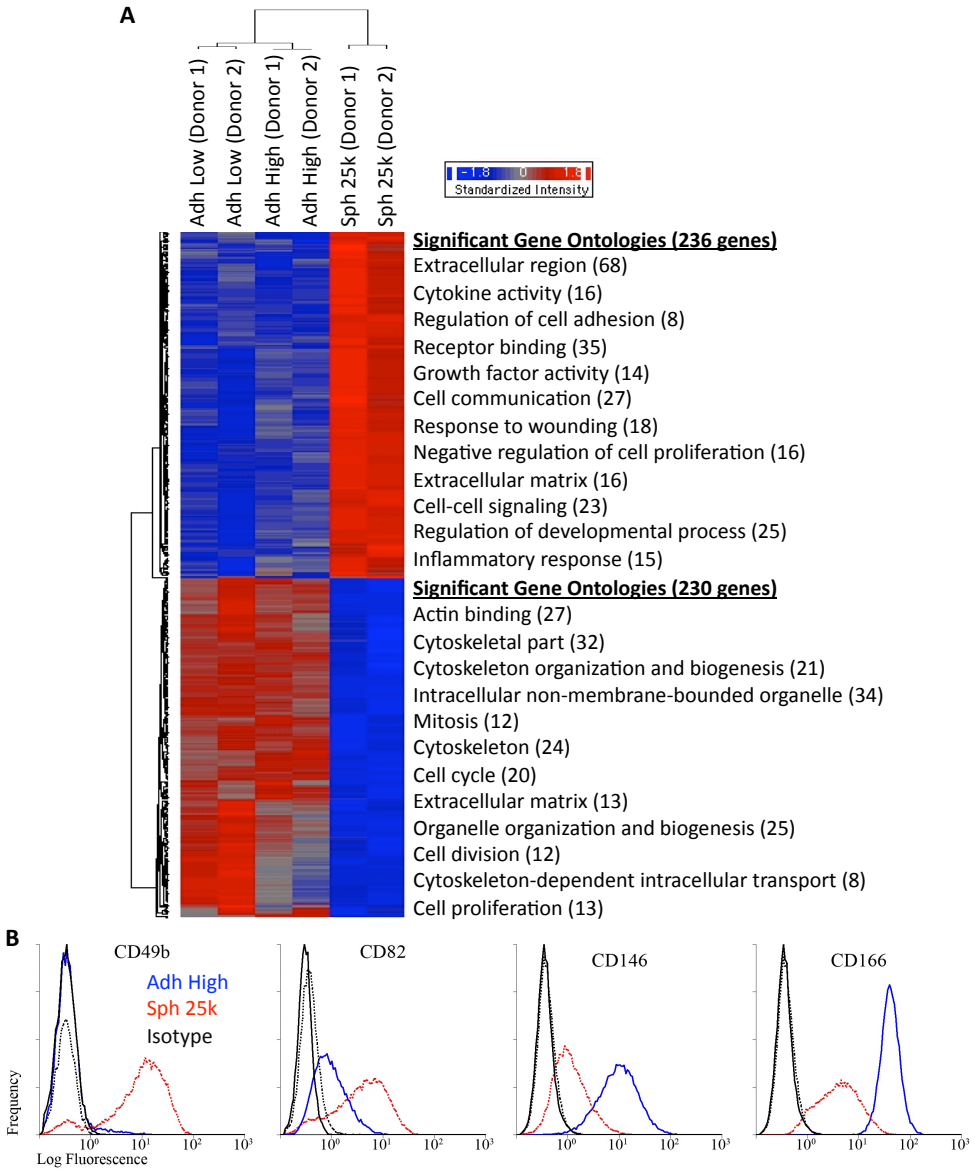

Figure III. 10. Microarray assays of hMSCs from two donors. (A) Hierarchical clustering of differentially expressed genes. Genes that were either up (236 genes) or downregulated (230 genes) in spheroids (Sph 25k) at least twofold compared with their adherent culture counterparts (Adh Low and Adh High), were used in hierarchical clustering. The most significant Gene Ontology terms for upregulated genes (red) and downregulated genes (blue) are shown next to the heat map. (B) Flow cytometry of differentially expressed surface epitopes on hMSCs. Abbreviations: as in Fig. 1. Bartosh et al. PNAS (2010) [198].

Table III. 2. Selected genes upregulated in hMSC spheroids

	Donor 1		Donor 2	
Gene (GeneID)	25k Sph vs. Adh Low	25k Sph vs. Adh High	25k Sph vs. Adh Low	25k Sph vs. Adh High
Secreted molecules				
IL8 (3576)	78	82	38	34
TSG-6 (7130)	55	61	51	40
IL1B (3553)	3	24	19	12
BMP2 (650)	16	14	23	12
CXCL1 (2919)	14	12	7	3
SPP1 (6696)	13	12	4	5
GDF15 (9518)	12	6	17	6
IL11 (3589)	11	10	9	10
LIF (3976)	10	12	7	9
SMOC1 (64093)	10	8	6	4
IL1A (3552)	9	7	5	3
IGFBP5 (3488)	8	11	11	14
C1S (716)	8	4	9	3
BMP6 (654)	7	8	3	4
TRAIL (8743)	7	7	11	6
PTHLH (5744)	6	6	3	3
NMB (4828)	6	5	5	3
APOD (347)	6	5	7	3
PLTP (5360)	6	7	5	4
IL24 (11009)	6	6	10	7
IL6 (3569)	6	3	3	3
STC1 (6781)	6	7	6	10
NAMPT (10135)	5	5	3	3
Cell surface receptors				
ITGA2 (3673)	26	23	13	18
EDNRA (1909)	21	15	7	9
GPR84 (53831)	18	13	11	5
BDKRB2 (624)	10	10	9	6
CXCR4 (7852)	7	7	4	5
DPP4 (1803)	7	6	5	4
CD82 (3732)	6	5	7	4
PLA2R1 (22925)	6	5	7	4
PTGDR (5729)	6	7	7	5
ICAM1 (3383)	5	6	8	5
COLEC12 (81035)	5	4	7	6
C3AR1 (719)	5	5	4	3
Extracellular matrix molecules				
MMP13 (4322)	64	66	39	37
CHI3L1 (1116)	42	33	72	36
TFPI2 (7980)	25	55	15	53
MMP3 (4314)	14	15	9	6
MMP1 (4312)	10	11	25	16
ADAMTS5 (11096)	8	7	5	3
GPC6 (10082)	6	4	3	2
LUM (4060)	6	3	6	3
LAMA4 (3910)	5	3	5	3
Transcription factors				
NR4A2 (4929)	11	12	13	10
ETV1 (2115)	10	11	6	6
MAFB (9935)	9	9	6	6
SATB1 (6304)	6	6	7	5

Values are fold changes of 25k Sph sample compared with either Adh Low or Adh High for two donors. Bartosh et al. PNAS (2010) [198].

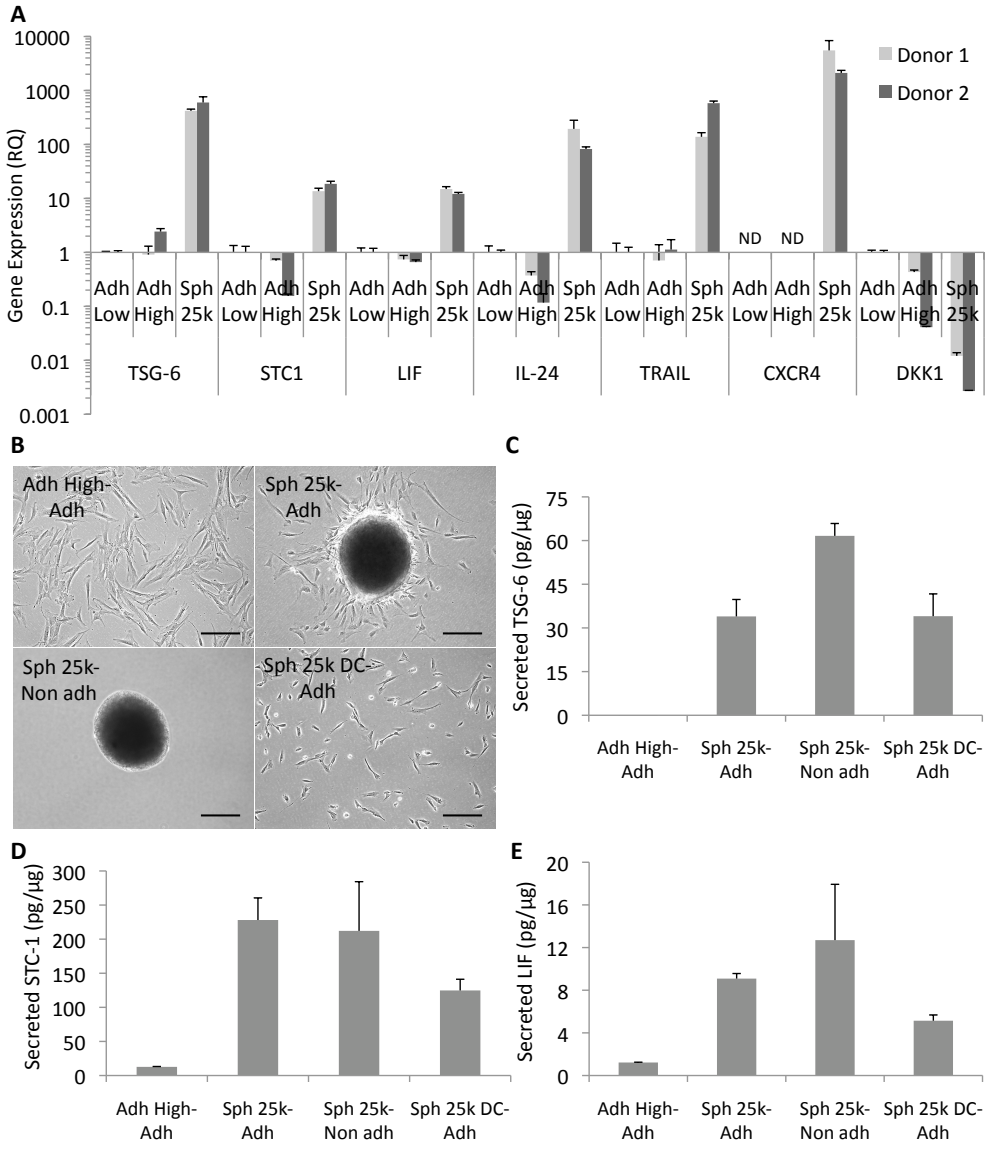

Figure III. 11. Spheroid hMSCs express high levels of anti-inflammatory and anti-tumorigenic molecules. (A) Real-time RT-PCR measurements for anti-inflammatory genes (TSG-6, STC-1, and LIF), anti-tumorigenic genes (IL-24 and TRAIL), gene for an MSC homing receptor (CXCR4), and gene for the Wnt signaling inhibitor (DKK1) for two donors. Values are mean RQ ± 95% confidence interval from triplicate assays compared with Adh Low sample. (B) Images of high density monolayer (Adh High), spheroids (Sph 25k), and spheroid derived hMSCs (Sph 25k DC) 24 h after transfer onto adherent (Adh) or non-adherent (Non adh) surfaces. Cultures were in six-well plates containing 1.5 mL CCM and either 200,000 hMSCs from high density cultures, eight spheroids, or 200,000 hMSCs dissociated from spheroids. After 24 h, medium was recovered for ELISAs and cells lyzed for protein assays. (Scale bar, 200 µm.) TSG-6 (C), STC-1 (D), and LIF (E) ELISAs on medium, normalized to total cellular protein. Values are mean ± SD (n = 3). Abbreviations: as in Fig. 1 with ND indicating not detectable and Sph 25k DC-Adh indicating hMSCs dissociated from Sph 25k and plated on cell adherent surfaces. Bartosh et al., PNAS (2010) [198].

III.3.6. Changes in cell surface protein expression and cell cycle distribution in hMSC spheroids

Assays by flow cytometry demonstrated decreased expression of podocalyxin-like protein (PODXL), an anticell-adhesion protein; and α4-integrin (CD49d), an integrin subunit associated with lymphocyte homing (Figs. III.7-9). There was partial downregulation of the melanoma cell adhesion molecule (MCAM or CD146) that is used as a marker for endothelial cells and pericytes, and of ALCAM (CD166), a cell adhesion molecule (Fig. III.10B). At the same time, there was increased expression of an integrin subunit for cell adhesion (α2-integrin of CD49b), and a protein associated with suppression of metastases (CD82) (Fig. III.10B). As expected from microarray results, assays by flow cytometry also demonstrated a decrease of spheroid hMSCs in S-phase compared with monolayer hMSCs (Fig. III.12A–D).

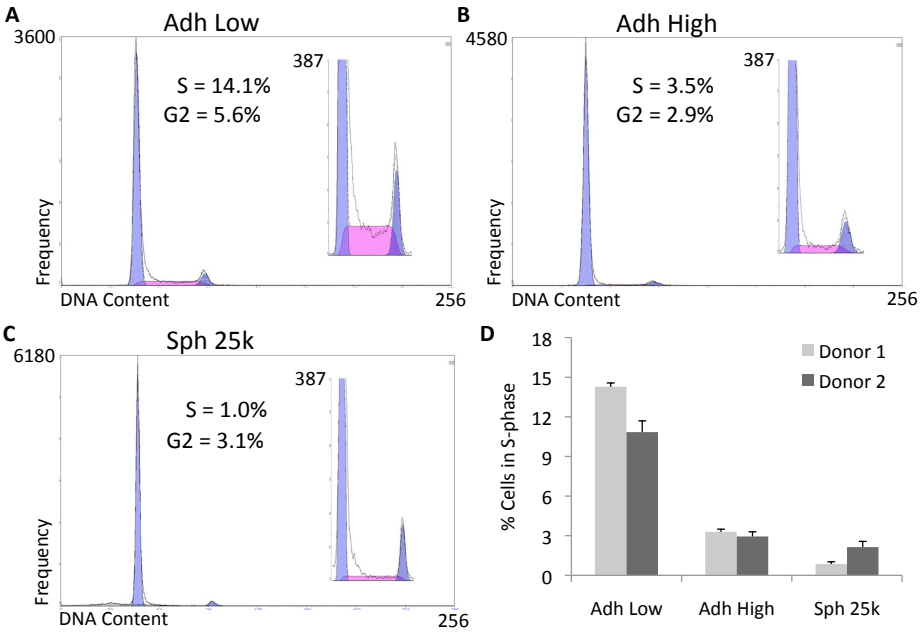

Figure III. 12. Cell cycle analysis of monolayer and spheroid hMSCs. Representative cell cycle distribution in hMSCs for donor 1 grown at low density (A), at high density (B), and as spheroids (C) was determined by analyzing DNA content of permeabilized hMSCs labeled with PI. DNA content was measured with a flow cytometer and data analyzed using MultiCycle software. (D) Summary of the cell cycle analysis data. Values are mean ± SD (n = 3). Bartosh et al. PNAS (2010) [198].

III.3.7. Spheroid hMSCs secrete anti-inflammatory proteins

Spheroids of hMSCs plated on adherent culture surfaces gradually generated spindle-shaped cells that migrated away from the spheroids (Fig. III.11B). No migration was seen with spheroids plated on non-adherent surfaces (Fig. III.11B). ELISAs demonstrated that hMSCs either in spheroids or dissociated from spheroids continued to secrete TSG-6, STC-1, and LIF when plated on culture dishes for 24 h (Fig. III.11C–E). The levels of all three factors were much higher than with adherent monolayer hMSCs. About the same levels of STC-1 and LIF were observed in spheroids cultured directly either on adherent or non-adherent plates, but spheroids cultured on non-adherent dishes secreted more TSG-6 (Fig. III.11C–E). The levels of TSG-6, STC-1, and LIF decreased when the hMSCs were dissociated from spheroids and cultured on adherent plates but the levels remained much higher than with adherent monolayers (Fig. III.11C–E).

III.3.8. Spheroid hMSCs decrease activation of macrophages in vitro and inflammation in vivo

The increased secretion of anti-inflammatory molecules TSG-6 and STC-1 by the spheroid hMSCs suggested that the cells would be more effective than adherent monolayer cultures of hMSCs in reducing inflammatory responses. To test this prediction, mouse macrophages were preactivated with LPS in the upper chamber of a transwell, followed by a transfer of the chamber to a test well (Fig. III.13A). Under the conditions of the experiment, the presence in the test well of hMSCs from adherent monolayers had no significant effect on the expression or secretion of TNFα by the stimulated macrophages (Fig. III.13B and Fig. III.14A). In contrast, TNFα expression and secretion was decreased significantly by the presence in the test well of intact spheroids or hMSCs dissociated from spheroids (Fig. III.13B and Fig. III.14A). The results indicated therefore that the spheroid derived hMSCs secreted more effective anti-inflammatory factors.

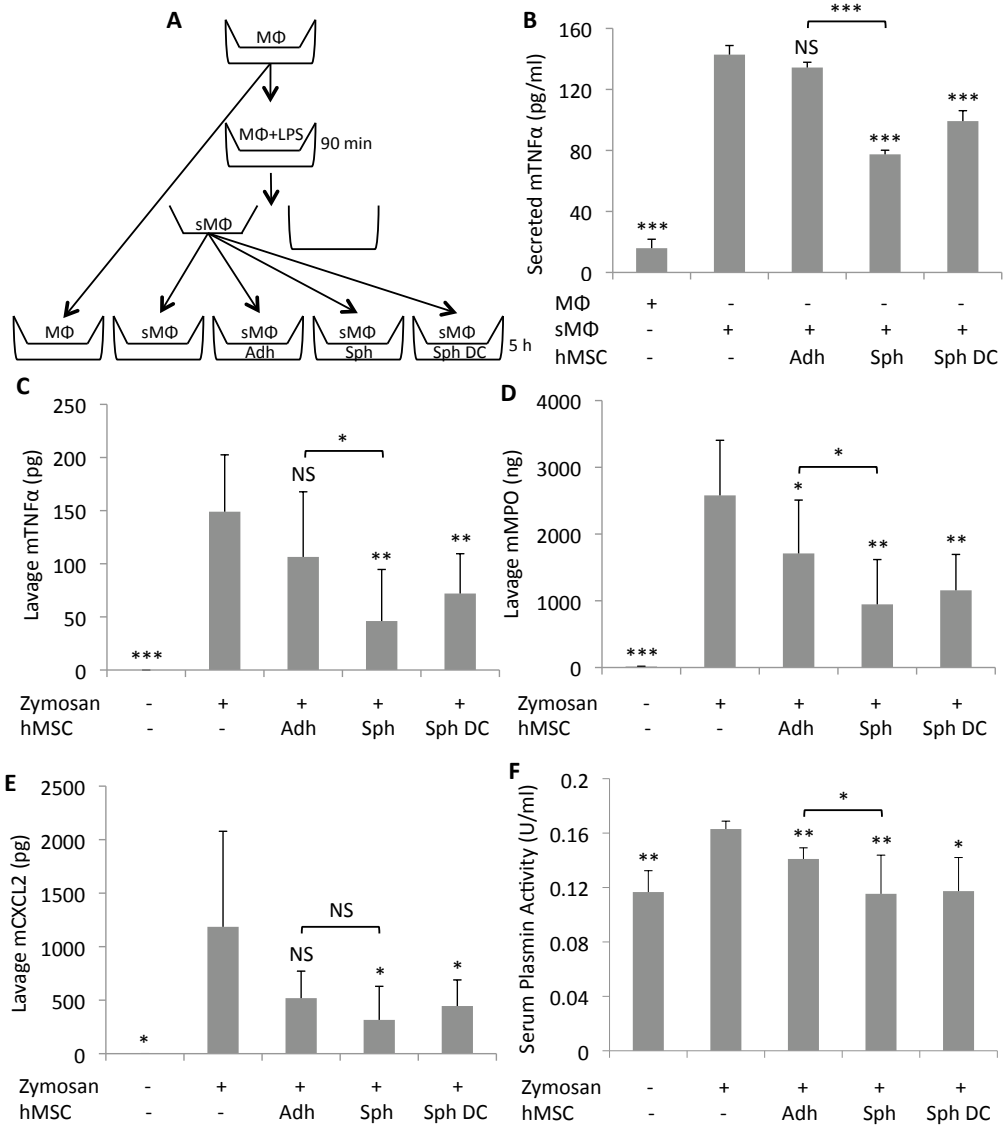

Figure III. 13. hMSC spheroids exhibit enhanced anti-inflammatory effects in vitro and in vivo. (A) Schematic of the mouse macrophage (mMΦ) assay. mMΦs were seeded in the upper chamber of a transwell, stimulated with LPS for 90 min, the LPS was removed, and the chamber transferred to a six-well dish plated with monolayer (Adh), spheroid (Sph), or spheroid derived hMSCs (Sph DC) at the same cell density. MΦ:hMSC (2:1). After 5 h, medium was collected for ELISAs. (B) ELISA for mTNFα in medium from cocultures (n = 3). (C–F) Anti-inflammatory activity of hMSCs in a mouse model of peritonitis. C57BL/6 mice were injected i.p. with zymosan to induce inflammation. After 15 min, the mice were injected i.p. with 1.5×10^6 monolayer hMSCs, 60 spheroids, or 1.5×10^6 spheroid derived cells. After 6 h, peritoneal lavage was collected and mTNFα (C), mMPO (D), and mCXCL2 (E) levels were determined with ELISAs. Total amounts of the specific molecules in the lavage are shown (n = 4–8). After 24 h, blood was collected and plasmin activity was measured from serum (n = 3–6). Values are mean ± SD. Not significant (NS) $P \geq 0.05$, *$P < 0.05$, **$P < 0.01$, and ***$P < 0.001$. Abbreviations: as in Figs. 1 and 6. Bartosh et al. PNAS (2010) [198].

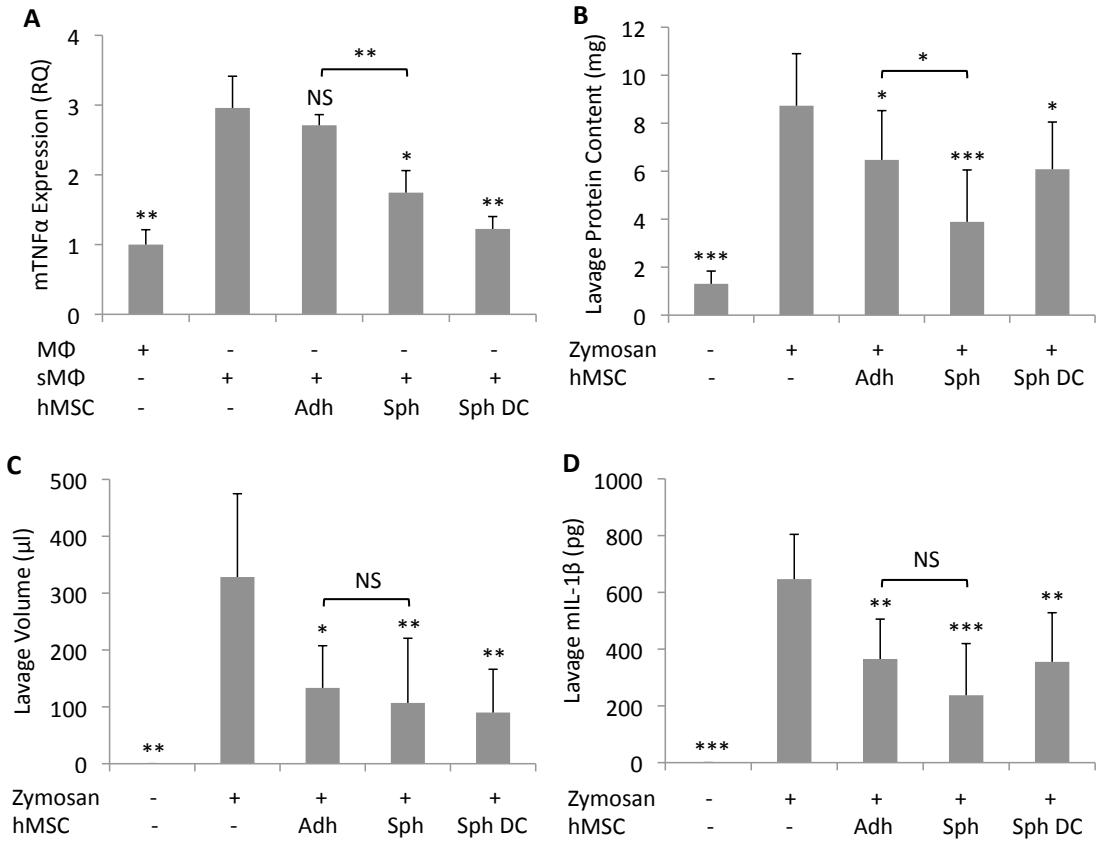

Figure III. 14. hMSC spheroids show increased anti-inflammatory effects in vitro and in vivo. (A) Real-time RT-PCR assays of RNA for mouse TNFα in mouse macrophages (MΦs). MΦs were seeded in the upper chamber of a transwell, stimulated with LPS for 90 min, the LPS was removed, and the chamber transferred to a six-well dish plated with monolayer (Adh), spheroid (Sph), or spheroid derived (Sph DC) hMSCs at equal cell density. MΦ:hMSC (2:1). After 5 h, MΦs were lyzed, RNA was isolated, and mTNFα expression was determined with real-time RT-PCR. Values are mean ± SD (n = 3) normalized to MΦ sample without LPS stimulation. (B–D) Anti-inflammatory activity of hMSCs in a mouse model of peritonitis. C57BL/6 mice were injected i.p. with zymosan to induce inflammation. After 15 min, the mice were injected i.p. with 1.5×10^6 monolayer hMSCs (Adh), 60 spheroids (Sph), or 1.5×10^6 spheroid derived cells (Sph DC). After 6 h, peritoneal lavage was collected and lavage protein content (B), volume (C), and mIL-1β (D) were determined. Values are mean ± SD (negative control, n = 4; vehicle control, n = 6; Adh treated, n = 6; Sph treated, n = 8; Sph DC treated, n = 6). Not significant (NS) $P \geq 0.05$, *$P < 0.05$, **$P < 0.01$, and ***$P < 0.001$. Bartosh et al. PNAS (2010) [198].

To test the effects of spheroid hMSCs on inflammation in vivo, a mouse model of zymosan-induced peritonitis was used [207]. Six hours after i.p. administration of monolayer, spheroid, or spheroid derived hMSCs, inflammatory exudates were collected and used in estimating the level of inflammation. hMSC spheroids significantly decreased the protein content of the lavage fluid (Fig. III.14B) and the volume (Fig. III.14C), neutrophil activity, as assayed by secreted MPO (Fig. III.13D), and levels of the pro-inflammatory molecules TNFα (Fig. III.13C), CXCL2 (Fig. III.13E), and IL-1β (Fig. III.14D). In addition, serum levels of plasmin activity, an inflammation associated protease that is inhibited by TSG-6 [62], were decreased significantly by hMSC spheroids (Fig. III.13F). Serum plasmin activity was reduced approximately to the levels of non-inflammatory control animals 24 h after spheroid injection (Fig. III.13F). Spheroid derived hMSCs also substantially decreased levels of the inflammatory markers assayed, although to a lesser extent than intact spheroids (Fig. III.13C–F and Fig. III.14B–D). Moreover, hMSC spheroids were significantly more effective than adherent monolayer hMSC in suppressing inflammation (Fig. III.13C–F and Fig. III.14B).

III.4. Discussion

Classically hMSCs were isolated and expanded as adherent monolayer cultures, but it was soon recognized that centrifugation of the cells to form micropellets or large aggregates greatly enhanced their chondrogenic differentiation that slowly occurred over several weeks [191,208]. However, several recent publications demonstrated that culture of MSCs in 3D or as spheroids for shorter periods of time improved their therapeutic potential by increased expression of genes such as CXCR4 to promote adhesion to endothelial cells or of IL-24 that has tumor suppressing properties [193,194,203]. The experiments presented here were designed to prepare hMSCs as spheroids that maximally expressed TSG-6, the anti-inflammatory protein that produced beneficial effects in mice with myocardial infarcts because it was expressed at high levels after i.v.-infused hMSCs were trapped in the lung [51].

The results demonstrated that the properties of hMSCs cultured as spheroids depend critically on the experimental conditions. In hanging drops, the cells first formed a network and then most of the cells coalesced into a single spheroid. Optimal levels of TSG-6 expression were observed with spheroids approximately 500 μm in diameter and incubated for 3 d. Expression levels remained high but were lower in larger spheroids, and more of the cells became apoptotic or necrotic in the larger spheroids. Also, more of the cells became apoptotic or necrotic with longer times of incubation. The cells in spheroids retained most of the surface epitopes of hMSCs from adherent cultures. Also, hMSCs dissociated from spheroids retained the potential to differentiate into mineralizing cells and adipocytes. They also expanded at a similar rate as hMSCs from adherent monolayer cultures after a delay through one passage. In addition, spheroid-dissociated hMSCs remained highly clonogenic.

As was observed previously with large hMSC spheroids [192] and hMSCs in 3D culture [203], surveys with mRNA/cDNA microarrays demonstrated marked differences in the transcriptomes compared with hMSCs from adherent cultures. Quantitative assays confirmed some of the important differences. As expected, there was a marked decrease in the anticell-adhesion protein PODXL [204] and a decrease in cell cycling. Of special note was that several of the differences had important implications for the potential therapeutic uses of hMSCs. There were higher levels of expression of the anti-inflammatory protein TSG-6 than previously observed by preincubation of hMSCs with TNFα [51]. Also, there was a high level of expression of STC-1, a protein with both anti-inflammatory and anti-apoptotic effects [67,135]. The high levels of expression of both TSG-6 and STC-1 were maintained for at least 1 d after the cells were dissociated from the spheroids. Therefore the results suggested that both spheroids and spheroid derived hMSCs may be more effective than hMSCs from adherent cultures in modulating inflammatory reactions. The suggestion was confirmed by the demonstration that the spheroids and spheroid derived hMSCs were more effective in suppressing TNFα production by LPS-stimulated macrophages in culture. In addition, they were more effective in suppressing inflammation in an in vivo model for zymosan-induced

peritonitis. Also of special interest was that the spheroid hMSCs expressed high levels of transcripts for the tumor suppressor protein IL-24, an observation made previously with 3D cultures of hMSCs prepared using spinner flasks and a rotating wall vessel bioreactor [203]. In addition, the spheroid hMSCs prepared under the conditions optimized to express TSG-6 also expressed high levels of transcripts for TRAIL that is selective for killing certain cancer cells [209,210] and for CD82 that suppresses some metastases [211]. Therefore, spheroids and spheroid derived hMSCs may be particularly effective as an adjunct therapy for some types of cancers, particularly for therapy of cancers sensitive to anti-inflammatory agents such as aspirin or steroids [212]. A further advantage of the spheroid hMSCs was that they were less than one-fourth the volume of hMSCs from adherent cultures. Therefore a significantly smaller number was trapped in the lung after i.v. infusion and thus larger numbers were found in many tissues [51,204].

The molecular forces that increase expression of anti-inflammatory and anti-tumorigenic genes in hMSCs assembled into spheroids are intriguing but unclear. Cells in spheroids are in close association with each other and probably signal cues to each other much easier than in monolayer cultures, where only a very small part of the cell can touch another cell and secreted molecules must be present in high amounts to ensure communication. The changes in the hMSCs as they form spheroids are probably the result of the non-adherent culture conditions, high degree of confluency, nutrient deprivation, air-liquid interface, and “microgravity” of hanging drops. More detailed studies of each of these and other possible factors must be conducted to have a better understanding of the changes hMSCs accrue when they aggregate into spheroids.

The results presented here indicated that hMSCs can be activated non-chemically in hanging drops to secrete substantial quantities of potent anti-inflammatory proteins and express anti-tumorigenic molecules. Therefore spheroid hMSCs may have advantages for many therapeutic applications. In addition, hMSCs dissociated from spheroids provide extremely small activated cells that could have major advantages for i.v. administration.

CHAPTER IV

MANUSCRIPT 2:

STANNIOCALCIN-1 SUPPRESSES MACROPHAGE RESPONSE TO DANGER SIGNALS BY REDUCING CD14 EXPRESSION AND ATTENUATES ISCHEMIC CARDIAC INJURY

Stanniocalcin-1 (STC-1) is a multifunctional glycoprotein that ameliorates inflammation and tissue injury by reducing oxidative stress. Cardiomyocyte necrosis in the ischemic heart generates 'danger' signals that trigger an often detrimental inflammatory reaction involving monocyte recruitment and differentiation. Therefore, we evaluated the effects of recombinant STC-1 (rSTC-1) on monocyte fate and in a mouse model of myocardial infarction. Using an established protocol to differentiate human monocytes to macrophages, we demonstrated that rSTC-1 did not alter macrophage morphology or expression of the monocyte/macrophage marker CD11b and toll-like receptor (TLR) 4. However rSTC-1 treatment prior to monocyte differentiation decreased expression of the TLR4 co-receptor CD14 and levels of TNFα, CXCL2, and CCL2 produced by the differentiated cells in response to the TLR4 ligand lipopolysaccharide. Moreover, rSTC-1 treatment reduced CD14 expression in monocytes stimulated with endogenous danger signals, and in the ischemic mouse heart. Intravenous administration of rSTC-1 also suppressed levels of IL-1β and MPO, and formation of scar tissue in the infarcted heart while enhancing cardiac function. The data suggests that one of the beneficial effects of STC-1 might be attributed to suppression of CD14 on recruited monocytes/macrophages that limits their inflammatory response. STC-1 may be a promising therapy to protect the heart and other tissues from ischemic injury.

IV.1. Introduction

STC-1 is a conserved glycoprotein with an unusual history both in terms of its evolution and as a subject for biological research [69,70,110]. STC-1, formerly called hypocalcin, was named after it was discovered to be secreted by the corpuscles of Stannius, small endocrine glands that were found in bony fish and that were initially assumed to be adrenal glands because of their location on the ventral surface of the kidneys. However, surgical removal of the glands caused toxic hypercalcemia and led to the finding that STC-1 is a critical regulator of plasma calcium and phosphate homeostasis in the fishes. This role has since been replaced in mammals by parathyroid hormone, calcitonin, and 1, 25-dihydroxyvitamin D [70]. Instead, STC-1 in mammals is produced by a variety of tissues and has been proposed to regulate a variety of physiological and cellular functions in a paracrine/intracrine fashion. A major intracellular target for STC-1 is mitochondria, the organelle also targeted by other intracrines such as angiotensin II, TGF-β, growth hormone, atrial natriuretic peptide, and Wnt 13 [69]. Binding sites for STC-1 have been identified on cell membrane fractions and on mitochondria [118], but the major effects of STC-1 have been difficult to define. Some observations demonstrated that STC-1 reversibly inhibits transmembrane calcium currents through L-type channels in cardiomyocytes [140] and decreases cytokine-induced intracellular calcium signals in macrophages [147] suggesting that it has a continuing but diminished role in calcium metabolism. Other observations emphasized that STC-1 increases expression of mitochondrial UCPs that dissipate the proton gradient and thereby effectively uncouple oxidation from phosphorylation [142,143]. The increase in UCPs reduces the surge of ROS that is often seen with tissue injury and appears to explain, at least in part, the anti-inflammatory and anti-apoptotic properties of STC-1 in mouse models of sepsis [152], glomerulonephritis [135], and retinal degeneration [151]. The decrease in ROS production also appears to explain some of the effects of STC-1 in altering macrophage function [186], and protecting cardiac myocytes from angiotensin II-mediated injury [145]. However, the role of STC-1 on macrophage differentiation and in ischemic myocardial injury has not been studied.

Myocardial infarction is a leading cause of morbidity and mortality worldwide despite advances in therapy [195,197]. Myocardial tissue injury induces the release of endogenous inflammatory mediators or 'danger' signals including cytokines, ROS, and numerous intracellular factors that are inaccessible to the immune system but that are liberated from necrotic cells [197]. TLRs are among the cellular receptors that sense many danger signals released by necrotic cells and provide a key molecular link between tissue injury and inflammatory response [195]. A growing body of evidence suggests that inflammation after ischemic cardiac injury, especially when persistent, can exacerbate pathological remodeling of the heart and promote heart failure; therefore, strategies to regulate inflammatory pathways will improve prognosis after myocardial infarction [196,197].

Accordingly in the present report, we tested the hypotheses that STC-1 regulates macrophage phenotype and response to inflammatory mediators, reduces inflammation in the post-infarcted heart, and protects the heart from damage associated with ischemic injury.

IV.2. Material and Methods

IV.2.1. Cell culture

The human monocyte cell line U937 was purchased from American Type Culture Collection (ATCC, Rockville, MD). The cells were cultured in a humidified atmosphere at 37°C and 5% (v/v) CO_2 in macrophage medium consisting of RPMI-1640 (ATCC) supplemented with 10% (v/v) heat-inactivated fetal bovine serum (FBS, Atlanta Biologicals, Flowery Branch, GA), 100 units/ml penicillin and 100 µg/ml streptomycin (Gibco, Grand Island, NY).

IV.2.2. Monocyte differentiation assay

To induce macrophage differentiation of U937 monocytes, the cells were suspended at 500,000 cells/ml in petri dishes (VWR international, Radnor, PA) and

stimulated for 48 hours with 100 ng/ml of phorbol 12-myristate 13-acetate (PMA, Sigma-Aldrich, St. Louis, MO). In separate experiments, U937 cells were stimulated concurrently with 5 μg/ml recombinant human HMGB1 (R&D systems, Minneapolis, MN) and recombinant human TNFα, IL-1β, and IL-6 (10 ng/ml each, R& D Systems). Differentiation assays were performed in the presence or absence of 1.0 μg/ml of human rSTC-1 (BioVendor Research and Diagnostic Products, Asheville, NC or Czech Republic). After 48 hours, images of the cells were captured on a Nikon Eclipse Ti-S inverted microscope using a Ds-Fi1 camera (Nikon, Melville, NY) and managed with NiS Elements AR 3.0 software (Nikon). The differentiated macrophages were subsequently harvested, counted, and processed for real-time RT-PCR or flow cytometry analysis.

IV.2.3. In vitro inflammatory assay

U937 monocytes stimulated for 48 hours with PMA (in the presence or absence of rSTC-1) were seeded at 600,000 cells/ml into 24-well culture plates (Corning Incorporated, Corning, NY). After a 3 hour recovery period, 50 ng/ml of LPS (Sigma-Aldrich) was added to the cultures. In some experiments cultures of differentiated macrophages were treated with 1.0 μg/ml rSTC-1 just prior to LPS stimulation. Five hours later, CM of unstimulated or LPS-stimulated macrophages were collected. Cells and debris were removed from the CM by centrifugation at 500 x g for 5-10 minutes. Several aliquots were prepared from the CM and stored at -80°C until they were used for ELISA.

IV.2.4. Ischemic cardiac injury model

The experimental protocols were approved by the Institutional Animal Care and Use Committee of Texas A&M University Health Science Center and in accordance with guidelines set forth by the National Institutes of Health. Male immunodeficient NOD/scid mice (NOD.CB17-Prkdcscid/J, Jackson Laboratory, Bar Harbor, Maine), 7–8 weeks of age and 25-30 grams of body weight, were used for this study to reduce the

immune reaction to human protein. The mice were kept on a 12 hour light-dark cycle and were provided sterile food and water ad libitum. To induce ischemic cardiac injury, mice were mechanically ventilated and maintained under anesthesia with isoflurane (1.5%, v/v) during the course of the procedure. The thoracic cavity was opened via an incision made at the left 5th intercostal space to visualize the left anterior descending coronary artery (LAD). An 8-0 prolene suture (Ethicon, Somerville, NJ) was positioned around the LAD distal to the first diagonal branch and permanently tied. After myocardial infarction was confirmed by ventricular blanching, the chest was closed. rSTC-1 (2.0 mg/kg body weight) in 0.9% (w/v) sodium chloride (Sigma-Aldrich) or equal volume of saline was injected intravenously 1 hour and 24 hours after ligation. To alleviate post-operative discomfort, buprenorphine (0.1 mg/kg) was administered subcutaneously twice daily for up to 5 days. For endpoint assays, the mice were euthanized by intraperitoneal injection of ketamine (80 mg/kg) and xylazine (8 mg/kg). Levels of inflammatory mediators in the heart were determined from cardiac tissue lysates prepared 48 hours after ligation. Cardiac function was evaluated on day 21 and mice were euthanized to determine infarct size.

IV.2.5. Evaluation of cardiac function

Cardiac ejection fraction was determined by transthoracic echocardiography 21 days after ligation of the LAD (LLDCA) using a 30 MHz transducer supported by a Vevo 2100 ultrasound instrument (VisualSonics Inc., Toronto, Canada). The procedure was performed on mice under isoflurane anesthesia. Heart rate was maintained at 350-400 beats per minute. Left ventricular ejection fraction (LVEF) was evaluated from parasternal long axis position. The average of two separate recordings containing 3 consecutive cardiac cycles were used per animal to obtain the LVEF.

IV.2.6. Infarct size measurement

Measurements of infarct size were performed on hearts obtained 21 days after surgery. Hearts were perfused with 3-5 ml of saline, excised from the chest, and fixed in

10-15 ml of 10% (v/v) formalin (Sigma-Aldrich) to be processed for staining. Paraffin-embedded heart samples were cut into 5 μm sections from the apex to the base. Every 20th section was stained with Masson Trichrome. Quantitative assays for infarct size were performed as described by Takagawa and colleagues [213]. Images of every fifth stained section covering both ventricles (total of 10 sections per heart) were acquired using a Photometrics Coolsnap HQ2 camera mounted on a Nikon Eclipse Ti-E inverted microscope (Nikon). NiS Elements AR 3.0 software (Nikon) was used to measure midline infarct length of heart.

IV.2.7. Real-time RT-PCR

Total RNA was isolated from cells using RNeasy Mini Kit (Qiagen, Valencia, CA) with DNase I (RNase-Free DNase Sel, Qiagen) digestion step. The isolated RNA was quantified with nanodrop spectrophotometer (ThermoFisher Scientific, Rockford, IL) and converted to cDNA with High-Capacity cDNA RT Kit (Applied Biosystems, Technologies, Grand Island, NY). Real-time RT-PCR was performed in triplicate for expression of *human GAPDH*, *CD11b* (*ITGAM*), *CD14*, *TLR2*, and *TLR4* using TaqMan® Gene Expression Assays (Applied Biosystems, Technologies) and TaqMan® Fast Master Mix (Life Technologies). Total of 20 ng of cDNA was used for each 20 μl reaction. Thermal cycling was performed with 7900HT System (Applied Biosystems, Technologies) by incubating the reactions at 95° C for 20 seconds followed by 40 cycles of 95° C for 1 second and 60° C for 20 seconds. Data were analyzed with Sequence Detection Software V2.3 (Applied Biosystems, Technologie) and relative quantitation (RQ)s were calculated with comparative critical threshold (Ct) method using RQ Manager V1.2 (Applied Biosystems, Life Technologies).

IV.2.8. Enzyme-linked immunosorbent assay (ELISA) for markers of inflammation

Levels of the inflammatory mediators TNFα, CXCL2, and CCL2 were determined in cell-free U937 CM using commercially available ELISA Kits (TNFα and CCL2 were from R&D Systems and CXCL2 from Abnova, Taipei City, Taiwan). To

determine levels of inflammation in the heart, ventricular tissue was minced with surgical scissors, transferred to tissue extraction reagent I (Life Technologies) containing 1x of Halt protease inhibitor cocktail (ThermoFisher Scientific), and homogenized using a PowerGen model 125 tissue grinder (ThermoFisher Scientific). The lysates were centrifuged at 1,000 x g for 10 minutes 4°C. The protein rich supernatant was transferred to new tubes and centrifuged at 12,000 x g for 10 minutes. Several aliquots were prepared from the supernatants and stored at -80°C. Protein concentration was determined with micro BCA protein assay kit (ThermoFisher Scientific) per manufacturer's instructions. Levels of mouse MPO, CD14, and IL-1β were measured using commercially available ELISA Kits (CD14 and IL-1β were form R&D Systems and MPO from Hycult Biotech, Plymouth Meeting, PA). The optical density was determined on a plate reader (FLUOstarOmega; BMG Labtech) at an absorbance of 450 nm with wavelength correction at 540 nm. Where appropriate, samples were diluted prior to running the assay so that the optical density detected for the sample fit within the standard curve of the ELISA kit.

IV.2.9. Flow cytometry analysis

Cell surface expression of CD11b and CD14 was determined by flow cytometry. U937 cells were suspended at 2,000 cells/μl in 100 μl of cold PBS (Gibco) containing 2% (v/v) FBS and then incubated for 20 min with 20 μl of human Fc receptor binding inhibitor (Affymetrix eBioscience, San Diego, CA). Without washing, cell suspensions were labeled with 0.2 μg of fluorescein-conjugated antibodies to CD11b (Clone Bear1, Beckman Coulter, Brea, CA) or CD14 (Clone RMO52, Beckman Coulter) for 20 min at room temperature. Isotype matched antibodies were used as controls. After 2 washes in PBS, cells were again suspended in PBS containing 2% FBS and analyzed on an FC500 flow cytometer (Beckman Coulter). A minimum of 10,000 events was examined from the viable cell population. Data were analyzed using CXP Software (Beckman Coulter).

IV.2.10. Statistical analyses

Unpaired two-tailed Student's t-test was used to compare data sets consisting of two treatment groups. One-way ANOVA was used to calculate levels of significance between multiple groups. Statistical analysis was performed with Graphpad Prism 5 software.

IV.3. Results

IV.3.1. Recombinant STC-1 modulates the inflammatory response of differentiated human monocytes in vitro

To evaluate the effects of rSTC-1 treatment on monocyte differentiation and inflammatory response, we modified an established protocol that uses the protein kinase C (PKC) activator PMA to promote the differentiation of U937 human monocytes into macrophages [214]. Here, U937 cells were stimulated with 100 ng/ml of PMA for 48 hours in the presence or absence of 1 μg/ml rSTC-1. The differentiated U937 cells were harvested, re-plated, and activated with 50 ng/ml of LPS. Five hours later, CM of the macrophages were collected (Fig. IV.1A) and used to evaluate levels of inflammatory cytokines/chemokines. As shown, PMA-differentiated U937 cells secreted high levels of TNFα, CXCL2, and CCL2 in response to LPS (Figs. IV.1B-D). Addition of rSTC-1 to the cultures prior to PMA treatment significantly reduced the secretion of these cytokines and chemokines (Figs. IV.1B-D). We then examined the effects of rSTC-1 on inflammatory response of newly differentiated macrophages. In these experiments, U937 monocytes were first differentiated with PMA for 48 hours and then treated with rSTC-1 just prior to LPS stimulation (Fig. IV.1E). Secretion of TNFα, CXCL2, and CCL2 in response to LPS was unchanged by treatment with rSTC-1 when it was applied to the cultures after the cells were differentiated (Figs. IV.1F-H). These results indicate that rSTC-1 therapy, during monocyte differentiation but not after, suppresses macrophage r esponse to inflammatory stimuli.

Figure IV. 1. Recombinant stanniocalcin-1 (rSTC-1) treatment, prior to monocyte differentiation but not after, suppressed the inflammatory response of macrophages to danger signals. (A) Schematic illustrating the strategy used to evaluate the effects of rSTC-1 pre-treatment on macrophage response to lipopolysaccharide (LPS). Human U937 monocytes were induced to differentiate into macrophages by treatment with 100 ng/ml of phorbol 12-myristate 13-acetate (PMA) in the presence or absence of 1 μg/ml of rSTC-1. After 48 hours, differentiated macrophages were harvested, plated, and incubated for another 3 hours. Then, macrophages were stimulated with 50 ng/ml of LPS. After 5 hours, media conditioned (CM) by unstimulated or LPS-stimulated macrophages were collected and used to evaluate changes in levels of secreted TNFα (B), CXCL2 (C), and CCL2 (D) by ELISA. (E) Schematic illustrating the strategy used to evaluate the effects of rSTC-1 on the response of differentiated macrophages to LPS. U937 monocytes were plated in macrophage medium supplemented with 100 ng/ml of PMA for 48 hours. Differentiated macrophages were harvested, re-plated, and incubated with or without 1 μg/ml of rSTC-1. After 3 hours, macrophages were stimulated with LPS for an additional 5 hours. The CM was collected, clarified by centrifugation and used to determine levels of TNFα (F), CXCL2 (G), and CCL2 (H) by ELISA. Values are presented as mean + SEM (n=3). Statistical significance was determined using ANOVA (B-D) or student's t-test (F-H) (not significant, ns $p \geq 0.05$; ***$p < 0.001$).

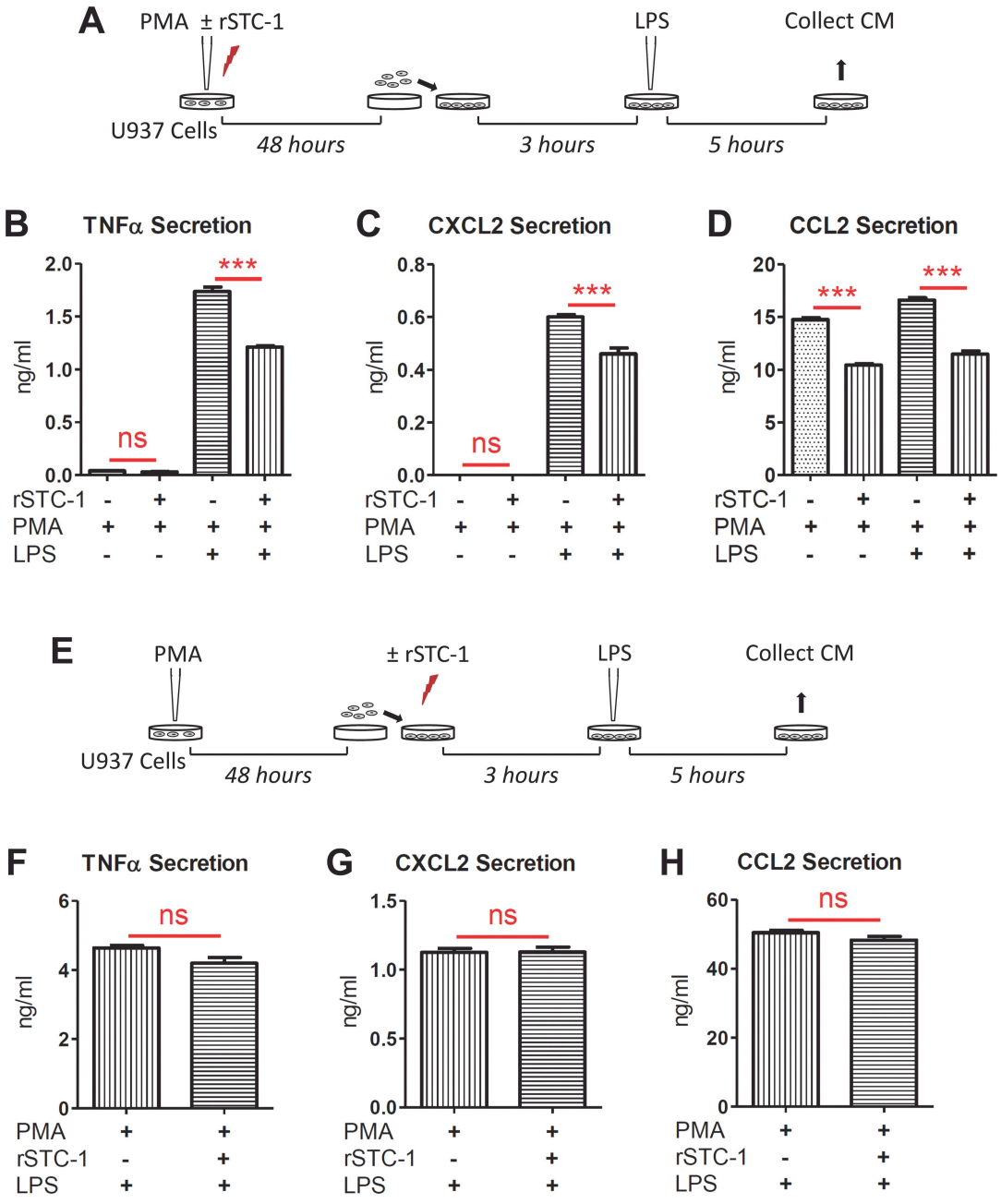
A
PMA ± rSTC-1
LPS
Collect CM
U937 Cells
48 hours
3 hours
5 hours
B
TNFα Secretion
C
CXCL2 Secretion
D
CCL2 Secretion
ng/ml
ns
***
rSTC-1
PMA
LPS
E
PMA
± rSTC-1
LPS
Collect CM
U937 Cells
48 hours
3 hours
5 hours
F
TNFα Secretion
G
CXCL2 Secretion
H
CCL2 Secretion

IV.3.2. Recombinant STC-1 regulates the expression of surface markers on differentiating macrophages

To explore the mechanism(s) that drive the inhibitory effects of rSTC-1 on differentiating monocytes, we evaluated phenotypic changes of U937 cells in response to PMA and rSTC-1. In these experiments, U937 cells were stimulated with PMA for 48 hours in the presence or absence of rSTC-1 and then analyzed by microscopy, flow cytometry, and real-time RT-PCR (Fig. IV.2A). In culture, undifferentiated U937 monocytes propagate in suspension as single cells that ultimately form adherent colonies in the presence of PMA (Fig. IV.2B). Analysis by microscopy revealed that cells treated simultaneously with PMA and rSTC-1 shared a similar morphology to cells incubated with PMA alone (Fig. IV.2B). We next assayed for changes in expression of monocyte/macrophage surface markers by flow cytometry. We observed a dramatic increase in cell surface expression of CD11b and CD14 on PMA-differentiated macrophages (Fig. IV.2C). Interestingly, rSTC-1 treatment caused a marked reduction in cell surface expression of CD14 without changing CD11b levels (Fig. IV.2C). Since CD14 is a well-known co-receptor for TLR2 and TLR4 [176], we examined mRNA levels of these TLRs in addition to CD11b and CD14 by real-time RT-PCR. As expected, the expression of CD11b, CD14, TLR2, and TLR4 was increased in U937 cells differentiated with PMA (Figs. IV.2D-G); however, we detected a notable decline in CD14 message levels after treatment with PMA and rSTC-1 (Fig. IV.2E) but did not detect significant effects of rSTC-1 on amount of CD11b and TLR4 mRNA (Figs. IV.2D and F). In contrast, the expression of TLR2 was significantly increased in U937 cells treated with rSTC-1 (Fig. IV.2G). These data suggest that rSTC-1 suppresses macrophage response to danger signals by attenuating the up-regulation of the TLR co-receptor CD14 in differentiating macrophages.

Figure IV. 2. Expression of CD14 was reduced in differentiating monocyte/macrophages by treatment with recombinant stanniocalcin-1 (rSTC-1). Human U937 monocytes were incubated in macrophage medium supplemented with 100 ng/ml of phorbol 12-myristate 13-acetate (PMA) in the presence or absence of 1.0 μg/ml of rSTC-1. After 48 hours, morphology of differentiated macrophages was evaluated by light microscopy. Then, macrophages were harvested and processed for real-time RT-PCR or flow cytometry analysis. (A) Schematic showing the workflow. (B) Representative images of undifferentiated U937 monocytes (No Treatment), PMA-differentiated U937 macrophages (PMA), and U937 cells stimulated with PMA and rSTC-1 (PMA+ rSTC-1). 10x magnification (C) Cell surface expression of CD11b and CD14 was assessed by flow cytometry. Real-time RT-PCR for CD11b (D), CD14 (E), TLR4 (F), and TLR2 (G) in undifferentiated U937 monocytes and cells stimulated with PMA for 48 hours (with and without rSTC-1 treatment). Values are expressed as mean + SEM (n=3). Data was analyzed using ANOVA (not significant, ns $p \geq 0.05$, *$p < 0.05$, **$p < 0.01$, ***$p < 0.001$).

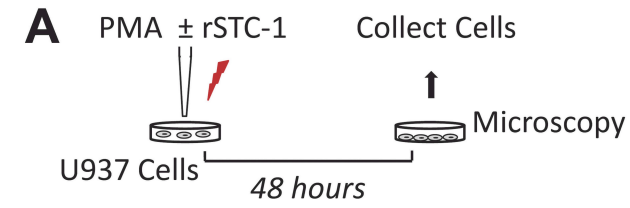
A
PMA ± rSTC-1
Collect Cells
Microscopy
U937 Cells
48 hours

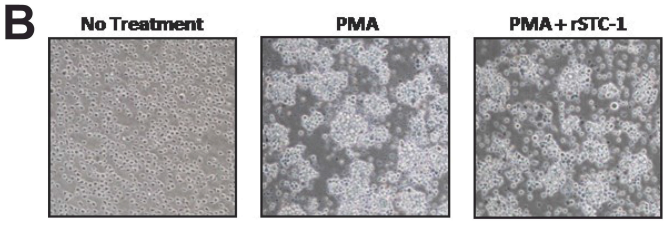
B
No Treatment
PMA
PMA + rSTC-1

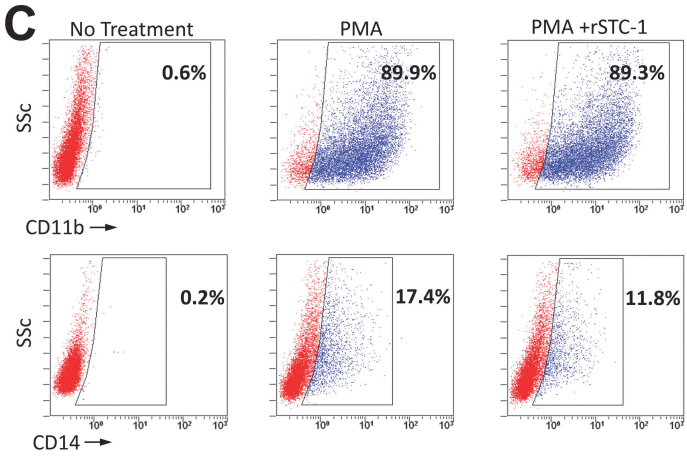
C
No Treatment
PMA
PMA +rSTC-1
0.6%
89.9%
89.3%
SSc
CD11b
0.2%
17.4%
11.8%
SSc
CD14

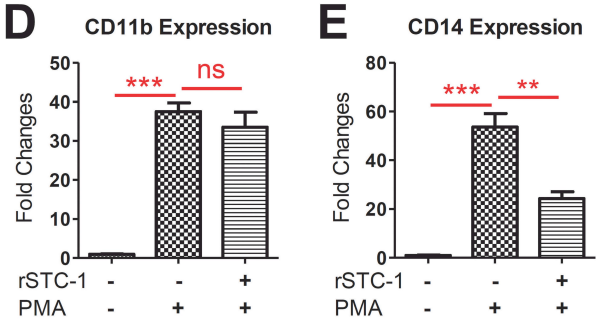
D
CD11b Expression
Fold Changes
***
ns
rSTC-1
PMA
E
CD14 Expression
Fold Changes
***
**
rSTC-1
PMA

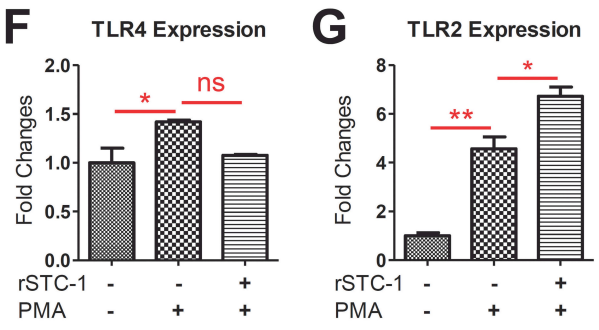
F
TLR4 Expression
Fold Changes
*
ns
rSTC-1
PMA
G
TLR2 Expression
Fold Changes
**
*
rSTC-1
PMA

IV.3.3. The effect of rSTC-1 on CD14 is PMA independent

To further explore the role of STC-1 on monocyte-to-macrophage differentiation, we evaluated the effects of rSTC-1 on expression of CD11b and CD14 in U937 monocytes in response to numerous inflammatory stimuli classically associated with ischemic tissue injury. As shown, U937 cells were stimulated with a pro-inflammatory cocktail consisting of 5 μg/ml human HMGB1 and 10 ng/ml each of recombinant human TNFα, IL-1β, and IL-6 (Figs. IV.3A). After 48 hours, differentiated macrophages were lysed to quantify mRNA levels of CD11b and CD14 by real-time RT-PCR. The expression of CD11b was increased significantly after the cells were stimulated with the inflammatory cocktail in the presence and absence of rSTC-1 (Fig. IV.3B). In contrast, we observed a dramatic reduction in U937 cell expression of CD14 (Fig. IV.3C) similar to that observed previously with PMA treated cells. The data indicates that STC-1 suppresses inflammatory response of newly differentiated macrophages driven by the ischemic tissue microenvironment, such as observed with myocardial infarction, by inhibiting CD14 expression.

IV.3.4. CD14 expression and inflammatory response in the ischemic heart were diminished by intravenous administration of rSTC-1

Based on our observations demonstrating the inhibitory effects of rSTC-1 on macrophage CD14 expression and response to LPS, we hypothesized that rSTC-1 treatment reduces inflammation following acute myocardial infarction and protects the ischemic heart. For these experiments a myocardial infarct was generated in NOD/scid mice by permanent LLDCA and rSTC-1 was administered intravenously (2.0 mg/kg) 1 hour and 24 hours after ligation. To study the effects of rSTC-1 on inflammation, the mice were euthanized 48 hours after surgery and the heart tissues were processed (Fig. IV.4A) for ELISA. The amount of CD14 protein was increased in heart lysates following

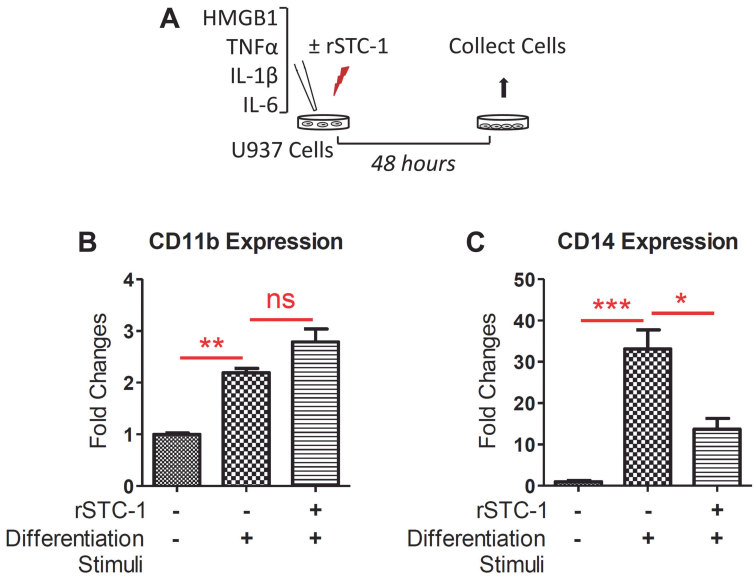

Figure IV. 3. Recombinant stanniocalcin-1 (rSTC-1) reduced CD14 expression in monocyte/macrophages stimulated with danger signals. Human U937 monocytes were stimulated with 5 μg/ml human high mobility group box1 (HMGB1) and 10 ng/ml each of recombinant human tumor necrosis factor alpha (TNFα), interleukin 1 beta (IL-1β), and IL-6 in the presence or absence of 1.0 μg/ml rSTC-1 treatment. After 48 hours, cells were lysed for real-time RT-PCR. (A) Schematic showing the workflow. The fold changes of mRNA levels for CD11b (B) and CD14 (C) were measured in unstimulated U937 monocytes, stimulated U937 monocytes, and stimulated cells treated simultaneously with rSTC-1. Values are expressed as mean + SEM (n=3). Data were analyzed with ANOVA (not significant, ns $p \geq 0.05$, *$p < 0.05$, **$p < 0.01$, ***$p < 0.001$).

infarction. In a manner similar to our in vitro data using U937 cells, administration of rSTC-1 significantly reduced levels of CD14 protein (Fig. IV.4B). Moreover rSTC-1 treatment reduced cardiac levels of MPO (Fig. IV.4C); a bio-marker of tissue injury that is produced mainly by activated neutrophils and macrophages, and that has powerful pro-oxidative and pro-inflammatory properties [197,215]. Since the life span of inflammatory cells can be prolonged in the pro-inflammatory environment due to the effects of several cytokine mediators such as IL-1β [216], we measured levels of IL-1β in the heart lysate. We observed that IL-1β amount was increased 48 hours after LLDCA; however, the amount of this cytokine was significantly reduced after rSTC-1 treatment (Fig. IV.4D). Collectively, these data suggest that STC-1 suppresses levels of

inflammatory mediators in the heart following myocardial infarction and can protect cardiomyocytes from injury directly caused by MPO.

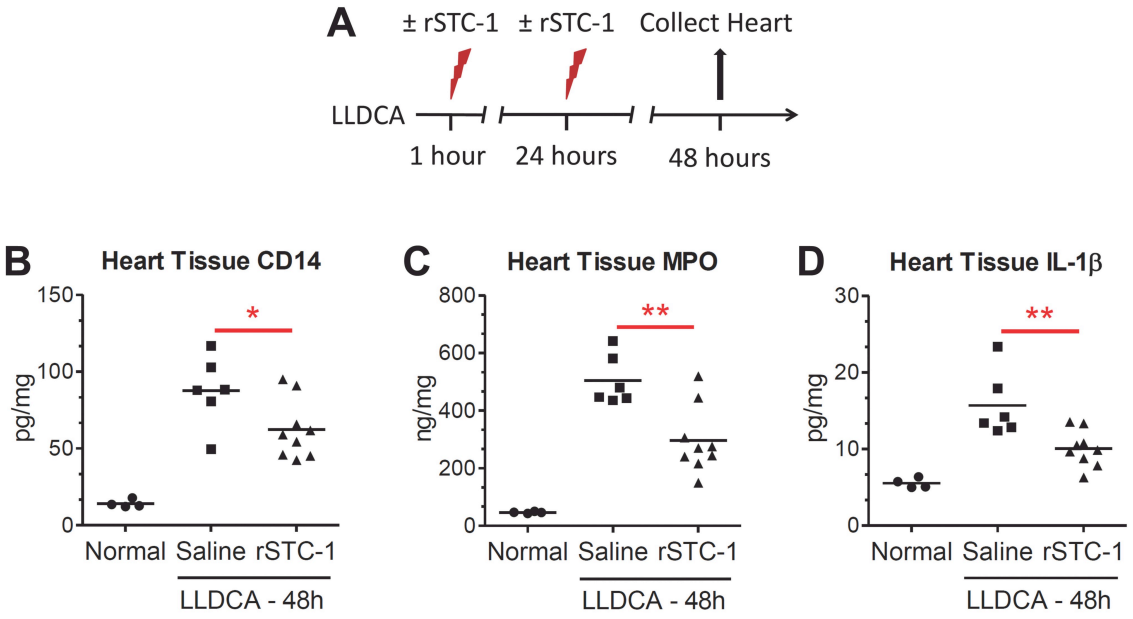

Figure IV. 4. Intravenous administration of recombinant stanniocalcin-1 (rSTC-1) reduced the expression of CD14 in cardiac tissue and attenuated inflammation following myocardial infarction. NOD/scid mice were subjected to ischemic cardiac injury by permanent ligation of the left anterior descending coronary artery (LLDCA). At 1 hour and 24 hours after ligation, 2.0 mg/kg of rSTC-1 or equal volume of 0.9% sodium chloride (saline) was administered intravenously. Mice were euthanized 48 hours after LLDCA to collect heart tissue and assess inflammatory response. (A) Diagram showing the workflow of the cardiac injury model. Amounts of CD14 (B), myeloperoxidase (MPO) (C), and interleukin 1 beta (IL-1β) (D) were determined by ELISA on heart tissue lysates prepared 48 hours after LLDCA. Values are expressed as mean (n=4-9). Statistical significance was determined using student's t-tests (* $p < 0.05$, ** $p < 0.01$).

IV.3.5. Intravenous administration of rSTC-1 improves heart function and reduced scar formation in ischemic cardiac injury

To examine the therapeutic effects of rSTC-1, myocardial infarction was induced in NOD/scid mice followed by 2 injections of rSTC-1 (2.0 mg/kg) as described previously. Changes in heart function were determined with echocardiography by measuring LVEF on anesthetized mice 21 days after LLDCA (Fig. IV.5A). The results

showed a substantial decrease in LVEF following coronary artery ligation that was improved significantly by treatment with rSTC-1 (Fig. IV.5B). After cardiac function was evaluated, the hearts were removed from the chest and infarct size measured from paraffin embedded sections stained with Masson Trichrome (Figs. IV.5C and D). We observed that rSTC-1 decreased the length of the ventricular infarct region (Figs. IV.5C and D). Thus, STC-1 treatment results in reduced cardiac scarring and functional improvements of the ischemic heart.

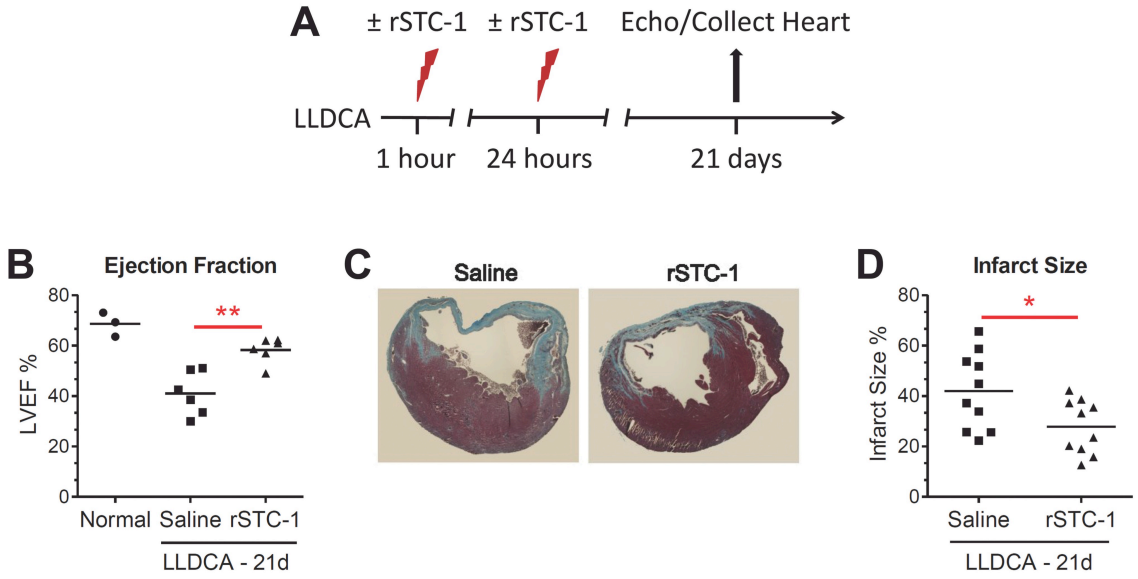

Figure IV. 5. Recombinant stanniocalcin-1 (rSTC-1) administered intravenously improved heart function and reduced infarct size. NOD/scid mice were subjected to ischemic cardiac injury by permanent ligation of the left anterior descending coronary artery (LLDCA). At 1 hour and 24 hours after ligation, 2.0 mg/kg of rSTC-1 or equal volume of 0.9% sodium chloride (saline) was administered intravenously. Twenty one days after permanent LLDCA, NOD/scid mice were anesthetized and their left ventricular ejection fraction (LVEF) was evaluated. Then, mice were euthanized to collect heart tissue and assess infarct size. (A) Diagram showing the workflow of the cardiac injury model. (B) Each data point represents the average LVEF of 2 independent recordings with 3 consecutive cardiac cycles (n=3-6). (C) Representative images showing fibrosis in heart sections stained with Masson Trichrome. 4x magnification. Infarct size was measured at the ventricular midline of each section and expressed as the percent length of the fibrotic region relative to the ventricular midline length. (D) Each data point represents the average of ten infarct size measurements per heart (n=10-12). Data was analyzed using student's t-tests (*p< 0.05, **p< 0.01).

IV.4. Discussion

Macrophages and their precursor -monocytes- are among important immune effector cells that instruct inflammatory processes to defend against pathogens and promote wound healing [160]. Upon tissue injury or infection, monocytes are recruited to foci of inflammation and, in response to a variety of signals emanating from the microenvironment, differentiate into functional tissue macrophages [160,197]. Tight control of these processes is essential to prevent excessive inflammation and collateral tissue destruction.

The glycoprotein STC-1 originally identified as a calcium regulatory hormone in fish [70,110] has emerged, for multiple reasons, as a candidate to modulate monocyte behavior and inflammatory response. First, STC-1 expression is widely distributed and responsive to numerous stress-inducing factors including hypoxia [128,129], oxidative stress, and inflammation [147,152]. We reported previously that STC-1 expression is upregulated in mesenchymal stem cells (MSCs) by signals from dying cells [67,185,217] and in response to caspase activation and inflammatory cytokines [185]. Second, STC-1 is reported to blunt the rise in levels of mitochondrial ROS generated in stimulated macrophages [143] and decrease activation of the NLRP3 inflammasome [186], a cytosolic multiprotein complex present in myeloid cells that promotes cytokine maturation [61,218]. While mechanisms for the pleiotropic actions of STC-1 have not been entirely defined, most studies emphasize that the antioxidant property of the protein involves induction of UCPs and dissipation of the mitochondrial proton gradient [143,145,146].

In exploring the effects of STC-1 here, we discovered that STC-1 can potentially regulate inflammation by controlling monocyte phenotype independent of its effects on ROS. Specifically, we observed that STC-1 suppresses the PKC-dependent rise in monocyte expression of CD14, a myeloid cell receptor that detects indicators of ‘danger’ originating from pathogens or damaged tissue, and delivers these products to specific pro-inflammatory TLRs. In subsequent experiments, we observed similar suppressive effects of STC-1 on CD14 expression in monocytes stimulated with a variety of

cytokines and danger signals classically associated with tissue injury. Interestingly, the effects on CD14 expression in monocytes were relatively specific given that STC-1 treatment did not alter levels of CD11b or TLR4 and promoted a moderate increase in expression of TLR2.

Our immune system is designed to combat the threat of both infection and injury by responding to a particular set of molecular cues or patterns that are normally undetectable or absent. TLRs play a major role in this process by distinguishing the conserved motifs of pathogens (PAMPs), and the endogenous factors released upon sterile tissue injury (DAMPs). There is considerable evidence that both PAMPs and DAMPs share many TLRs on macrophages and perpetuate inflammatory cytokine production [61]. There is also considerable evidence indicating that DAMP-mediated TLR signaling is implicated in the pathobiology of numerous inflammatory and autoimmune diseases [219-221]. For this reason, TLRs and factors associated with TLR signaling have become attractive therapeutic targets [61,195].

One of these factors, CD14, can be highly expressed by monocytes/macrophages and is heavily implicated in the behavior of these cells. It is best known as a pattern recognition receptor of the innate immune system that directly interacts with bacterial endotoxin (LPS) to induce intracellular pro-inflammatory signaling cascades through TLR4. However, CD14 also recognizes peptidoglycans and products of apoptotic/necrotic cells such as the transcription factor HMGB1 [179]. The role of CD14 in disease progression has become apparent with studies revealing that CD14 deficient mice are protected against LPS-induced cardiac inflammation [222], ischemic tissue injury [223], and septic shock [178]. Moreover, several studies have demonstrated that TLR4 inhibition with antibodies or knockout strategies is associated with cardiac benefits following infarction that include attenuation of myocardial inflammation and reduction in infarct size [224-226].

Together these findings here and from others support our initial observation that STC-1 effectively reduced cytokine production by monocytes/macrophages stimulated with LPS but only when the protein was applied concurrently with PMA to prevent the

cells from acquiring a CD14 positive phenotype. These findings also explain, at least in part, our observations that STC-1 treatment suppressed inflammation in the heart and improved cardiac function after ischemic injury by reducing levels of cardiac CD14.

Similar to the sequence of events that accompany ischemic injury in many tissues, myocardial ischemia and the resulting formation of necrotic cells triggers an intense inflammatory reaction that is important for monocyte recruitment and tissue repair but when lingering can become disadvantageous for tissue function [195-197]. It has been shown that both DAMP/TLR and IL-1 signaling can exacerbate post-infarction cardiac inflammation and lead to symptoms of heart failure [195,197]. Here we showed that STC-1 can potentially protect the heart by reducing levels of IL-1β suggesting that it could be employed in therapeutic regimens for treatment of patients suffering from ischemic cardiac injury. Previous studies support this concept having demonstrated that STC-1 inhibits ischemic injury to the kidney [227] and brain [128]. The improvements we noted in heart function with STC-1 treatment were also preceded by efficient reduction in levels of MPO, an enzyme found in neutrophils that catalyzes production of hypochlorous acid and other highly reactive moieties with important microbicidal properties [228]. However, MPO can be toxic to cells and detrimental to the remodeling process after myocardial infarction therefore, reduction in levels of MPO can prevent deterioration of cardiac tissue. Our data suggest that STC-1 treatment might reduce cardiac MPO through downregulation of CD14 in the heart and subsequent decrease in macrophage response to DAMPs that signal through CD14. Alternatively, reduction of MPO in the infarcted heart could be a result of the ability for STC-1 to decrease permeability of vascular endothelial cells [229] and prevent migration of neutrophils.

Regardless, STC-1 is an intriguing protein that exerts multiple beneficial effects in damaged mammalian tissue. Yet, the signaling pathways that drive STC-1 action have not been clearly defined and specific receptors that bind STC-1 have not been determined. Moreover, knowledge of the distribution of STC-1 following intravenous administration is lacking as well as our understanding of how STC-1 might regulate monocyte function in vivo. Future studies are being designed to find answers to these

concepts. With a recent study identifying a reservoir of splenic monocytes that are deployed to the infarcted heart [157], it is feasible to hypothesize that STC-1 does not suppress inflammation by directly binding to cardiac cells but instead associates with monocytes from the blood and spleen, and suppresses CD14 expression in these cell populations. This hypothesis is supported by previous observations that TLR inhibition prevents systemic inflammation following myocardial infarction [224-226,230-232].

In conclusion, as shown in Figure IV.6, our data demonstrate the STC-1 regulates monocyte phenotype in response to a variety of differentiation stimuli and, in turn, suppresses levels of inflammatory factors produced by activated monocytes/macrophages. Moreover, we demonstrate that STC-1 treatment effectively attenuates inflammation in the ischemic heart and improves cardiac function. Our observations provide a novel mechanism for STC-1 action that could be important for tissue repair by preventing excessive inflammatory response without disrupting the tissue healing properties of macrophages.

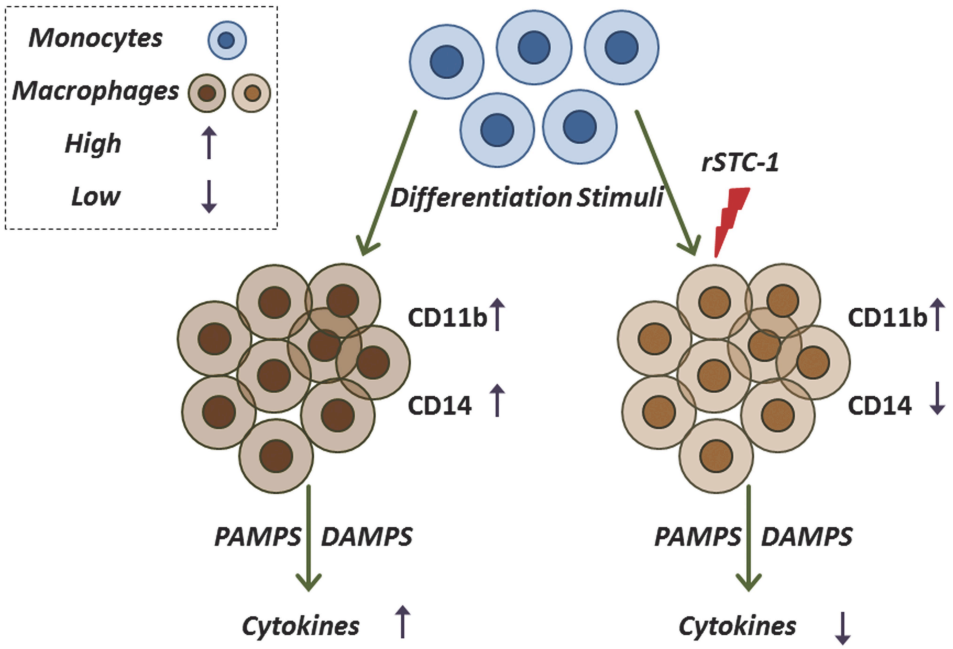

Figure IV. 6. Summary of recombinant stanniocalcin-1 (rSTC-1) effects on monocyte/macrophage differentiation and function. Tissue injury induces release of differentiation stimuli (such as pathogen-associated molecular pattern molecules (PAMPs), damage-associated molecular pattern molecules (DAMPs), cytokines, and chemokines) that promotes monocyte differentiation and recruitment to the site of injury. Differentiation stimuli cause an increase in expression of surface molecules such as CD11b and CD14 in monocyte/macrophage and enhance secretion of inflammatory cytokines and chemokines (for example TNFα, IL-1β, CXCL2, and CCL2) in these cells. Administration of rSTC-1 during differentiation process reduces the expression of CD14 in monocyte/macrophage, which decreases the secretion of inflammatory cytokines and chemokines and reduces the inflammatory response to the tissue injury.

CHAPTER V
CONCLUSION

Inflammation is an essential mechanism for removing infectious agents, protecting tissue from insults, and promoting repair in damaged organ. The usual outcome of the acute inflammatory action is successful elimination of infection and repair of tissue damage. However, failure in removing offending agents, or constant exposure to the irritants can lead to persistent activation of immune cells. The production of proteases, ROS, and growth factors by activated neutrophils and macrophages can cause tissue destruction. In addition, aberrant collagen formation by activated fibroblasts leads to excessive scarring and loss of organ function; therefore, activated immune cells such as monocytes/macrophages function as a double-edged sword with both offensive as well as defensive actions at a site of injury.

Multipotent MSCs can respond to the microenvironment of injured tissues. The cells generate immune-modulatory and anti-inflammatory effects via cell-to-cell interaction, secretion of regulatory factors, and exosomes. The dramatic beneficial effects of MSCs observed in various disease models have supported their use in numerous clinical trials. Since MSCs have low immunogenicity with limited risks of tumorigenicity, their applications for allogeneic transplantation are known to be safe. Signals from injured tissues activate MSCs to secrete beneficial factors and contribute in immune/inflammatory modulation and tissue healing; however, several reports indicate that MSCs have a short half-life in the host [3]. Different strategies have been considered in order to activate MSCs prior to in vivo administration, which could eliminate the lag period required to upregulate expression of appropriate genes, and thus, enhance the therapeutic potentials of the cells. In addition, application of secreted proteins from MSCs has been tested as an alternative approach in different disease models.

In the present work, the effects of 3D cultures on production of anti-inflammatory factors by aggregated MSCs were tested. A hanging drop culture method was used to produce uniform MSC aggregates as spheroids in culture. Gene expression

and secretion of anti-inflammatory proteins such asTSG-6 and STC-1 were shown to increase dramatically early after incubation of the cells in the drops. Previous studies reported that MSCs do not secrete TSG-6 and STC-1 in standard 2D cultures; however, MSCs dissociated from spheroids could maintain high levels of TSG-6 and STC-1 expression for at least one day in standard 2D culture highlighting the enhanced anti-inflammatory potential of spheroid and spheroid derived MSCs as compared to the non-activated MSCs. Interestingly, spheroid MSCs, cultured in the conditions optimized for secretion of TSG-6 and STC-1, retain the properties of MSCs from standard 2D cultures. The enhanced anti-inflammatory effects of spheroids and spheroid derived cells were further examined in a co-culture system with LPS-stimulated macrophages and a mouse model of zymosan-induced peritonitis. These observations suggest that the rapid anti-inflammatory effect of spheroid MSCs reduces the early cascade of inflammatory responses in the host, and therefore, improve the therapeutic potential of MSCs in acute tissue injuries.

Data from microarray assays demonstrated significant differences in the transcriptomes of spheroid MSCs compared with cells from standard 2D cultures. Several of these differentially expressed genes suggest potential therapeutic uses of spheroid MSCs, including anticancer proteins (TRAIL, IL-24, and CD82) and chemokine receptor CXCR4 as well as anti-inflammatory factors. Thus, while a large number of non-activated MSCs from 2D cultures undergo cell death during activation in vivo, self-activated spheroid MSCs generate a variety of beneficial factors right after their administration into the host. In addition, the media conditioned by spheroid MSCs in drops contain high concentrations of these factors and can potentially be used in different pathological conditions.

In this study, local administration of spheroid MSCs was shown to reduce acute peritonitis in mice. MSCs have been previously demonstrated to reduce inflammation and tissue injuries from distance site in a number of mouse models, including myocardial infarction and cornea injury [51,64]. Therefore, intraperitoneal administration of intact spheroid can also be used for systemic modulation of

immune/inflammatory responses. Another potential therapeutic advantage of spheroid MSCs was their size. MSCs dissociated from spheroids were about one/forth the volume of 2D cultured MSCs, and thus, larger numbers of these cells could pass through pulmonary microvasculature and home to other tissues. Together these results suggest that intact spheroids and spheroid derived MSCs may have major advantages for different strategies of MSC administration.

Spheroid MSCs are in close contact with each other comparable as they are in vivo. In addition, the cells experience nutrient deprivation, air-liquid interface, and microgravity. These factors alter the microenvironment in hanging drops and could lead to activation of MSCs in spheroids. Bartosh and colleagues have demonstrated recently that caspase-dependent IL-1 signaling, activated by aggregated MSCs in hanging drops, was required for upregulation of TSG-6, STC-1, and another potent anti-inflammatory factor PGE_2 in MSCs [185]. Since the cells can produce similar aggregates in vivo, these results can explain, at least in part, the beneficial effects of MSCs in animal models. More detailed studies can help identify the key factors for self-activation of MSCs in vitro and in vivo in order to optimize culture conditions for different therapeutic potentials of the cells. Meanwhile, the hanging drop method can be used to produce MSCs with enhanced therapeutic potential for different diseases; therefore, it is essential to determine any loss of activity in freshly thawed cells from frozen cell banks to evaluate the clinical applications of spheroids and spheroid derived MSCs.

Previous studies have shown that STC-1 produces some of the beneficial effects of MSCs in vitro and in vivo. This protein can protect injured tissues by reducing the generation of ROS, apoptosis, and immune/inflammatory response, and thereby, its therapeutic potential has been considered for various diseases.

In the present work, the effects of STC-1 on stimulated monocytes/macrophages were studied. Monocytes differentiate to pro-inflammatory macrophages in the early stages of tissue damage and play important roles in immune/inflammatory actions. Administration of recombinant human STC-1 concurrent with monocyte-to-macrophage differentiation was shown to suppress the secretion of inflammatory mediators (TNFα,

CCL2, and CXCL2) by differentiated cells in response to LPS in vitro; however, treatment with this protein after maturation of monocytes/macrophages did not have any significant effects on their inflammatory actions. Therefore, the distinct characteristics of the differentiating monocytes/macrophages in the presence or absence of STC-1 were tested. Treatment with STC-1 was shown to reduce the expression of TLR4 co-receptor CD14 in monocytes/macrophages stimulated with both PMA and various endogenous danger signals, whereas there were no significant differences in the expression of TLR4 or monocyte/macrophage marker CD11b. In contrast, the expression of TLR2 was increased. These observations suggest that STC-1 can modulate inflammatory responses of stimulated monocytes/macrophages by regulating the expression of CD14.

CD14 is predominantly expressed by myeloid cells. This TLR co-receptor plays major roles in recognition and responses of immune cells to numerous PAMPs and DAMPs [176,177,179]. In addition, the involvement of CD14 in progression of different diseases such as cardiac inflammation has been demonstrated recently [178,222,223]; Although little is known about the factors controlling the expression of CD14 on monocytes/macrophages, a number of factors have been reported to reduce the transcription of CD14 such as IL-4 [233]. Therefore, it would be of interest to determine the correlation between STC-1 and expression level of these factors, especially IL-4, in differentiating monocytes/macrophages.

Also, mechanisms for the pleiotropic actions of STC-1 have not been entirely defined; nevertheless, the expression of mammalian STC-1 is responsive to numerous stress-inducing factors. The protein has been identified to modulate the calcium influx, which suggests its regulatory role on the calcium-dependent signaling pathways; therefore, in order to determine the key factors involved in inhibition of CD14 expression, differentiation assay could be performed in the presence or absence of calcium channel blockers. The downregulation of CD14 in differentiating monocytes/macrophages blocked for calcium entry would suggest the mechanisms for STC-1 action on modulation of CD14 expression. This hypothesis could be further tested

to demonstrate STC-1 binding to the calcium channels in stimulated monocytes/macrophages using immunoprecipitation assay.

In addition, STC-1 has been shown to suppress generation of mitochondrial ROS, at least in part, by upregulation of UCPs. To identify the role of UCPs in expression of CD14, first the mRNA levels of UCP2 should be determined in differentiating monocytes/macrophages. If STC-1 treatment results in upregulation of UCP2, small interfering RNA (siRNA) could be used to suppress the expression of this protein in monocytes prior to differentiation assay. The upregulation of CD14 in UCP2 knocked-down cells, despite presence or absence of STC-1, would suggest an UCP-dependent controlling mechanism for CD14 expression in myeloid cells.

Interestingly in the current study, i.v. administration of STC-1 decreased the amount of CD14 in the hearts of mice after LLDCA. CD14 is expressed in other immune cells as well as non-immune cells, which makes it difficult to assume that STC-1 therapy reduced the expression of CD14 only in monocytes/macrophages. Detailed studies, including immunostaining for co-expression of CD14 and monocyte/macrophage markers in the heart sections as well as flow cytometry of immune cells isolated from blood and spleen of healthy and injured animals would lead to better understand anti-inflammatory and immune modulatory potentials of STC-1.

STC-1 also reduced the amount of cardiac IL-1β and MPO. Mature form of IL-1β is involved in a wide range of immune/inflammatory responses and can exacerbate post-infarction cardiac injury [197]. Excessive MPO can be toxic to cardiomyocytes and deteriorate ventricular remodeling; therefore, STC-1 can protect cardiomyocytes and prevent heart failure by reducing these inflammatory mediators. Since STC-1 administration reduced the amount of CD14 in the heart, it can be suggested that decreased sensitivity of monocytes/macrophages to DAMPs can result in reduction of these mediators. STC-1 has been previously shown to decrease permeability of vascular endothelial cells and prevent migration of immune cells [148,229]; thus it can also be suggested that STC-1 inhibits cardiac inflammation by reducing the migration of

immune cells to the site of injury. This hypothesis could be examined by counting the number of infiltrated cells to the heart in the sections.

Long-term evaluation of experimental mice demonstrated that cardiac function and infarct size were improved three weeks after STC-1 treatment. CD14 deficiency has been shown to protect CD14 knockout mice against LPS-induced cardiac inflammation and ischemic tissue injury [222,223]; therefore, it can be assumed that STC-1 protects heart from excessive inflammation and supports tissue repair by a novel mechanism to control monocyte/macrophage functions.

In conclusion, the current study demonstrates that self-activated MSCs in spheroids provide enhanced therapeutic potential for the clinical use of the cells. Also, this study reveals a novel mechanism for STC-1 and promotes the potential therapeutic use of STC-1 for tissue injury.

LITERATURE CITED

[1] A. Caplan, J. Dennis, Mesenchymal stem cells as trophic mediators. J. Cell. Biochem. 98 (2006) 1076-84.

[2] A. Uccelli, L. Moretta, V. Pistoia, Mesenchymal stem cells in health and disease. Nat. Rev. Immunol. 8 (2008) 726-36.

[3] D.J. Prockop, D.J. Kota, N. Bazhanov, R.L. Reger, Evolving paradigms for repair of tissues by adult stem/progenitor cells (MSCs). J. Cell. Mol. Med. 14 (2010) 2190-2199.

[4] A.J. Friedenstein, R.K. Chailakhyan, N.V. Latsinik, A.F. Panasyuk, I.V. Keiliss Borok, Stromal cells responsible for transferring the microenvironment of the hemopoietic tissues. Cloning in vitro and retransplantation in vivo. Transplantation. 17 (1974) 331-40.

[5] M. Owen, Marrow stromal stem cells. J. Cell Sci. Suppl. 10 (1988) 63-76.

[6] A.J. Friedenstein, K.V. Petrakova, A.I. Kurolesova, G.P. Frolova, Heterotopic of bone marrow. Analysis of precursor cells for osteogenic and hematopoietic tissues. Transplantation. 6 (1968) 230-47.

[7] A.J. Friedenstein, R.K. Chailakhjan, K.S. Lalykina, The development of fibroblast colonies in monolayer cultures of guinea-pig bone marrow and spleen cells. Cell Tissue Kinet. 3 (1970) 393-403.

[8] A.J. Friedenstein, Precursor cells of mechanocytes. Int. Rev. Cytol. 47 (1976) 327-59.

[9] A.J. Friedenstein, R.K. Chailakhyan, U.V. Gerasimov, Bone marrow osteogenic stem cells: in vitro cultivation and transplantation in diffusion chambers. Cell Tissue Kinet. 20 (1987) 263-72.

[10] A.I. Caplan, Mesenchymal stem cells. J. Orthop. Res. 9 (1991) 641-50.

[11] C. Gregory, D. Prockop, J. Spees, Non-hematopoietic bone marrow stem cells: molecular control of expansion and differentiation. Exp. Cell Res. 306 (2005) 330-5.

[12] P. Zuk, M. Zhu, P. Ashjian, D. De Ugarte, J. Huang, H. Mizuno, Z. Alfonso, J. Fraser, P. Benhaim, M. Hedrick, Human adipose tissue is a source of multipotent stem cells. Mol. Biol. Cell. 13 (2002) 4279-95.

[13] M. Miura, S. Gronthos, M. Zhao, B. Lu, L. Fisher, P. Robey, S. Shi, SHED: stem cells from human exfoliated deciduous teeth. Proc. Natl. Acad. Sci. U. S. A. 100 (2003) 5807-12.

[14] M. Lee, J. Choi, M. Yang, Y. Moon, J. Park, H. Kim, Y. Kim, Mesenchymal stem cells from cryopreserved human umbilical cord blood. Biochem. Biophys. Res. Commun. 320 (2004) 273-8.

[15] P.S. In 't Anker, S. Scherjon, C. Kleijburg-van der Keur, G.M. de Groot-Swings, F.H. Claas, W.E. Fibbe, H.H. Kanhai, Isolation of mesenchymal stem cells of fetal or maternal origin from human placenta. Stem Cells. 22 (2004) 1338-45.

[16] M. Dominici, K. Le Blanc, I. Mueller, I. Slaper Cortenbach, F. Marini, D. Krause, R. Deans, A. Keating, D. Prockop, E. Horwitz, Minimal criteria for defining multipotent mesenchymal stromal cells. The International Society for Cellular Therapy position statement. Cytotherapy. 8 (2006) 315-7.

[17] D.C. Colter, R. Class, C.M. DiGirolamo, D.J. Prockop, Rapid expansion of recycling stem cells in cultures of plastic-adherent cells from human bone marrow. Proc. Natl. Acad. Sci. U. S. A. 97 (2000) 3213-8.

[18] I. Sekiya, B. Larson, J. Smith, R. Pochampally, J. Cui, D. Prockop, Expansion of human adult stem cells from bone marrow stroma: conditions that maximize the yields of early progenitors and evaluate their quality. Stem Cells. 20 (2002) 530-41.

[19] J. Spees, C. Gregory, H. Singh, H.A. Tucker, A. Peister, P. Lynch, S. Hsu, J. Smith, D. Prockop, Internalized antigens must be removed to prepare hypoimmunogenic mesenchymal stem cells for cell and gene therapy. Mol. Ther. 9 (2004) 747-56.

[20] S. Gronthos, S.E. Graves, S. Ohta, P.J. Simmons, The STRO-1^+ fraction of adult human bone marrow contains the osteogenic precursors. Blood. 84 (1994) 4164-73.

[21] C.J. Eaves, J.D. Cashman, H.J. Sutherland, T. Otsuka, R.K. Humphries, D.E. Hogge, P.L. Lansdorp, A.C. Eaves, Molecular analysis of primitive hematopoietic cell proliferation control mechanisms. Ann. N. Y. Acad. Sci. 628 (1991) 298-306.

[22] A.D. Whetton, T.M. Dexter, Influence of growth factors and substrates on differentiation of haemopoietic stem cells. Curr. Opin. Cell Biol. 5 (1993) 1044-9.

[23] S.E. Haynesworth, M.A. Baber, A.I. Caplan, Cytokine expression by human marrow-derived mesenchymal progenitor cells in vitro: effects of dexamethasone and IL-1 alpha. J. Cell. Physiol. 166 (1996) 585-92.

[24] D.J. Prockop, Marrow stromal cells as stem cells for nonhematopoietic tissues. Science. 276 (1997) 71-4.

[25] B. Sacchetti, A. Funari, S. Michienzi, S. Di Cesare, S. Piersanti, I. Saggio, E. Tagliafico, S. Ferrari, P. Robey, M. Riminucci, P. Bianco, Self-renewing osteoprogenitors in bone marrow sinusoids can organize a hematopoietic microenvironment. Cell. 131 (2007) 324-36.

[26] O.N. Koç, S.L. Gerson, B.W. Cooper, S.M. Dyhouse, S.E. Haynesworth, A.I. Caplan, H.M. Lazarus, Rapid hematopoietic recovery after coinfusion of autologous-

blood stem cells and culture-expanded marrow mesenchymal stem cells in advanced breast cancer patients receiving high-dose chemotherapy. J. Clin. Oncol. 18 (2000) 307-16.

[27] M.F. Pittenger, A.M. Mackay, S.C. Beck, R.K. Jaiswal, R. Douglas, J.D. Mosca, M.A. Moorman, D.W. Simonetti, S. Craig, D.R. Marshak, Multilineage potential of adult human mesenchymal stem cells. Science. 284 (1999) 143-7.

[28] S. Wakitani, T. Saito, A.I. Caplan, Myogenic cells derived from rat bone marrow mesenchymal stem cells exposed to 5-azacytidine. Muscle Nerve. 18 (1995) 1417-26.

[29] S.A. Azizi, D. Stokes, B.J. Augelli, C. DiGirolamo, D.J. Prockop, Engraftment and migration of human bone marrow stromal cells implanted in the brains of albino rats--similarities to astrocyte grafts. Proc. Natl. Acad. Sci. U. S. A. 95 (1998) 3908-13.

[30] G. Ferrari, G. Cusella-De Angelis, M. Coletta, E. Paolucci, A. Stornaiuolo, G. Cossu, F. Mavilio, Muscle regeneration by bone marrow-derived myogenic progenitors. Science. 279 (1998) 1528-30.

[31] S. Makino, K. Fukuda, S. Miyoshi, F. Konishi, H. Kodama, J. Pan, M. Sano, T. Takahashi, S. Hori, H. Abe, J. Hata, A. Umezawa, S. Ogawa, Cardiomyocytes can be generated from marrow stromal cells in vitro. J. Clin. Invest. 103 (1999) 697-705.

[32] B.E. Petersen, W.C. Bowen, K.D. Patrene, W.M. Mars, A.K. Sullivan, N. Murase, S.S. Boggs, J.S. Greenberger, J.P. Goff, Bone marrow as a potential source of hepatic oval cells. Science. 284 (1999) 1168-70.

[33] D. Woodbury, E.J. Schwarz, D.J. Prockop, I.B. Black, Adult rat and human bone marrow stromal cells differentiate into neurons. J. Neurosci. Res. 61 (2000) 364-70.

[34] J. Sanchez Ramos, Neural cells derived from adult bone marrow and umbilical cord blood. J. Neurosci. Res. 69 (2002) 880-93.

[35] M. Dezawa, Systematic neuronal and muscle induction systems in bone marrow stromal cells: the potential for tissue reconstruction in neurodegenerative and muscle degenerative diseases. Med. Mol. Morphol. 41 (2008) 14-9.

[36] S.P. Bruder, D.J. Fink, A.I. Caplan, Mesenchymal stem cells in bone development, bone repair, and skeletal regeneration therapy. J. Cell. Biochem. 56 (1994) 283-94.

[37] R.F. Pereira, K.W. Halford, M.D. O'Hara, D.B. Leeper, B.P. Sokolov, M.D. Pollard, O. Bagasra, D.J. Prockop, Cultured adherent cells from marrow can serve as long-lasting precursor cells for bone, cartilage, and lung in irradiated mice. Proc. Natl. Acad. Sci. U. S. A. 92 (1995) 4857-61.

[38] R.F. Pereira, M.D. O'Hara, A.V. Laptev, K.W. Halford, M.D. Pollard, R. Class, D. Simon, K. Livezey, D.J. Prockop, Marrow stromal cells as a source of progenitor cells for nonhematopoietic tissues in transgenic mice with a phenotype of osteogenesis imperfecta. Proc. Natl. Acad. Sci. U. S. A. 95 (1998) 1142-7.

[39] G.C. Kopen, D.J. Prockop, D.G. Phinney, Marrow stromal cells migrate throughout forebrain and cerebellum, and they differentiate into astrocytes after injection into neonatal mouse brains. Proc. Natl. Acad. Sci. U. S. A. 96 (1999) 10711-6.

[40] E.M. Horwitz, D.J. Prockop, L.A. Fitzpatrick, W.W. Koo, P.L. Gordon, M. Neel, M. Sussman, P. Orchard, J.C. Marx, R.E. Pyeritz, M.K. Brenner, Transplantability and therapeutic effects of bone marrow-derived mesenchymal cells in children with osteogenesis imperfecta. Nat. Med. 5 (1999) 309-13.

[41] O.N. Koç, C. Peters, P. Aubourg, S. Raghavan, S. Dyhouse, R. DeGasperi, E.H. Kolodny, Y.B. Yoseph, S.L. Gerson, H.M. Lazarus, A.I. Caplan, P.A. Watkins, W. Krivit, Bone marrow-derived mesenchymal stem cells remain host-derived despite successful hematopoietic engraftment after allogeneic transplantation in patients with lysosomal and peroxisomal storage diseases. Exp. Hematol. 27 (1999) 1675-81.

[42] M. Chopp, Y. Li, Z. Zhang, Mechanisms underlying improved recovery of neurological function after stroke in the rodent after treatment with neurorestorative cell-based therapies. Stroke. 40 (2009) S143-5.

[43] U. Krause, C. Harter, A. Seckinger, D. Wolf, A. Reinhard, F. Bea, T. Dengler, S. Hardt, A. Ho, H. Katus, H. Kuecherer, A. Hansen, Intravenous delivery of autologous mesenchymal stem cells limits infarct size and improves left ventricular function in the infarcted porcine heart. Stem Cells Dev. 16 (2007) 31-7.

[44] F. Tögel, C. Westenfelder, Stem cells in acute kidney injury repair. Minerva Urol. Nefrol. 61 (2009) 205-13.

[45] R. Lee, M. Seo, R. Reger, J. Spees, A. Pulin, S. Olson, D. Prockop, Multipotent stromal cells from human marrow home to and promote repair of pancreatic islets and renal glomeruli in diabetic NOD/scid mice. Proc. Natl. Acad. Sci. U. S. A. 103 (2006) 17438-43.

[46] F. Ezquer, M. Ezquer, V. Simon, F. Pardo, A. Yañez, D. Carpio, P. Conget, Endovenous administration of bone-marrow-derived multipotent mesenchymal stromal cells prevents renal failure in diabetic mice. Biol. Blood Marrow Transplant. 15 (2009) 1354-65.

[47] J. Munoz, B. Stoutenger, A. Robinson, J. Spees, D. Prockop, Human stem/progenitor cells from bone marrow promote neurogenesis of endogenous neural stem cells in the hippocampus of mice. Proc. Natl. Acad. Sci. U. S. A. 102 (2005) 18171-6.

[48] H. Ohtaki, J. Ylostalo, J. Foraker, A. Robinson, R. Reger, S. Shioda, D. Prockop, Stem/progenitor cells from bone marrow decrease neuronal death in global ischemia by modulation of inflammatory/immune responses. Proc. Natl. Acad. Sci. U. S. A. 105 (2008) 14638-43.

[49] M. Horie, I. Sekiya, T. Muneta, S. Ichinose, K. Matsumoto, H. Saito, T. Murakami, E. Kobayashi, Intra-articular Injected synovial stem cells differentiate into meniscal cells directly and promote meniscal regeneration without mobilization to distant organs in rat massive meniscal defect. Stem Cells. 27 (2009) 878-87.

[50] S. Kidd, E. Spaeth, J. Dembinski, M. Dietrich, K. Watson, A. Klopp, V. Battula, M. Weil, M. Andreeff, F. Marini, Direct evidence of mesenchymal stem cell tropism for tumor and wounding microenvironments using in vivo bioluminescent imaging. Stem Cells. 27 (2009) 2614-23.

[51] R.H. Lee, A.A. Pulin, M.J. Seo, D.J. Kota, J. Ylostalo, B.L. Larson, L. Semprun-Prieto, P. Delafontaine, D.J. Prockop, Intravenous hMSCs improve myocardial infarction in mice because cells embolized in lung are activated to secrete the anti-inflammatory protein TSG-6. Cell Stem Cell. 5 (2009) 54-63.

[52] L. Timmers, S. Lim, F. Arslan, J. Armstrong, I. Hoefer, P. Doevendans, J. Piek, R. El Oakley, A. Choo, C. Lee, G. Pasterkamp, D.P.V. de Kleijn, Reduction of myocardial infarct size by human mesenchymal stem cell conditioned medium. Stem Cell Res. 1 (2007) 129-37.

[53] J. Oh, M. Kim, M. Shin, H. Lee, J. Ko, W. Wee, J. Lee, The anti-inflammatory and anti-angiogenic role of mesenchymal stem cells in corneal wound healing following chemical injury. Stem Cells. 26 (2008) 1047-55.

[54] W. Gunn, A. Conley, L. Deininger, S. Olson, D. Prockop, C. Gregory, A crosstalk between myeloma cells and marrow stromal cells stimulates production of DKK1 and interleukin-6: a potential role in the development of lytic bone disease and tumor progression in multiple myeloma. Stem Cells. 24 (2006) 986-91.

[55] G. Ren, X. Zhao, L. Zhang, J. Zhang, A. L'Huillier, W. Ling, A. Roberts, A. Le, S. Shi, C. Shao, Y. Shi, Inflammatory cytokine-induced intercellular adhesion molecule-1

and vascular cell adhesion molecule-1 in mesenchymal stem cells are critical for immunosuppression. J. Immunol. 184 (2010) 2321-8.

[56] D. Prockop, J. Oh, Medical therapies with adult stem/progenitor cells (MSCs): a backward journey from dramatic results in vivo to the cellular and molecular explanations. J. Cell. Biochem. 113 (2012) 1460-9.

[57] A. Bartholomew, C. Sturgeon, M. Siatskas, K. Ferrer, K. McIntosh, S. Patil, W. Hardy, S. Devine, D. Ucker, R. Deans, A. Moseley, R. Hoffman, Mesenchymal stem cells suppress lymphocyte proliferation in vitro and prolong skin graft survival in vivo. Exp. Hematol. 30 (2002) 42-8.

[58] E. Zappia, S. Casazza, E. Pedemonte, F. Benvenuto, I. Bonanni, E. Gerdoni, D. Giunti, A. Ceravolo, F. Cazzanti, F. Frassoni, G. Mancardi, A. Uccelli, Mesenchymal stem cells ameliorate experimental autoimmune encephalomyelitis inducing T-cell anergy. Blood. 106 (2005) 1755-61.

[59] E. Gerdoni, B. Gallo, S. Casazza, S. Musio, I. Bonanni, E. Pedemonte, R. Mantegazza, F. Frassoni, G. Mancardi, R. Pedotti, A. Uccelli, Mesenchymal stem cells effectively modulate pathogenic immune response in experimental autoimmune encephalomyelitis. Ann. Neurol. 61 (2007) 219-27.

[60] K. Le Blanc, I. Rasmusson, B. Sundberg, C. Götherström, M. Hassan, M. Uzunel, O. Ringdén, Treatment of severe acute graft-versus-host disease with third party haploidentical mesenchymal stem cells. Lancet (London, England). 363 (2004) 1439-41.

[61] G. Chen, G. Nuñez, Sterile inflammation: sensing and reacting to damage. Nat. Rev. Immunol. 10 (2010) 826-37.

[62] H. Wisniewski, J. Vilcek, Cytokine-induced gene expression at the crossroads of innate immunity, inflammation and fertility: TSG-6 and PTX3/TSG-14. Cytokine Growth Factor Rev. 15 (2004) 129-46.

[63] C.M. Milner, V.A. Higman, A.J. Day, TSG-6: a pluripotent inflammatory mediator? Biochem. Soc. Trans. 34 (2006) 446-50.

[64] G.W. Roddy, J.Y. Oh, R.H. Lee, T.J. Bartosh, J. Ylostalo, K. Coble, R.H. Rosa Jr, D.J. Prockop, Action at a distance: systemically administered adult stem/progenitor cells (MSCs) reduce inflammatory damage to the cornea without engraftment and primarily by secretion of TNF-alpha stimulated gene/protein 6. Stem Cells. 29 (2011) 1572-1579.

[65] H. Choi, R. Lee, N. Bazhanov, J. Oh, D. Prockop, Anti-inflammatory protein TSG-6 secreted by activated MSCs attenuates zymosan-induced mouse peritonitis by decreasing TLR2/NF-KB signaling in resident macrophages. Blood. 118 (2011) 330-8.

[66] S. Hung, R. Pochampally, S. Chen, S. Hsu, D. Prockop, Angiogenic effects of human multipotent stromal cell conditioned medium activate the PI3K-Akt pathway in hypoxic endothelial cells to inhibit apoptosis, increase survival, and stimulate angiogenesis. Stem Cells. 25 (2007) 2363-70.

[67] G.J. Block, S. Ohkouchi, F. Fung, J. Frenkel, C. Gregory, R. Pochampally, G. DiMattia, D.E. Sullivan, D.J. Prockop, Multipotent stromal cells are activated to reduce apoptosis in part by upregulation and secretion of stanniocalcin-1. Stem Cells. 27 (2009) 670-681.

[68] Y. Yoshiko, J. Aubin, Stanniocalcin 1 as a pleiotropic factor in mammals. Peptides. 25 (2004) 1663-9.

[69] R.N. Re, J.L. Cook, The mitochondrial component of intracrine action. Am. J. Physiol. Heart Circ. Physiol. 299 (2010) H577-83.

[70] B.H. Yeung, A.Y. Law, C.K. Wong, Evolution and roles of stanniocalcin. Mol. Cell. Endocrinol. 349 (2012) 272-280.

[71] G. Wagner, G. Dimattia, The stanniocalcin family of proteins. J. Exp. Zool. A Comp. Exp. Biol. 305 (2006) 769-80.

[72] J.C. Fenwick, Y.P. So, A perfusion study of the effect of stanniectomy on the net influx of calcium 45 across an isolated eel gill (1). J. Exp. Zool. 188 (1974) 125-31.

[73] P.K. Pang, R.K. Pang, W.H. Sawyer, Effects of environmental calcium and replacement therapy on the killifish, Fundulus heteroclitus, after the surgical removal of the corpuscles of Stannius. Endocrinology. 93 (1973) 705-10.

[74] Y.P. So, J.C. Fenwick, In vivo and in vitro effects of Stannius corpuscle extract on the branchial uptake of 45Ca in stanniectomized North American eels (Anguilla rostrata). Gen. Comp. Endocrinol. 37 (1979) 143-9.

[75] P.K. Pang, R.K. Pang, W.H. Sawyer, Environmental calcium and the sensitivity of killifish (Fundulus heteroclitus) in bioassays for the hypocalcemic response to Stannius corpuscles from killifish and cod (Gadus morhua). Endocrinology. 94 (1974) 548-55.

[76] P.K. Pang, R.K. Pang, Environmental calcium and hypocalcin activity in the Stannius corpuscles of the channel catfish, Ictalurus punctatus (Rafinesque). Gen. Comp. Endocrinol. 23 (1974) 239-41.

[77] I.C. Jones, I.W. Henderson, D.K. Chan, J.C. Rankin, W. Mosley, J.J. Brown, A.F. Lever, J.I. Robertson, M. Tree, Pressor activity in extracts of the corpuscles of Stannius from the European eel (Anguilla anguilla L.). J. Endocrinol. 34 (1966) 393-408.

[78] V.G. Krishnamurthy, Cytophysiology of corpuscles of Stannius. Int. Rev. Cytol. 46 (1976) 177-249.

[79] G.F. Wagner, M. Hampong, C.M. Park, D.H. Copp, Purification, characterization, and bioassay of teleocalcin, a glycoprotein from salmon corpuscles of Stannius. Gen. Comp. Endocrinol. 63 (1986) 481-491.

[80] D. Butler, J. Brown, Stanniectomy attenuates the renin-angiotensin response to hypovolemic hypotension in freshwater eels (Anguilla rostrata) but not blood pressure recovery. J. Comp. Physiol. B. 177 (2007) 143-51.

[81] A. Butkus, P.J. Roche, R.T. Fernley, J. Haralambidis, J.D. Penschow, G.B. Ryan, J.F. Trahair, G.W. Tregear, J.P. Coghlan, Purification and cloning of a corpuscles of Stannius protein from Anguilla australis. Mol. Cell. Endocrinol. 54 (1987) 123-33.

[82] F.P. Lafeber, R.G. Hanssen, Y.M. Choy, G. Flik, M.P. Herrmann Erlee, P.K. Pang, S.E. Bonga, Identification of hypocalcin (teleocalcin) isolated from trout Stannius corpuscles. Gen. Comp. Endocrinol. 69 (1988) 19-30.

[83] I. Hulova, H. Kawauchi, Assignment of disulfide linkages in chum salmon stanniocalcin. Biochem. Biophys. Res. Commun. 257 (1999) 295-9.

[84] G. Flik, T. Labedz, J.A. Neelissen, R.G. Hanssen, S.E. Wendelaar Bonga, P.K. Pang, Rainbow trout corpuscles of Stannius: stanniocalcin synthesis in vitro. Am. J. Physiol. 258 (1990) R1157-64.

[85] Y. Amemiya, L. Marra, N. Reyhani, J. Youson, Stanniocalcin from an ancient teleost: a monomeric form of the hormone and a possible extracorpuscular distribution. Mol. Cell. Endocrinol. 188 (2002) 141-50.

[86] C.E. Milliken, R.C. Fargher, A. Butkus, M. McDonald, D.H. Copp, Effects of synthetic peptide fragments of teleocalcin (hypocalcin) on calcium uptake in juvenile rainbow trout (Salmo gairdneri). Gen. Comp. Endocrinol. 77 (1990) 416-22.

[87] P.M. Verbost, A. Butkus, W. Atsma, P. Willems, G. Flik, S.E. Bonga, Studies on stanniocalcin: characterization of bioactive and antigenic domains of the hormone. Mol. Cell. Endocrinol. 93 (1993) 11-6.

[88] K. Yamashita, Y. Koide, H. Itoh, N. Kawada, H. Kawauchi, The complete amino acid sequence of chum salmon stanniocalcin, a calcium-regulating hormone in teleosts. Mol. Cell. Endocrinol. 112 (1995) 159-67.

[89] C.R. McCudden, M.R. Kogon, G.E. DiMattia, G.F. Wagner, Novel expression of the stanniocalcin gene in fish. J. Endocrinol. 171 (2001) 33-44.

[90] Y. Amemiya, J. Youson, Primary structure of stanniocalcin in two basal Actinopterygii. Gen. Comp. Endocrinol. 135 (2004) 250-7.

[91] G.F. Wagner, R.C. Fargher, C. Milliken, B.A. McKeown, D.H. Copp, The gill calcium transport cycle in rainbow trout is correlated with plasma levels of bioactive, not immunoreactive, stanniocalcin. Mol. Cell. Endocrinol. 93 (1993) 185-91.

[92] D. Radman, C. McCudden, K. James, E. Nemeth, G. Wagner, Evidence for calcium-sensing receptor mediated stanniocalcin secretion in fish. Mol. Cell. Endocrinol. 186 (2002) 111-9.

[93] M. Greenwood, G. Flik, G. Wagner, R. Balment, The corpuscles of Stannius, calcium-sensing receptor, and stanniocalcin: responses to calcimimetics and physiological challenges. Endocrinology. 150 (2009) 3002-10.

[94] G. Flik, Hypocalcin physiology. Prog. Clin. Biol. Res. 342 (1990) 578-85.

[95] T.J. Ellis, G.F. Wagner, Post-transcriptional regulation of the stanniocalcin gene by calcium. J. Biol. Chem. 270 (1995) 1960-5.

[96] P.M. Pierson, A. Lamers, G. Flik, N. Mayer Gostan, The stress axis, stanniocalcin, and ion balance in rainbow trout. Gen. Comp. Endocrinol. 137 (2004) 263-71.

[97] M. Lu, G.F. Wagner, J.L. Renfro, Stanniocalcin stimulates phosphate reabsorption by flounder renal proximal tubule in primary culture. Am. J. Physiol. 267 (1994) R1356-62.

[98] H.S. Olsen, M.A. Cepeda, Q.Q. Zhang, C.A. Rosen, B.L. Vozzolo, G.F. Wagner, Human stanniocalcin: a possible hormonal regulator of mineral metabolism. Proc. Natl. Acad. Sci. U. S. A. 93 (1996) 1792-6.

[99] P.M. Verbost, G. Flik, J.C. Fenwick, A.M. Greco, P.K. Pang, S.E. Wendelaar Bonga, Branchial calcium uptake: possible mechanisms of control by stanniocalcin. Fish Physiol. Biochem. 11 (1993) 205-15.

[100] D.G. Butler, G.Y. Oudit, Corpuscles of Stannius and blood flow regulation in freshwater North American eels, Anguilla rostrata LeSueur. J. Endocrinol. 145 (1995) 181-94.

[101] D. Tseng, M. Chou, Y. Tseng, C. Hsiao, C. Huang, T. Kaneko, P. Hwang, Effects of stanniocalcin 1 on calcium uptake in zebrafish (Danio rerio) embryo. Am. J. Physiol. Regul. Integr. Comp. Physiol. 296 (2009) R549-57.

[102] G.F. Wagner, C.C. Guiraudon, C. Milliken, D.H. Copp, Immunological and biological evidence for a stanniocalcin-like hormone in human kidney. Proc. Natl. Acad. Sci. U. S. A. 92 (1995) 1871-5.

[103] A.C. Chang, J. Janosi, M. Hulsbeek, D. de Jong, K.J. Jeffrey, J.R. Noble, R.R. Reddel, A novel human cDNA highly homologous to the fish hormone stanniocalcin. Mol. Cell. Endocrinol. 112 (1995) 241-7.

[104] A.C. Chang, R.R. Reddel, Identification of a second stanniocalcin cDNA in mouse and human: stanniocalcin 2. Mol. Cell. Endocrinol. 141 (1998) 95-9.

[105] G.E. DiMattia, R. Varghese, G.F. Wagner, Molecular cloning and characterization of stanniocalcin-related protein. Mol. Cell. Endocrinol. 146 (1998) 137-40.

[106] K. Ishibashi, K. Miyamoto, Y. Taketani, K. Morita, E. Takeda, S. Sasaki, M. Imai, Molecular cloning of a second human stanniocalcin homologue (STC2). Biochem. Biophys. Res. Commun. 250 (1998) 252-8.

[107] E.E. Moore, R.E. Kuestner, D.C. Conklin, T.E. Whitmore, W. Downey, M.M. Buddle, R.L. Adams, L.A. Bell, D.L. Thompson, A. Wolf, L. Chen, M.R. Stamm, F.J. Grant, S. Lok, H. Ren, K.S. De Jongh, Stanniocalcin 2: characterization of the protein and its localization to human pancreatic alpha cells. Horm. Metab. Res. 31 (1999) 406-14.

[108] C. Luo, M. Pisarska, A.J.W. Hsueh, Identification of a stanniocalcin paralog, stanniocalcin-2, in fish and the paracrine actions of stanniocalcin-2 in the mammalian ovary. Endocrinology. 146 (2005) 469-76.

[109] A.C. Chang, D.A. Jellinek, R.R. Reddel, Mammalian stanniocalcins and cancer. Endocr. Relat. Cancer. 10 (2003) 359-73.

[110] D. Sheikh-Hamad, Mammalian stanniocalcin-1 activates mitochondrial antioxidant pathways: new paradigms for regulation of macrophages and endothelium. Am. J. Physiol. Renal Physiol. 298 (2010) F248-54.

[111] P. De Niu, D.P. Radman, E.M. Jaworski, H. Deol, R. Gentz, J. Su, H.S. Olsen, G.F. Wagner, Development of a human stanniocalcin radioimmunoassay: serum and tissue hormone levels and pharmacokinetics in the rat. Mol. Cell. Endocrinol. 162 (2000) 131-44.

[112] K. James, M. Seitelbach, C. McCudden, G. Wagner, Evidence for stanniocalcin binding activity in mammalian blood and glomerular filtrate. Kidney Int. 67 (2005) 477-82.

[113] P. De Niu, H.S. Olsen, R. Gentz, G.F. Wagner, Immunolocalization of stanniocalcin in human kidney. Mol. Cell. Endocrinol. 137 (1998) 155-9.

[114] C.K. Wong, M.A. Ho, G.F. Wagner, The co-localization of stanniocalcin protein, mRNA and kidney cell markers in the rat kidney. J. Endocrinol. 158 (1998) 183-9.

[115] C. McCudden, K. James, C. Hasilo, G. Wagner, Characterization of mammalian stanniocalcin receptors. Mitochondrial targeting of ligand and receptor for regulation of cellular metabolism. J. Biol. Chem. 277 (2002) 45249-58.

[116] M. Paciga, C. McCudden, C. Londos, G. DiMattia, G. Wagner, Targeting of big stanniocalcin and its receptor to lipid storage droplets of ovarian steroidogenic cells. J. Biol. Chem. 278 (2003) 49549-54.

[117] C. McCudden, A. Majewski, S. Chakrabarti, G. Wagner, Co-localization of stanniocalcin-1 ligand and receptor in human breast carcinomas. Mol. Cell. Endocrinol. 213 (2004) 167-72.

[118] O. Sazonova, K.A. James, C.R. McCudden, D. Segal, A. Talebian, G.F. Wagner, Stanniocalcin-1 secretion and receptor regulation in kidney cells. Am. J. Physiol. Renal Physiol. 294 (2008) F788-94.

[119] A.C. Chang, J. Hook, F. Lemckert, M. McDonald, M. Nguyen, E. Hardeman, D. Little, P. Gunning, R. Reddel, The murine stanniocalcin 2 gene is a negative regulator of postnatal growth. Endocrinology. 149 (2008) 2403-10.

[120] S. Honda, M. Kashiwagi, K. Ookata, A. Tojo, S. Hirose, Regulation by 1alpha,25-dihydroxyvitamin D(3) of expression of stanniocalcin messages in the rat kidney and ovary. FEBS Lett. 459 (1999) 119-22.

[121] D. Sheikh-Hamad, D. Rouse, Y. Yang, Regulation of stanniocalcin in MDCK cells by hypertonicity and extracellular calcium. Am. J. Physiol. Renal Physiol. 278 (2000) F417-24.

[122] J. Kahn, F. Mehraban, G. Ingle, X. Xin, J.E. Bryant, G. Vehar, J. Schoenfeld, C.J. Grimaldi, F. Peale, A. Draksharapu, D.A. Lewin, M.E. Gerritsen, Gene expression profiling in an in vitro model of angiogenesis. Am. J. Pathol. 156 (2000) 1887-900.

[123] S.E. Bell, A. Mavila, R. Salazar, K.J. Bayless, S. Kanagala, S.A. Maxwell, G.E. Davis, Differential gene expression during capillary morphogenesis in 3D collagen matrices: regulated expression of genes involved in basement membrane matrix assembly, cell cycle progression, cellular differentiation and G-protein signaling. J. Cell. Sci. 114 (2001) 2755-73.

[124] D.I.R. Holmes, I. Zachary, Vascular endothelial growth factor regulates stanniocalcin-1 expression via neuropilin-1-dependent regulation of KDR and synergism with fibroblast growth factor-2. Cell. Signal. 20 (2008) 569-79.

[125] D. Klein, A. Demory, F. Peyre, J. Kroll, C. Géraud, N. Ohnesorge, K. Schledzewski, B. Arnold, S. Goerdt, Wnt2 acts as an angiogenic growth factor for non-sinusoidal endothelial cells and inhibits expression of stanniocalcin-1. Angiogenesis. 12 (2009) 251-65.

[126] N. Sato, K. Kokame, K. Shimokado, H. Kato, T. Miyata, Changes of gene expression by lysophosphatidylcholine in vascular endothelial cells: 12 up-regulated distinct genes including 5 cell growth-related, 3 thrombosis-related, and 4 others. J. Biochem. 123 (1998) 1119-26.

[127] A. Lal, H. Peters, B. St Croix, Z.A. Haroon, M.W. Dewhirst, R.L. Strausberg, J.H. Kaanders, van der Kogel, A J, G.J. Riggins, Transcriptional response to hypoxia in human tumors. J. Natl. Cancer Inst. 93 (2001) 1337-43.

[128] J.A. Westberg, M. Serlachius, P. Lankila, M. Penkowa, J. Hidalgo, L.C. Andersson, Hypoxic preconditioning induces neuroprotective stanniocalcin-1 in brain via IL-6 signaling. Stroke. 38 (2007) 1025-1030.

[129] J. Westberg, M. Serlachius, P. Lankila, L. Andersson, Hypoxic preconditioning induces elevated expression of stanniocalcin-1 in the heart. Am. J. Physiol. Heart Circ. Physiol. 293 (2007) H1766-71.

[130] V.R. Iyer, M.B. Eisen, D.T. Ross, G. Schuler, T. Moore, J.C. Lee, J.M. Trent, L.M. Staudt, J. Hudson, M.S. Boguski, D. Lashkari, D. Shalon, D. Botstein, P.O. Brown, The transcriptional program in the response of human fibroblasts to serum. Science. 283 (1999) 83-7.

[131] P. Welcsh, M. Lee, R. Gonzalez Hernandez, D. Black, M. Mahadevappa, E. Swisher, J. Warrington, M. King, BRCA1 transcriptionally regulates genes involved in breast tumorigenesis. Proc. Natl. Acad. Sci. U. S. A. 99 (2002) 7560-5.

[132] Y. Tohmiya, Y. Koide, S. Fujimaki, H. Harigae, T. Funato, M. Kaku, T. Ishii, Y. Munakata, J. Kameoka, T. Sasaki, Stanniocalcin-1 as a novel marker to detect minimal residual disease of human leukemia. Tohoku J. Exp. Med. 204 (2004) 125-33.

[133] E. Filvaroff, S. Guillet, C. Zlot, M. Bao, G. Ingle, H. Steinmetz, J. Hoeffel, S. Bunting, J. Ross, R.A.D. Carano, L. Powell Braxton, G. Wagner, R. Eckert, M. Gerritsen, D. French, Stanniocalcin 1 alters muscle and bone structure and function in transgenic mice. Endocrinology. 143 (2002) 3681-90.

[134] R. Varghese, A. Gagliardi, P. Bialek, S. Yee, G. Wagner, G. Dimattia, Overexpression of human stanniocalcin affects growth and reproduction in transgenic mice. Endocrinology. 143 (2002) 868-76.

[135] L. Huang, G. Garcia, Y. Lou, Q. Zhou, L.D. Truong, G. DiMattia, X.R. Lan, H.Y. Lan, Y. Wang, D. Sheikh-Hamad, Anti-inflammatory and renal protective actions of

stanniocalcin-1 in a model of anti-glomerular basement membrane glomerulonephritis. Am. J. Pathol. 174 (2009) 1368-1378.

[136] A.C. Chang, J. Cha, F. Koentgen, R. Reddel, The murine stanniocalcin 1 gene is not essential for growth and development. Mol. Cell. Biol. 25 (2005) 10604-10.

[137] K.L. Madsen, M.M. Tavernini, C. Yachimec, D.L. Mendrick, P.J. Alfonso, M. Buergin, H.S. Olsen, M.J. Antonaccio, A.B. Thomson, R.N. Fedorak, Stanniocalcin: a novel protein regulating calcium and phosphate transport across mammalian intestine. Am. J. Physiol. 274 (1998) G96-102.

[138] G.F. Wagner, B.L. Vozzolo, E. Jaworski, M. Haddad, R.L. Kline, H.S. Olsen, C.A. Rosen, M.B. Davidson, J.L. Renfro, Human stanniocalcin inhibits renal phosphate excretion in the rat. J. Bone Miner. Res. 12 (1997) 165-71.

[139] Y. Yoshiko, N. Maeda, J. Aubin, Stanniocalcin 1 stimulates osteoblast differentiation in rat calvaria cell cultures. Endocrinology. 144 (2003) 4134-43.

[140] D. Sheikh-Hamad, R. Bick, G.Y. Wu, B.M. Christensen, P. Razeghi, B. Poindexter, H. Taegtmeyer, A. Wamsley, R. Padda, M. Entman, S. Nielsen, K. Youker, Stanniocalcin-1 is a naturally occurring L-channel inhibitor in cardiomyocytes: relevance to human heart failure. Am. J. Physiol. Heart Circ. Physiol. 285 (2003) H442-8.

[141] K.z. Zhang, P.J. Lindsberg, T. Tatlisumak, M. Kaste, H.S. Olsen, L.C. Andersson, Stanniocalcin: A molecular guard of neurons during cerebral ischemia. Proc. Natl. Acad. Sci. U. S. A. 97 (2000) 3637-42.

[142] J. Ellard, C. McCudden, C. Tanega, K. James, S. Ratkovic, J. Staples, G. Wagner, The respiratory effects of stanniocalcin-1 (STC-1) on intact mitochondria and cells: STC-1 uncouples oxidative phosphorylation and its actions are modulated by nucleotide triphosphates. Mol. Cell. Endocrinol. 264 (2007) 90-101.

[143] Y. Wang, L. Huang, M. Abdelrahim, Q. Cai, A. Truong, R. Bick, B. Poindexter, D. Sheikh-Hamad, Stanniocalcin-1 suppresses superoxide generation in macrophages through induction of mitochondrial UCP2. J. Leukoc. Biol. 86 (2009) 981-988.

[144] R. Mailloux, M. Harper, Uncoupling proteins and the control of mitochondrial reactive oxygen species production. Free Radic. Biol. Med. 51 (2011) 1106-15.

[145] D. Liu, L. Huang, Y. Wang, W. Wang, X.H. Wehrens, T. Belousova, M. Abdelrahim, G. DiMattia, D. Sheikh-Hamad, Human stanniocalcin-1 suppresses angiotensin II-induced superoxide generation in cardiomyocytes through UCP3-mediated anti-oxidant pathway. PLoS One. 7 (2012) e36994.

[146] S. Ohkouchi, G.J. Block, A.M. Katsha, M. Kanehira, M. Ebina, T. Kikuchi, Y. Saijo, T. Nukiwa, D.J. Prockop, Mesenchymal stromal cells protect cancer cells from ROS-induced apoptosis and enhance the Warburg effect by secreting STC1. Mol. Ther. 20 (2012) 417-423.

[147] J. Kanellis, R. Bick, G. Garcia, L. Truong, C.C. Tsao, D. Etemadmoghadam, B. Poindexter, L. Feng, R.J. Johnson, D. Sheikh-Hamad, Stanniocalcin-1, an inhibitor of macrophage chemotaxis and chemokinesis. Am. J. Physiol. Renal Physiol. 286 (2004) F356-62.

[148] A. Chakraborty, H. Brooks, P. Zhang, W. Smith, M.R. McReynolds, J.B. Hoying, R. Bick, L. Truong, B. Poindexter, H. Lan, W. Elbjeirami, D. Sheikh-Hamad, Stanniocalcin-1 regulates endothelial gene expression and modulates transendothelial migration of leukocytes. Am. J. Physiol. Renal Physiol. 292 (2007) F895-904.

[149] V. Tergaonkar, NFkappaB pathway: a good signaling paradigm and therapeutic target. Int. J. Biochem. Cell Biol. 38 (2006) 1647-53.

[150] L. Huang, T. Belousova, M. Chen, G. DiMattia, D. Liu, D. Sheikh-Hamad, Overexpression of stanniocalcin-1 inhibits reactive oxygen species and renal ischemia/reperfusion injury in mice. Kidney Int. 82 (2012) 867-877.

[151] G.W. Roddy, R.H. Rosa Jr, J.Y. Oh, J.H. Ylostalo, T.J. Bartosh Jr, H. Choi, R.H. Lee, D. Yasumura, K. Ahern, G. Nielsen, M.T. Matthes, M.M. LaVail, D.J. Prockop, Stanniocalcin-1 rescued photoreceptor degeneration in two rat models of inherited retinal degeneration. Mol. Ther. 20 (2012) 788-797.

[152] S.E. Tang, C.P. Wu, S.Y. Wu, C.K. Peng, W.C. Perng, B.H. Kang, S.J. Chu, K.L. Huang, Stanniocalcin-1 ameliorates lipopolysaccharide-induced pulmonary oxidative stress, inflammation, and apoptosis in mice. Free Radic. Biol. Med. 71C (2014) 321-331.

[153] F. Ginhoux, S. Jung, Monocytes and macrophages: developmental pathways and tissue homeostasis. Nat. Rev. Immunol. 14 (2014) 392-404.

[154] R. van Furth, Z.A. Cohn, The origin and kinetics of mononuclear phagocytes. J. Exp. Med. 128 (1968) 415-35.

[155] F. Geissmann, M. Manz, S. Jung, M. Sieweke, M. Merad, K. Ley, Development of monocytes, macrophages, and dendritic cells. Science. 327 (2010) 656-61.

[156] J. Hettinger, D. Richards, J. Hansson, M. Barra, A. Joschko, J. Krijgsveld, M. Feuerer, Origin of monocytes and macrophages in a committed progenitor. Nat. Immunol. 14 (2013) 821-30.

[157] F.K. Swirski, M. Nahrendorf, M. Etzrodt, M. Wildgruber, V. Cortez-Retamozo, P. Panizzi, J.L. Figueiredo, R.H. Kohler, A. Chudnovskiy, P. Waterman, E. Aikawa, T.R. Mempel, P. Libby, R. Weissleder, M.J. Pittet, Identification of splenic reservoir monocytes and their deployment to inflammatory sites. Science. 325 (2009) 612-616.

[158] C. Robbins, A. Chudnovskiy, P. Rauch, J. Figueiredo, Y. Iwamoto, R. Gorbatov, M. Etzrodt, G. Weber, T. Ueno, N. van Rooijen, M. Mulligan Kehoe, P. Libby, M. Nahrendorf, M. Pittet, R. Weissleder, F. Swirski, Extramedullary hematopoiesis generates Ly-6C(high) monocytes that infiltrate atherosclerotic lesions. Circulation. 125 (2012) 364-74.

[159] X. Dai, G. Ryan, A. Hapel, M. Dominguez, R. Russell, S. Kapp, V. Sylvestre, E.R. Stanley, Targeted disruption of the mouse colony-stimulating factor 1 receptor gene results in osteopetrosis, mononuclear phagocyte deficiency, increased primitive progenitor cell frequencies, and reproductive defects. Blood. 99 (2002) 111-20.

[160] T. Wynn, A. Chawla, J. Pollard, Macrophage biology in development, homeostasis and disease. Nature. 496 (2013) 445-55.

[161] E. Zigmond, S. Jung, Intestinal macrophages: well educated exceptions from the rule. Trends Immunol. 34 (2013) 162-8.

[162] S. Gordon, P. Taylor, Monocyte and macrophage heterogeneity. Nat. Rev. Immunol. 5 (2005) 953-64.

[163] C. Shi, E. Pamer, Monocyte recruitment during infection and inflammation. Nat. Rev. Immunol. 11 (2011) 762-74.

[164] J. Yang, L. Zhang, C. Yu, X. Yang, H. Wang, Monocyte and macrophage differentiation: circulation inflammatory monocyte as biomarker for inflammatory diseases. Biomark. Res. 2 (2014) 1.

[165] P. Murray, T. Wynn, Protective and pathogenic functions of macrophage subsets. Nat. Rev. Immunol. 11 (2011) 723-37.

[166] N. McGovern, A. Schlitzer, M. Gunawan, L. Jardine, A. Shin, E. Poyner, K. Green, R. Dickinson, X. Wang, D. Low, K. Best, S. Covins, P. Milne, S. Pagan, K.

Aljefri, M. Windebank, D. Saavedra, A. Larbi, P. Wasan, K. Duan, M. Poidinger, V. Bigley, F. Ginhoux, M. Collin, M. Haniffa, Human dermal $CD14^{+}$ cells are a transient population of monocyte-derived macrophages. Immunity. 41 (2014) 465-77.

[167] D. Mosser, J. Edwards, Exploring the full spectrum of macrophage activation. Nat. Rev. Immunol. 8 (2008) 958-69.

[168] L. Carlin, E. Stamatiades, C. Auffray, R. Hanna, L. Glover, G. Vizcay Barrena, C. Hedrick, H.T. Cook, S. Diebold, F. Geissmann, Nr4a1-dependent Ly6C(low) monocytes monitor endothelial cells and orchestrate their disposal. Cell. 153 (2013) 362-75.

[169] K. Nguyen, S. Fentress, Y. Qiu, K. Yun, J. Cox, A. Chawla, Circadian gene Bmal1 regulates diurnal oscillations of Ly6C(hi) inflammatory monocytes. Science. 341 (2013) 1483-8.

[170] J. Pollard, Trophic macrophages in development and disease. Nat. Rev. Immunol. 9 (2009) 259-70.

[171] J. Stefater, I. Lewkowich, S. Rao, G. Mariggi, A. Carpenter, A. Burr, J. Fan, R. Ajima, J. Molkentin, B. Williams, M. Wills Karp, J. Pollard, T. Yamaguchi, N. Ferrara, H. Gerhardt, R. Lang, Regulation of angiogenesis by a non-canonical Wnt-Flt1 pathway in myeloid cells. Nature. 474 (2011) 511-5.

[172] C. Gordy, H. Pua, G. Sempowski, Y. He, Regulation of steady-state neutrophil homeostasis by macrophages. Blood. 117 (2011) 618-29.

[173] K. Kawane, H. Fukuyama, G. Kondoh, J. Takeda, Y. Ohsawa, Y. Uchiyama, S. Nagata, Requirement of DNase II for definitive erythropoiesis in the mouse fetal liver. Science. 292 (2001) 1546-9.

[174] S. Jenkins, D. Ruckerl, P. Cook, L. Jones, F. Finkelman, N. van Rooijen, A. MacDonald, J. Allen, Local macrophage proliferation, rather than recruitment from the blood, is a signature of TH2 inflammation. Science. 332 (2011) 1284-8.

[175] S. Frantz, G. Ertl, J. Bauersachs, Mechanisms of disease: Toll-like receptors in cardiovascular disease. Nat. Clin. Pract. Cardiovasc. Med. 4 (2007) 444-54.

[176] M. Di Gioia, I. Zanoni, Toll-like receptor co-receptors as master regulators of the immune response. Mol. Immunol. (2014).

[177] A.I. Tukhvatulin, D.Y. Logunov, D.N. Shcherbinin, M.M. Shmarov, B.S. Naroditsky, A.V. Gudkov, A.L. Gintsburg, Toll-like receptors and their adapter molecules. Biochemistry (Mosc). 75 (2010) 1098-1114.

[178] A. Haziot, E. Ferrero, F. Köntgen, N. Hijiya, S. Yamamoto, J. Silver, C.L. Stewart, S.M. Goyert, Resistance to endotoxin shock and reduced dissemination of gram-negative bacteria in CD14-deficient mice. Immunity. 4 (1996) 407-14.

[179] S. Kim, S.Y. Kim, J.P. Pribis, M. Lotze, K.P. Mollen, R. Shapiro, P. Loughran, M.J. Scott, T.R. Billiar, Signaling of high mobility group box 1 (HMGB1) through toll-like receptor 4 in macrophages requires CD14. Mol. Med. 19 (2013) 88-98.

[180] A. Nauta, W. Fibbe, Immunomodulatory properties of mesenchymal stromal cells. Blood. 110 (2007) 3499-506.

[181] D. Prockop, Repair of tissues by adult stem/progenitor cells (MSCs): controversies, myths, and changing paradigms. Mol. Ther. 17 (2009) 939-46.

[182] S. Ranganath, O. Levy, M. Inamdar, J. Karp, Harnessing the mesenchymal stem cell secretome for the treatment of cardiovascular disease. Cell Stem Cell. 10 (2012) 244-58.

[183] M. Islam, S. Das, M. Emin, M. Wei, L. Sun, K. Westphalen, D. Rowlands, S. Quadri, S. Bhattacharya, J. Bhattacharya, Mitochondrial transfer from bone-marrow-derived stromal cells to pulmonary alveoli protects against acute lung injury. Nat. Med. 18 (2012) 759-65.

[184] R. Lee, J. Yu, A. Foskett, G. Peltier, J. Reneau, N. Bazhanov, J. Oh, D. Prockop, TSG-6 as a biomarker to predict efficacy of human mesenchymal stem/progenitor cells (hMSCs) in modulating sterile inflammation in vivo. Proc. Natl. Acad. Sci. U. S. A. 111 (2014) 16766-71.

[185] T.J. Bartosh, J.H. Ylostalo, N. Bazhanov, J. Kuhlman, D.J. Prockop, Dynamic compaction of human mesenchymal stem/precursor cells (MSC) into spheres self-activates caspase-dependent IL1 signaling to enhance secretion of modulators of inflammation and immunity (PGE2, TSG6 and STC1). Stem Cells. (2013).

[186] J.Y. Oh, J.H. Ko, H.J. Lee, J.M. Yu, H. Choi, M.K. Kim, W.R. Wee, D.J. Prockop, Mesenchymal stem/stromal cells inhibit the NLRP3 inflammasome by decreasing mitochondrial reactive oxygen species. Stem Cells. 32 (2014) 1553-1563.

[187] P. Crisostomo, Y. Wang, T. Markel, M. Wang, T. Lahm, D. Meldrum, Human mesenchymal stem cells stimulated by TNF-alpha, LPS, or hypoxia produce growth factors by an NF kappa B- but not JNK-dependent mechanism. Am. J. Physiol. Cell Physiol. 294 (2008) C675-82.

[188] W. Wang, K. Itaka, S. Ohba, N. Nishiyama, U.I. Chung, Y. Yamasaki, K. Kataoka, 3D spheroid culture system on micropatterned substrates for improved differentiation efficiency of multipotent mesenchymal stem cells. Biomaterials. 30 (2009) 2705-2715.

[189] H. Page, P. Flood, E. Reynaud, Three-dimensional tissue cultures: current trends and beyond. Cell Tissue Res. 352 (2013) 123-31.

[190] E. Steck, H. Bertram, R. Abel, B. Chen, A. Winter, W. Richter, Induction of intervertebral disc-like cells from adult mesenchymal stem cells. Stem Cells. 23 (2005) 403-11.

[191] M.C. Arufe, A. De la Fuente, I. Fuentes-Boquete, F.J. De Toro, F.J. Blanco, Differentiation of synovial CD-105(+) human mesenchymal stem cells into chondrocyte-like cells through spheroid formation. J. Cell. Biochem. 108 (2009) 145-155.

[192] I. Potapova, G. Gaudette, P. Brink, R. Robinson, M. Rosen, I. Cohen, S. Doronin, Mesenchymal stem cells support migration, extracellular matrix invasion, proliferation, and survival of endothelial cells in vitro. Stem Cells. 25 (2007) 1761-8.

[193] I. Potapova, P. Brink, I. Cohen, S. Doronin, Culturing of human mesenchymal stem cells as three-dimensional aggregates induces functional expression of CXCR4 that regulates adhesion to endothelial cells. J. Biol. Chem. 283 (2008) 13100-7.

[194] C. Wang, C. Chen, S. Hwang, W. Lin, C. Huang, W. Lee, Y. Chang, H. Sung, Spherically symmetric mesenchymal stromal cell bodies inherent with endogenous extracellular matrices for cellular cardiomyoplasty. Stem Cells. 27 (2009) 724-32.

[195] F. Arslan, D. de Kleijn, G. Pasterkamp, Innate immune signaling in cardiac ischemia. Nat. Rev. Cardiol. 8 (2011) 292-300.

[196] T. Kempf, A. Zarbock, D. Vestweber, K. Wollert, Anti-inflammatory mechanisms and therapeutic opportunities in myocardial infarct healing. J. Mol. Med. 90 (2012) 361-9.

[197] N.G. Frangogiannis, Regulation of the inflammatory response in cardiac repair. Circ. Res. 110 (2012) 159-173.

[198] T.J. Bartosh, J.H. Ylostalo, A. Mohammadipoor, N. Bazhanov, K. Coble, K. Claypool, R.H. Lee, H. Choi, D.J. Prockop, Aggregation of human mesenchymal

stromal cells (MSCs) into 3D spheroids enhances their antiinflammatory properties. Proc. Natl. Acad. Sci. U. S. A. 107 (2010) 13724-13729.

[199] A.J. Friedenstein, J.F. Gorskaja, N.N. Kulagina, Fibroblast precursors in normal and irradiated mouse hematopoietic organs. Exp. Hematol. 4 (1976) 267-274.

[200] M. Owen, A.J. Friedenstein, Stromal stem cells: marrow-derived osteogenic precursors. Ciba Found. Symp. 136 (1988) 42-60.

[201] R. Romieu-Mourez, M. François, M. Boivin, M. Bouchentouf, D. Spaner, J. Galipeau, Cytokine modulation of TLR expression and activation in mesenchymal stromal cells leads to a proinflammatory phenotype. J. Immunol. 182 (2009) 7963-73.

[202] Z. Qihao, C. Xigu, C. Guanghui, Z. Weiwei, Spheroid formation and differentiation into hepatocyte-like cells of rat mesenchymal stem cell induced by co-culture with liver cells. DNA Cell Biol. 26 (2007) 497-503.

[203] J. Frith, B. Thomson, P. Genever, Dynamic three-dimensional culture methods enhance mesenchymal stem cell properties and increase therapeutic potential. Tissue Eng. Part C: Methods. 16 (2010) 735-49.

[204] R. Lee, M. Seo, A. Pulin, C. Gregory, J. Ylostalo, D. Prockop, The CD34-like protein PODXL and alpha6-integrin (CD49f) identify early progenitor MSCs with increased clonogenicity and migration to infarcted heart in mice. Blood. 113 (2009) 816-26.

[205] C. McBride, D. Gaupp, D.G. Phinney, Quantifying levels of transplanted murine and human mesenchymal stem cells in vivo by real-time PCR. Cytotherapy. 5 (2003) 7-18.

[206] C. Gregory, H. Singh, A. Perry, D. Prockop, The Wnt signaling inhibitor dickkopf-1 is required for reentry into the cell cycle of human adult stem cells from bone marrow. J. Biol. Chem. 278 (2003) 28067-78.

[207] J. Schwab, N. Chiang, M. Arita, C. Serhan, Resolvin E1 and protectin D1 activate inflammation-resolution programmes. Nature. 447 (2007) 869-74.

[208] B. Johnstone, T.M. Hering, A.I. Caplan, V.M. Goldberg, J.U. Yoo, In vitro chondrogenesis of bone marrow-derived mesenchymal progenitor cells. Exp. Cell Res. 238 (1998) 265-72.

[209] Z. Mahmood, Y. Shukla, Death receptors: targets for cancer therapy. Exp. Cell Res. 316 (2010) 887-99.

[210] G. Mellier, S. Huang, K. Shenoy, S. Pervaiz, TRAILing death in cancer. Mol. Aspects Med. 31 (2010) 93-112.

[211] S. Smith, D. Theodorescu, Learning therapeutic lessons from metastasis suppressor proteins. Nat. Rev. Cancer. 9 (2009) 253-64.

[212] S. Grivennikov, F. Greten, M. Karin, Immunity, inflammation, and cancer. Cell. 140 (2010) 883-99.

[213] J. Takagawa, Y. Zhang, M.L. Wong, R.E. Sievers, N.K. Kapasi, Y. Wang, Y. Yeghiazarians, R.J. Lee, W. Grossman, M.L. Springer, Myocardial infarct size measurement in the mouse chronic infarction model: comparison of area- and length-based approaches. J. Appl. Physiol. (1985). 102 (2007) 2104-2111.

[214] J. Ylöstalo, T. Bartosh, K. Coble, D. Prockop, Human mesenchymal stem/stromal cells cultured as spheroids are self-activated to produce prostaglandin E2 that directs stimulated macrophages into an anti-inflammatory phenotype. Stem Cells. 30 (2012) 2283-2296.

[215] V. Loria, I. Dato, F. Graziani, L.M. Biasucci, Myeloperoxidase: a new biomarker of inflammation in ischemic heart disease and acute coronary syndromes. Mediators Inflamm. 2008 (2008) 135625.

[216] F. Colotta, F. Re, N. Polentarutti, S. Sozzani, A. Mantovani, Modulation of granulocyte survival and programmed cell death by cytokines and bacterial products. Blood. 80 (1992) 2012-2020.

[217] T.J. Bartosh, Z. Wang, A.A. Rosales, S.D. Dimitrijevich, R.S. Roque, 3D-model of adult cardiac stem cells promotes cardiac differentiation and resistance to oxidative stress. J. Cell. Biochem. 105 (2008) 612-623.

[218] K. Schroder, J. Tschopp, The inflammasomes. Cell. 140 (2010) 821-32.

[219] M. Magna, D. Pisetsky, The role of HMGB1 in the pathogenesis of inflammatory and autoimmune diseases. Mol. Med. 20 (2014) 138-46.

[220] S. Smith, C. Jefferies, Role of DNA/RNA sensors and contribution to autoimmunity. Cytokine Growth Factor Rev. 25 (2014) 745-57.

[221] R. Thwaites, G. Chamberlain, S. Sacre, Emerging role of endosomal toll-like receptors in rheumatoid arthritis. Front. Immunol. 16 (2014) 1.

[222] P. Knuefermann, S. Nemoto, A. Misra, N. Nozaki, G. Defreitas, S. Goyert, B. Carabello, D. Mann, J. Vallejo, CD14-deficient mice are protected against lipopolysaccharide-induced cardiac inflammation and left ventricular dysfunction. Circulation. 106 (2002) 2608-15.

[223] D. Kaczorowski, A. Nakao, R. Vallabhaneni, K. Mollen, R. Sugimoto, J. Kohmoto, B. Zuckerbraun, K. McCurry, T. Billiar, Mechanisms of Toll-like receptor 4 (TLR4)-mediated inflammation after cold ischemia/reperfusion in the heart. Transplantation. 87 (2009) 1455-63.

[224] A.J. Chong, A. Shimamoto, C.R. Hampton, H. Takayama, D.J. Spring, C.L. Rothnie, M. Yada, T.H. Pohlman, E.D. Verrier, Toll-like receptor 4 mediates ischemia/reperfusion injury of the heart. J. Thorac. Cardiovasc. Surg. 128 (2004) 170-179.

[225] A. Shimamoto, A.J. Chong, M. Yada, S. Shomura, H. Takayama, A.J. Fleisig, M.L. Agnew, C.R. Hampton, C.L. Rothnie, D.J. Spring, T.H. Pohlman, H. Shimpo, E.D. Verrier, Inhibition of Toll-like receptor 4 with eritoran attenuates myocardial ischemia-reperfusion injury. Circulation. 114 (2006) I270-4.

[226] L. Timmers, J.P.G. Sluijter, J.K. van Keulen, I. Hoefer, M.G.J. Nederhoff, M. Goumans, P. Doevendans, van Echteld, Cees J A, J. Joles, P. Quax, J. Piek, G. Pasterkamp, D.P.V. de Kleijn, Toll-like receptor 4 mediates maladaptive left ventricular remodeling and impairs cardiac function after myocardial infarction. Circ. Res. 102 (2008) 257-64.

[227] J. Pan, L. Huang, T. Belousova, L. Lu, Y. Yang, R. Reddel, A. Chang, H. Ju, G. DiMattia, Q. Tong, D. Sheikh Hamad, Stanniocalcin-1 Inhibits Renal Ischemia/Reperfusion Injury via an AMP-Activated Protein Kinase-Dependent Pathway. J. Am. Soc. Nephrol. 26 (2015) 364-78.

[228] H. Rosen, J.R. Crowley, J.W. Heinecke, Human neutrophils use the myeloperoxidase-hydrogen peroxide-chloride system to chlorinate but not nitrate bacterial proteins during phagocytosis. J. Biol. Chem. 277 (2002) 30463-30468.

[229] C. Chen, M.S. Jamaluddin, S. Yan, D. Sheikh-Hamad, Q. Yao, Human stanniocalcin-1 blocks TNF-alpha-induced monolayer permeability in human coronary artery endothelial cells. Arterioscler. Thromb. Vasc. Biol. 28 (2008) 906-912.

[230] Y. Sakata, J.W. Dong, J.G. Vallejo, C.H. Huang, J.S. Baker, K.J. Tracey, O. Tacheuchi, S. Akira, D.L. Mann, Toll-like receptor 2 modulates left ventricular function

following ischemia-reperfusion injury. Am. J. Physiol. Heart Circ. Physiol. 292 (2007) H503-9.

[231] J. Favre, P. Musette, V. Douin-Echinard, K. Laude, J.P. Henry, J.F. Arnal, C. Thuillez, V. Richard, Toll-like receptors 2-deficient mice are protected against postischemic coronary endothelial dysfunction. Arterioscler. Thromb. Vasc. Biol. 27 (2007) 1064-1071.

[232] F. Arslan, M.B. Smeets, L.A. O'Neill, B. Keogh, P. McGuirk, L. Timmers, C. Tersteeg, I.E. Hoefer, P.A. Doevendans, G. Pasterkamp, D.P. de Kleijn, Myocardial ischemia/reperfusion injury is mediated by leukocytic toll-like receptor-2 and reduced by systemic administration of a novel anti-toll-like receptor-2 antibody. Circulation. 121 (2010) 80-90.

[233] R.P. Lauener, S.M. Goyert, R.S. Geha, D. Vercelli, Interleukin 4 down-regulates the expression of CD14 in normal human monocytes. Eur. J. Immunol. 20 (1990) 2375-2381.